DEFORMATION BASED SEISMIC DESIGN OF PILE SUPPORTED MARINE FACILITIES

by

Şamil Şeref POLAT

B.S., Civil Engineering, YTU, 1996

M.S., Earthquake Engineering, Boğaziçi University, 1999

Submitted to the Kandilli Observatory and Earthquake Research Institute
for Graduate Studies in Earthquake Engineering in partial fulfillment of
the requirements for degree of
Doctor of Philosophy

Graduate Program in Earthquake Engineering
Boğaziçi University
2008

DEFORMATION BASED SEISMIC DESIGN OF PILE SUPPORTED MARINE FACILITIES

APPROVED BY:

Prof. Dr. M. Nuray AYDINOĞLU (Thesis Supervisor)	.....
Prof. Dr. Mustafa ERDİK	.....
Prof. Dr. Atilla ANSAL	.....
Prof. Dr. Erkan ÖZER	.....
Assoc. Dr. Prof. Eser DURUKAL	.....

DATE OF APPROVAL : 18.07.2008

To my beloved wife, Handan and my precious children

ACKNOWLEDGMENTS

I would like to express my gratitude to Professor Nuray Aydınoğlu for his invaluable guidance and help during the preparation of this dissertation. I would also like to thank for his patience and understanding. On the other hand I would like to express my appreciation to the faculty of Earthquake Engineering during my PhD education with whom I had the opportunity to work with and take courses, Prof. Mustafa Erdik, Prof. Özal Yüzügüllü, Prof. Bilge Siyahi, Assoc. Prof. Yasin Fahjan. Their concern and support is greatly acknowledged.

I would like to express my special thanks to my dear colleagues Utku Celep, Göktürk Önem and Cüneyt Tüzün for their kind support.

I would like to express my gratitude to my beloved wife Handan, for her endless patience, love and support, which flourished further during the course of this thesis together with her inspiration all through my endless working days and nights.

Last but not least my deepest appreciation goes to my mother and my father for all the love and support they provided to me all through my life.

ABSTRACT

DEFORMATION BASED SEISMIC DESIGN OF PILE SUPPORTED MARINE FACILITIES

Pile supported marine structures with batter piles comprise a considerable share in the modern marine structure stock built in seismic zones. Their stiff nature offers significant advantages to structural engineers in resisting non-seismic loads such as, berthing, mooring etc. On the other hand the poor performance of marine structures supported by batter piles in recent earthquakes has revealed certain disadvantages of these systems in resisting seismic loads. The general design approach for pile supported marine structures is to ensure that the cap-beam and the deck system will remain elastic and the yielding will occur either at the pile-to-cap beam connection or along the pile itself. Traditionally those structures were designed with force-based design methods to withstand seismic forces reduced by response modification factors or to a force equal to a fraction of the total weight of the structure. The past research in last decade have shown that the poor behavior of batter piles is mainly related to this force-based approach, which lack to identify the problems associated to post-yield behavior of these piles.

When batter piles yield in tension, either in the form of pile-to-cap-beam connection or pile pull-out of soil pile-cap starts to pole vault over the compression piles as the structure deforms laterally. As the structure rises, substantial tension forces are developed both in the vertical and orthogonal batter piles and create additional shear and moment to the cap-beam. The non-linear analysis performed on generic pier frames in this study revealed that substantial amplifications in section forces have been observed at the pile-cap with decrease in strength and increase in batter.

Even though section compactness is a well known requirement in steel design most of the modern marine structure design codes does not provide a compactness criteria. When the connection of the tension batter pile is designed to develop high axial forces, the

compression piles with non-compact steel section have a tendency to yield under the action of earthquake induced bending moments and high compression forces at the pile-soil interface. The inelastic response history analysis performed on generic pier frames indicate formation of inelastic local buckling on compression piles results in partial or total collapse of the structure. Design recommendations are provided based on the results of the performed nonlinear analysis.

ÖZET

KAZIKLI KIYI YAPILARININ ŞEKİL DEĞİŞTİRMEYE GÖRE TASARIMI

Eğik kazıklı kıyı yapıları deprem bölgelerinde inşaa edilmiş olan denizyapı stoğunun önemli bir kısmını oluşturmaktadır. Bu yapıların rijit yapısı deprem harici yatay yüklere karşı dayanım açısından mühendislere önemli avantajlar sağlamaktadır. Öte yandan eğik kazıklı kıyı yapılarının son yıllarda olan büyük depremlerdeki kötü perfromansı, bu tür yapıların deprem yüklerine direnme noktasında ciddi dezavantajarını ortaya çıkarmıştır. Kazıklı kıyı yapılarının genel tasarım esası, deprem sırasında kazık başlığı ve döşemenin hasar görmememesine ve oluşacak olan hasarın ya kazıkta yada kazık-kazık başlığı birleşim noktasında oluşması prensibine dayanmaktadır. Geleneksel olarak bu yapılar deprem yükü azaltma katsayıları ile azaltılmış deprem yükleri veya toplam yapı ağırlığının belirli bir yüzdesi ile orantılı yüklerden oluşan deprem yüklerine karşı koymak üzere dayanım esaslı tasarım metodları ile tasarlanmaktaydılar. Son yıllarda yapılmış olan çalışmalar, bu kötü performansın eğik kazıkların elastic ötesi davranışına dayanan problemleri tanımlayamayan dayanım easalı tasarım metodları ile bağlantılı olduğunu göstermektedir.

Eğik kazıklar, kazığı kazık başlığına bağlayan betonarme bağlantının akması veya çekme yükleri altındaki kazığın zeminden sıyrılması ile, yapı yatayda hareket ettikçe, basıç kuvvetleri altındaki kazığın üzerinde yükselmeye başlar. Yapı yukarı doğru kalktıkça bu kazıklara dik eğik veya düşey kazıklarda ciddi çekme kuvvetleri ile kazık başlığında ekstra eğilme ve kesme kuvvetleri oluşmaktadır. Temsili iskele yapılarında yapılan doğrusal olmayan analizler, azalan yapı dayanımı ve artan kazık eğimi ile kazık başlıklarında oluşan tasarım kuvvetlerinde önemli artımlar olduğunu göstermektedir.

Kesit kompaklığı çelik yapıları tasarımında çok önemli bir kriter olduğu halda çoğu modern kıyı yapıları kodu bu konuda herhangi bir kısıtlama getirmemiştir. Çekme altındaki kazığın kazık başlığı bağlantısının yeterince güçlü tasarlanması durumunda, basınç altındaki çelik kazıkların kazığın zemine girdiği bölgede deprem sırasında oluşan eğilme momentleri ve yüksek basıç kuvvetleri altında akma ihtimali vardır. Temsili iskele yapılarında zaman tanım alanında yapılan doğrusal olmayan analizlerden elde edilen veriler basınç altındaki kazıklarda oluşan elastic olmayan burkulmaların yapıda kısmi veya toptan çökmeye sebep olduğunu göstermektedir. Dogrusal olmayan analizlerin verilerine bağlı olarak kıyı yapılarının tasarımında kullanılabilecek bazı tasarım onerimleri yapılmıştır.

TABLE OF CONTENTS

LIST OF FIGURES

LIST OF TABLES

LIST OF SYMBOLS /ABREVIATIONS

A	Total section area of the pile
A_p	Cross section area of the pile
C	Damping matrix
C_a	Compressive stress at the side of the pile
C_{Rn}	Spectral displacement amplification factor
C_u	Undrained shear strength
C_1	Dimensionless coefficient
C_2	Dimensionless coefficient
C_3	Dimensionless coefficient
D	Diameter of the pipe pile
d_b	Diameter of Reinforcing Bar
$d_n\ (t)$	Deformation response of the *n*th-"mode" inelastic SDF system
E_s	Young's modulus for steel
E_s	Modulus of soil reaction
E_p	Modulus of elasticity of the pile
f	Shaft Friction
F_a	Short period amplification factor
$\mathrm{f_m}$	P multiplier
F_{sn}	A nonlinear hysteretic function of q_n
F_{sy}	Yield force of the nonlinear spring
F_y	Yield Stress of Steel
f_y	Yield Stress of Mild Steel
F_{xc}	Local buckling stress
F_v	Amplification factor for 1.00 second period spectral acceleration
h	Tributary length between the nodes of the pile
H_e	Embedding length of the steel pile to the pile cap
I	Moment of inertia of the section
I_p	Moment of inertia of the pile section
J	Dimensionless empirical constant with values ranging from 0.25 to 0.5

k	Initial modulus of subgrade reaction in force per volume
K	Coefficient for lateral earth pressure
k_{py}	Elastic stiffness nonlinear spring element
L_p	Plastic Hinge Length
l_{sp}	Strain Penetration Length
M	Mass matrix
M_{pc}	Plastic Moment Capacity of Connection
N_q	Dimensionless bearing capacity factor
P	Lateral soil reaction per unit length
$\mathbf{p}_{\text{eff,n}}(t)$	Effective earthquake force
P_p	Axial compression or tension force at the pile section
P_y	Compression force at yield
Q	Axial load on the pile
$q_n(t)$	Modal coordinate of the nth mode
Q_p	Total end bearing
Q_u	Ultimate resistance
R	Strength reduction factor
r_t	Response of the system to excitation
R_t	Diameter-to-wall-thickness ratio defined by Japanese code
S_{di}	Predicted inelastic displacement
S_{de}	Elastic spectral displacement
S_s	Short Period Acceleration value
S_1	Spectral Acceleartion value at 1.00 second
t	Wall thickness of the pipe pile
T_L	Long period values of the design spectrum
T_o	Shorth period values of the design spectrum
T_s	Characteristic period of the spectrum
$u_n(t)$	Floor displacement at time t
u_{rxn}	Roof displacement of the nth mode
u_{ryn}	Roof displacement of the nth mode
$u_{r\theta n}$	Roof displacement of the nth mode
U_{rg}	The lateral roof displacement due to gravity loads

V_p	Pile shear force
V_{bn}	Base shear
x	Vertical depth
y	Lateral deflection of the pile at point x along the length of the pile
α	Ratio of bending moments evaluated with nonlinear analysis to bending moments evaluated with response modification factors
α_i	Coefficient for mass proportional damping
β_i	Coefficient for stiffness proportional damping
β_c	Correction factors comparing the downslope of horizontal p-y curves
δ	Friction angle between the soil and pile
δ_y	Yield displacement of the elasto-plastic nonlinear spring element
ΔM_p	Increase in flexural capacity due to contact of steel pipe with pile cap cover concrete
ε_{cy}	Yield strain of compact steel section in compression
ε_{cny}	Yield strain of non-compact steel section in compression
ε_{cm}	Strain at maximum compression stress of steel
ε_{max}	Maximum Steel Strain
ε_{ty}	Yield strain of steel in tension
ε_{tm}	Strain at maximum tension stress of steel
ε_{50}	Soil strain at 50% ultimate stess
Φ	Internal friction angle
Φ_n	nth vibration mode
Γ_n	Partipating factor of the nth mode
ϕ_t	Total curvature
ϕ_p	Total plastic curvature
ϕ_y	Yield curvature of the bilinearized moment curvature curve
γ	Effective soil weight
μ_a	Allowable plasticity ratio
ξ_i	Damping ratio
ξn	Damping ratio of the nth mode of the corresponding linear system
θ_p	Total plastic rotation

σ_{cny}	Yield stress of non-compact steel section in compression
σ_{cr}	Critical local buckling stress
σ_{cy}	Yield stress of compact steel section in compression
σ_{cm}	Maximum compression stress of steel
σ_{sy}	Stress drop after local buckling
σ_{ty}	Yield stress of steel in tension
σ_{y}	Yield stress of steel
σ_{tm}	Maximum tension stress of steel
σ_{0}	Effective overburden pressure at the point in question
ν	Poisson's ratio

API	American Petroleum Institute
ASCE	American Society of Civil Engineers
ATC	Applied Technology Council
CQC	Complete Quadratic Combination
SRSS	Square Root of Sum of Squares
EQE	Earthquake Engineering
FEMA	Federal Emergency Management Agency
FRP	Fiber Reinforced Polymer
IRHA	Inelastic Response History Analysis
MPA	Multi-Mode Pushover Analysis
MOTEMS	Marine Oil Terminal Engineering and Maintenance Standards
POLA	Port of Los Angeles
SMPA	Single Mode Pushover Analysis
TCLEE	Technical Council on Lifeline Earthquake Engineering
USA	United States of America

1. INTRODUCTION

In the last decades there has been an extraordinary increase in the sea trade worldwide, which has led to a significant growth in port facilities. Those facilities represent a large economical investment for the society and the economic loss resulting from their interruption can be substantial. A very important source of interruption is the earthquake induced damage. It was estimated that the direct damage to Port of Kobe, Japan, during the 1995 earthquake exceeded US $ 11 billion (EQE International, 1995). However actual financial loss exceeds this amount through loss of economical activity. By the year 2000, Port of Kobe had recovered only 80% of its 1994 container traffic volume, while surrounding ports in Japan and Asia increased their volume by 40% to 100% (Landers, 2001).

Most of the pile supported marine structures with batter piles suffered significant damage in the past earthquakes such as Loma Prieta (1989), Northridge (1994), and Kobe (1995). This poor performance has discouraged owners and engineers, even a number of seismic design codes, using batter piles in new port facilities. Traditionally those structures were designed with force-based design methods to withstand seismic forces reduced by response modification factors or to a force equal to a fraction of the total weight of the structure. The general design approach for pile supported marine structures is to ensure that the cap-beam and the deck system will remain elastic and the yielding will occur either at the pile-to-cap beam connection or along the pile itself. This design approach without considering the post-yield behavior could lead to a structural behavior much different from what the designer intended.

Driven piles must be robust to withstand the high driving forces. Such piles usually have more capacity in compression than in tension and the axial capacity of the pile in tension or compression will be higher than the capacity of the soil or the pile-to-cap beam connection, which indicates that the yielding is concentrated to the tension connection or the tensile force is bounded with the pile pull-out in the soil. When the batter pile in tension yields, the structure will “pole-vault” (Harn, 2004) over the compression pile and move both horizontally and vertically. As the structure rises, substantial tension forces are

developed both in the vertical and orthogonal batter piles and create additional shear and moment to the cap beam. Ignoring this post-yield mode by using force-based design methods may lead to yielding and heavy damage of the cap beam or the deck, which is normally required to remain elastic during a design earthquake event.

Steel piles with non-compact sections have a fragile post-yield behavior mode. When the connection of the tension batter pile is designed to develop high axial forces, the compression piles with non-compact steel section have a tendency to yield under the action of earthquake induced bending moments and high compression forces at the pile-soil interface. The occurrence of such a yielding under high compression forces may result in premature failure modes in the form of inelastic local buckling, which could cause a partial or total collapse.

Since there are only a very limited number of studies in the literature on these particular issues, quantified explanation of these behavior modes is still an open field of research.

Most of the modern design codes use displacement-based design approach, which requires the application of nonlinear analysis methods, such as pushover analysis. However behavior of irregular structures, such as wharfs and L or T shape piers need special attention, because their complex seismic response is very difficult to simulate by conventional pushover analysis tools. Thus, application of such methods to irregular pile supported marine structures also needs further investigation.

1.1. Scope of Work

The problems associated with the post-yield behavior of marine structures with batter piles, such as “pole vaulting” due to yielding of the pile-to-cap-beam connection or the pile pull-out from soil as well as the fragile post-yield behavior of steel piles with non-compact steel sections have been investigated within the scope of this study. The structural modeling issues related to each of these post-yield behavior modes, such as the plastic deformation of pile-to-cap-beam connections under high tension forces and the modeling

techniques of nonlinear spring elements representing the soil-pile interaction are discussed in detail.

A number of codes allow the use of special pile-to-pile-cap connections, namely structural fuses, for the purpose of improving the connection and hence the structural ductility. The application of such fuses is very difficult due to erection problems at site. A new and easily applicable structural fuse system in the form of a tension fuse at the pile-to-cap beam connection (Harn, 2004) is particularly investigated in this study to demonstrate the feasibility of such fuses.

Previous studies on post-yield behavior of pile supported marine structures, evolution of seismic guidelines and codes from force-based design methods to deformation-based design methods have been covered in Chapter 2 of the thesis.

Identification of marine structures with structural characteristics and definition of structural elements are presented in Chapter 3 and Chapter 4. Structural modeling and design aspects of pile supported marine structures are explained in Chapter 5. Alternative designs incorporating seismic isolation, use of structural fuse systems and identification of seismic input with inelastic analysis techniques are presented in Chapter 6 and 7.

The results obtained from extensive non-linear pushover and nonlinear time-history analyses performed on generic pier structures supported on batter piles are given in Chapter 8. The results of 3-Dimesional nonlinear pushover and inelastic response history analyses performed on wharf structures are given in Chapter 9. Finally design recommendations based on nonlinear analysis results are discussed in Chapter 10.

2. LITERATURE REVIEW

Till the end of the 20th century marine structures much like building structures were designed with force-based design methods to withstand the seismic forces reduced by response modification factors or to a force equal to a fraction of the total weight of the structure.

Early design approaches were based on elastic seismic design forces and the structures were designed to resist these forces with batter piles only. After the damaging earthquakes in 90's new guidelines such as ASCE TCLEE (1998) and US Navy Seismic Design Guidelines (1997) were compiled, which mainly discussed the ductile detailing errors in piles or pile to pile-cap connections and discouraged the use of batter piles in high seismic zones due to poor performance of those piles in recent earthquakes. The design was still advised to be done with force-based design methods with explicitly defined response modification factors. A two-level design approach is introduced in these guidelines where the structures were expected to remain undamaged or experience minor damage in a frequent earthquake and no collapse in a design earthquake.

Technical Standards for Ports, Harbor Facilities in Japan (1999) have provided a similar dual level design approach, but the analysis is performed with a nonlinear pushover analysis with specified ductility limits for different classes of structures. Also strain limits are defined for steel piles based on their wall-thickness-to-diameter ratio.

The first and most comprehensive publication written to provide the seismic design guidelines with displacement based design methods is the Seismic Criteria for California Marine Oil Terminals (1999) by Ferrito *et al*. This document discusses the main sources of failure of pile supported structures in past earthquakes and provides a detailed guideline of a displacement-based design approach for pile supported marine structures.

This guideline discouraged the use of batter piles in high seismic zones, but contrary to other guidelines it provided a strain-based damage criterion for multiple performance levels and discouraged the use of force-based design methods. Seismic Design Guidelines

for Port Structures (Balkema, 2001) is based on a similar approach with detailed information about structural modeling and nonlinear static analysis procedure to be used for design.

A seismic design code was subsequently written for port structures in Los Angeles Port, POLA (2002), which followed the footsteps of the above-mentioned guidelines and forbidden the use of batter piles. It also provided a displacement based design methodology with similar damage criteria to the pile elements and their connections.

Another recent code written in California is MOTEMS (2007), which provided a displacement-based design approach like POLA (2002) for marine oil terminals, but contrary to the others it allowed the use of batter piles either with detailed analysis that reflects the effects of post-yield behavior of batter piles or with the use of structural fuses, in which case such batter piles are called “special batter piles”.

Technical Standards for Ports, Harbor Facilities, Railroads, and Airports in Turkey (2007) provided a new approach with both deformation-based and force-based design methods. As in the previously cited codes, the new code defines performance through nonlinear strains as well as explicitly defined response modification factors.

The deformation-based design methods helped engineers to realize the post-yield or post-failure behavior of batter pile structures. Harn (2004) has been the first to mention about post-yield behavior of batter piles where he introduced the “pole vaulting effect” and warned engineering community about the possible design errors of force-based design methods in pile supported marine structures with batter piles. He concluded that the special nature of pile supported marine structures requires them to be designed by deformation-based methods.

Many design engineers following the poor performance of batter piles in the 90’s looked for advanced solution to the problems associated to the use of batter piles. Zmuda *et al* (1995) have shown that seismic isolation is feasible for marine structures and provided a deck isolated wharf through a series of sliding isolators and displacement restrainers. Later an analytical study about the feasibility of seismic isolation is carried out in Seismic

Criteria for California Marine Oil Terminals (1999) and concluded that, with a separated fender system from the deck, such applications were feasible.

Another advance solution was offered by Johnson et al (1998), providing a special seismic fuse connection to limit the forces transmitted to the batter piles. Harn (2004) encouraged the use of batter piles with structural fuses and provided a detailed design algorithm for the tension fuses. He also concluded that, with the use of such fuses structures, with batter piles could be as ductile as structures with vertical piles only and more efficient in resisting non-seismic lateral loads, such as berthing, mooring, etc. due to stiffer nature of batter piles.

Seismic Criteria for California Marine Oil Terminals (1999) studied the effect of soil flexibility and pile-soil interaction through a series of horizontal and vertical nonlinear springs defined per API recommendations (1994). Through a detailed study based on nonlinear response history analysis, it concluded that such a modeling technique can be used for batter piles. Subsequent seismic design criteria and codes such as MOTEMS (2007) have allowed the use of nonlinear soil spring models indicating that such an analysis should be performed with upper and lower bound limits of soil parameters.

3. IDENTIFICATION OF PILE SUPPORTED MARINE STRUCTURES

With the introduction of container concept in 1956, marine structures have evolved exponentially, which made port facilities an extremely important source for transportation. These facilities can be classified into two major categories. Those providing a fully closed structure on the seaward face of the structure and those with an open structure profile. Fully closed structure is consisted of either steel sheet bulkheads or concrete caisson units positioned on a foundation bed of dense gravel and crushed stone. Open structures are those with a deck supported by piles. Since the subject of this study is the pile supported marine structures, only open structures will be mentioned in the following.

3.1. Types of Pile Supported Marine Structures

There are two major types of pile supported marine facilities, namely, wharfs and piers (or jetties).

3.1.1. Wharfs

A wharf is a marine structure for berthing vessels, which is constructed parallel to the shore-line. It is generally constructed with a wall or a sheet-pile to retain the soil pressure and dredging in front of the structure to create sufficient water depth for the vessel. There are two types of open wharf structures mainly related to their platform level:

I) The low level pile supported platforms: Those platforms have short length precast concrete or steel sheet pile cut-off wall located in-shore edge of the platform. The pile supported platform structure then extends from the face of the cut-off wall to the seaward face of the wharf. The lateral stability can be provided by the use of batter piles or by a number of tie-rod systems. The fill material on top of platform provides the dead weight to ensure that the vertical piles are not subjected to significant tension forces due to the uplift component of the batter piles. Such a system is illustrated in Figure 3.1.

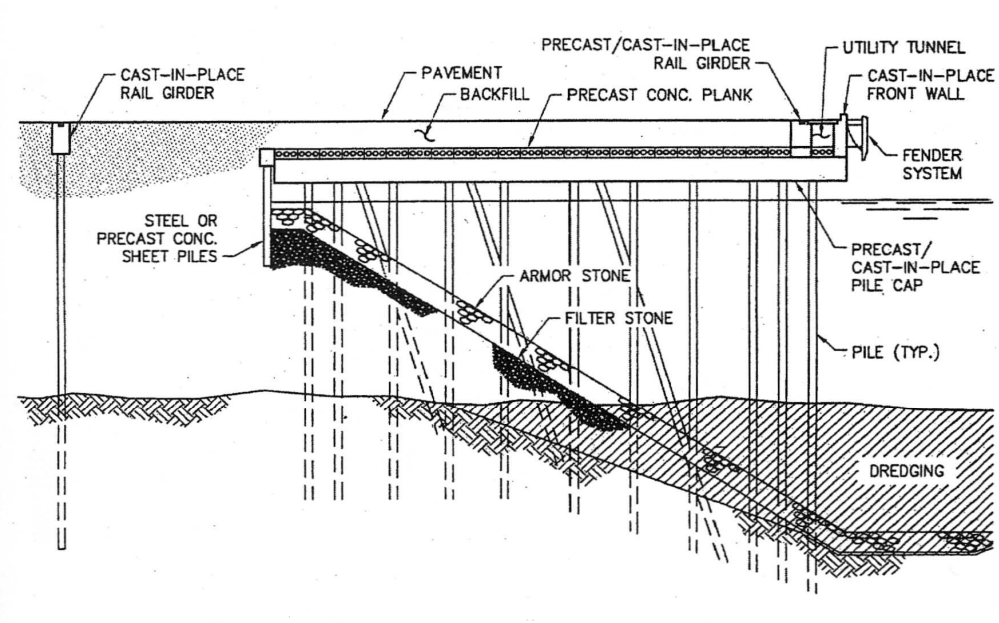

Figure 3.1. Wharf with low platform supported by a combination of batter and vertical piles (Port Engineering, 2004)

II) The high level pile supported platforms: The width of the deck in these platforms can be increased backward and the under-deck slope is extended to meet the deck slab, which eliminates most of the soil pressure or a precast retaining wall can be used to resist the soil pressure that permits the use of vertical piles only. This type of wharfs with high level decks is usually preferred in high seismic areas due to their relatively light weight (compared to low level platforms) and their relatively flexible nature (compared to batter piles systems). Figure 3.2 illustrates an example of this type.

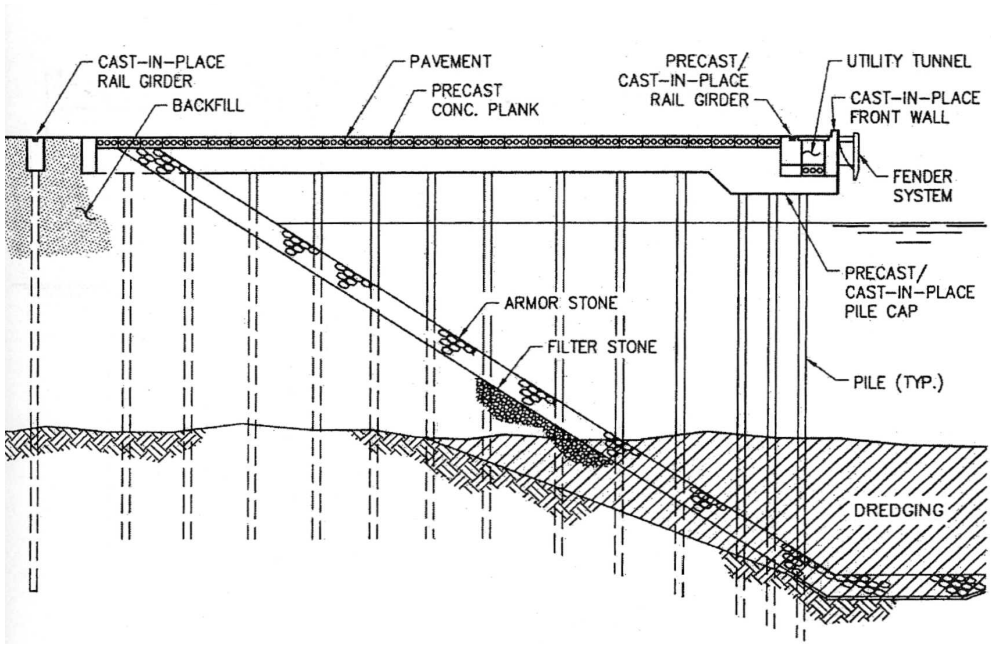

Figure 3.2. Wharf with high level platform supported by all vertical piles (Port Engineering, 2004)

3.1.2. Piers (Jetties)

A pier is a shore connected marine structure for berthing vessels which may be of several types of configuration and in principle categorized as finger, T head and L shaped. A finger pier (jetty) is generally oriented more or less perpendicular to the shore line and usually provides two sided berthing. A T head pier is generally oriented essentially parallel to the shoreline with an access trestle that connects to the shore line at a point near center of the pier. It generally provides berthing only on the shoreline side but can provide two sided berthing if the T head is of sufficient length. An L shaped pier is similar to T head pier but access trestle connects one end of the pier to the shoreline and both sides of the pier may readily be used for berthing. Figure 3.3 illustrates each category.

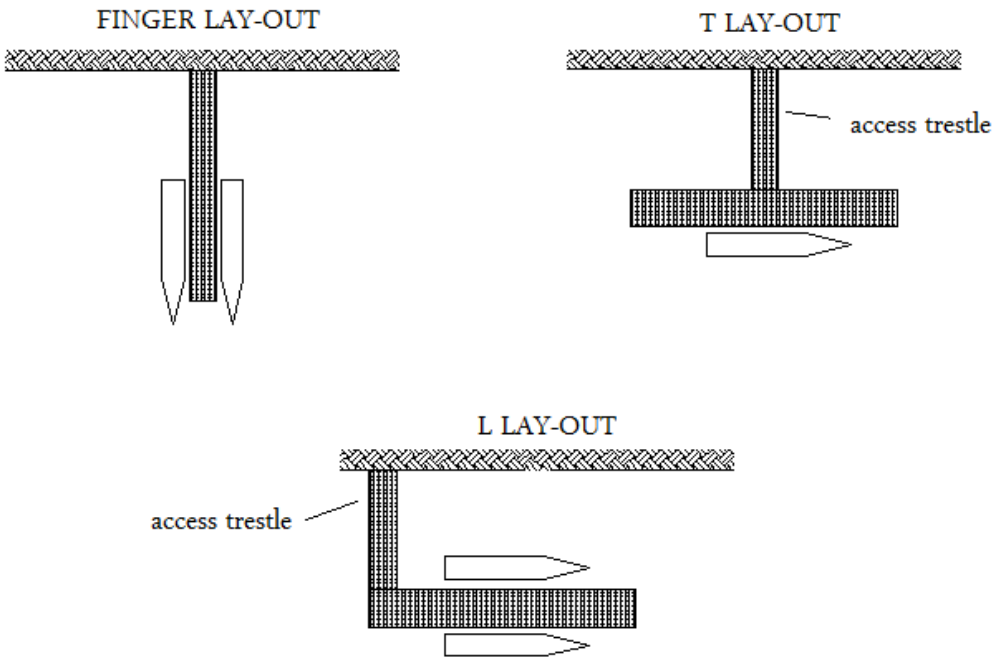

Figure 3.3. Types of pier lay-out

Even though piers can also be designed as closed structures, in practice most of them are designed as open structures. Open piers supported on piles are categorized as those supported by vertical piles only, those supported by a combination of vertical and batter piles and those supported by batter piles only. Figures 3.4 to 3.6 illustrate each of these categories.

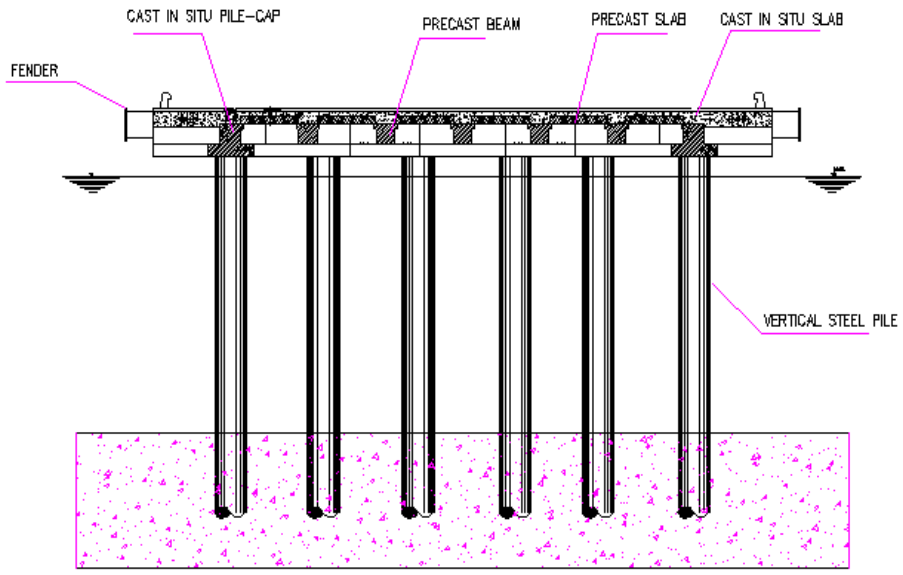

Figure 3.4. Pier with all vertical piles

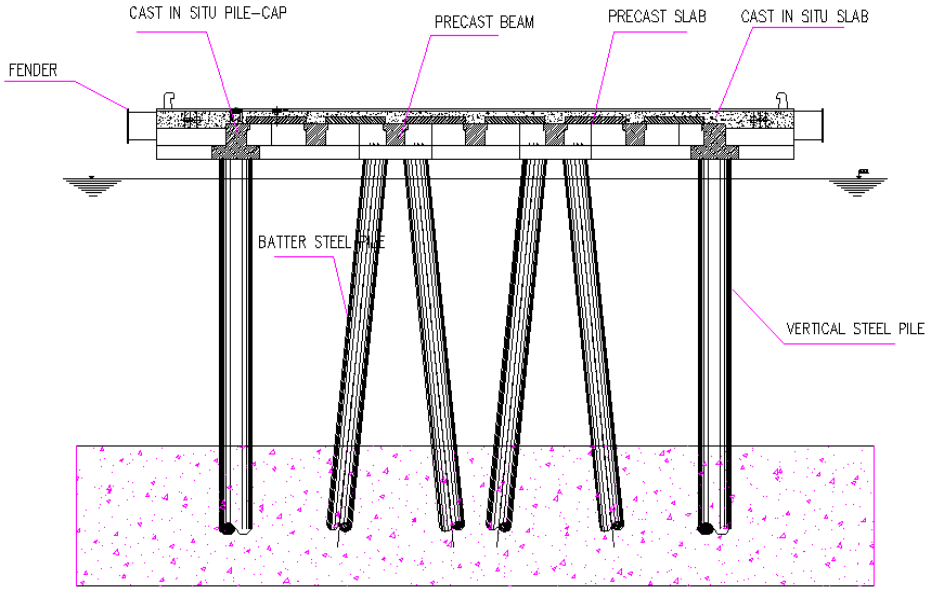

Figure 3.5. Pier with a combination of batter and vertical piles

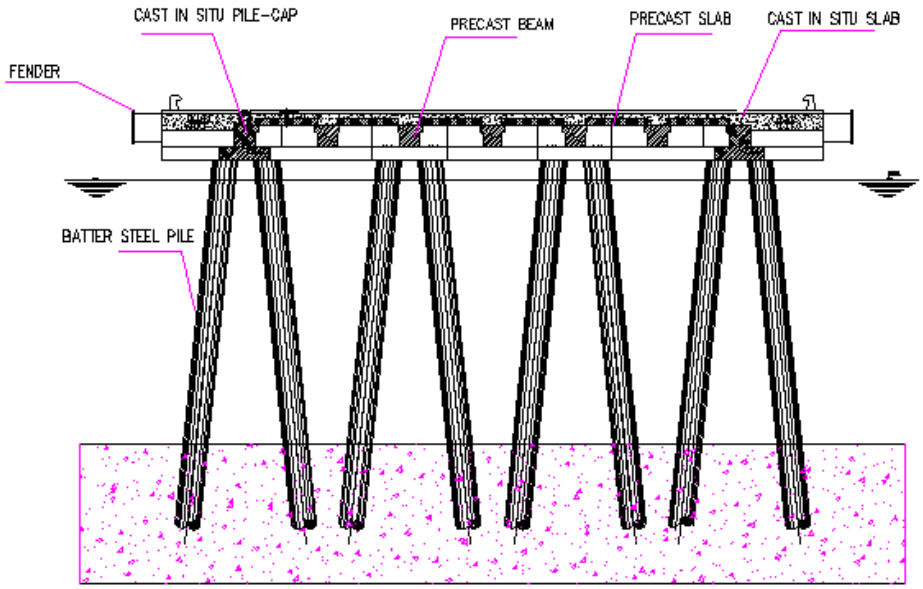

Figure 3.6. Pier with all batter piles

3.2. Earthquake Induced Damage to of Pile Supported Marine Structures

In general seismic response of pile supported marine structures is influenced by complex soil-structure interaction effects during an earthquake. Expected failures in pile supported marine structures are due to heavy lateral pressure from backfill, liquefaction, localized ground movement, or failures due to inertia forces. The major failure modes are presented in Figure 3.7 to 3.9. Some of the observed damages in recent earthquakes in Turkey and around the world related to pile supported marine structures are summarized in Table 3.1.

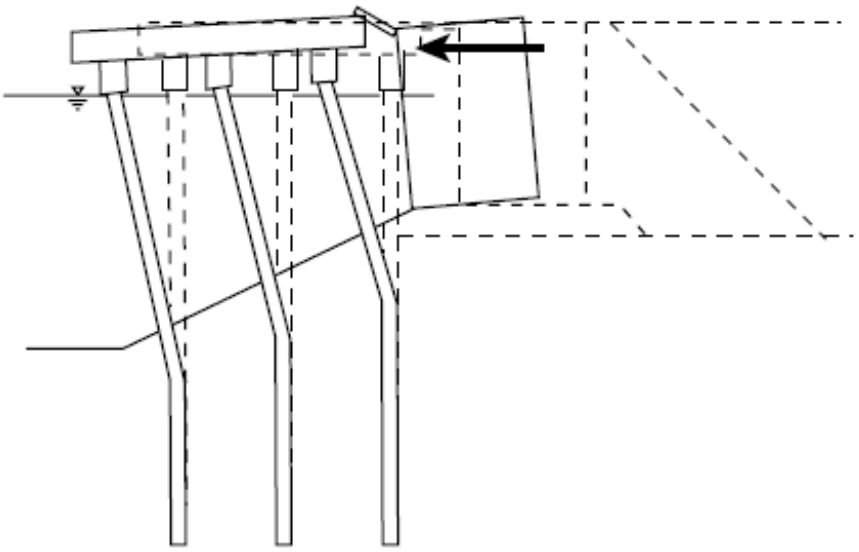

Figure 3.7. Damage due to heavy lateral pressure from backfill (Balkema , 2001)

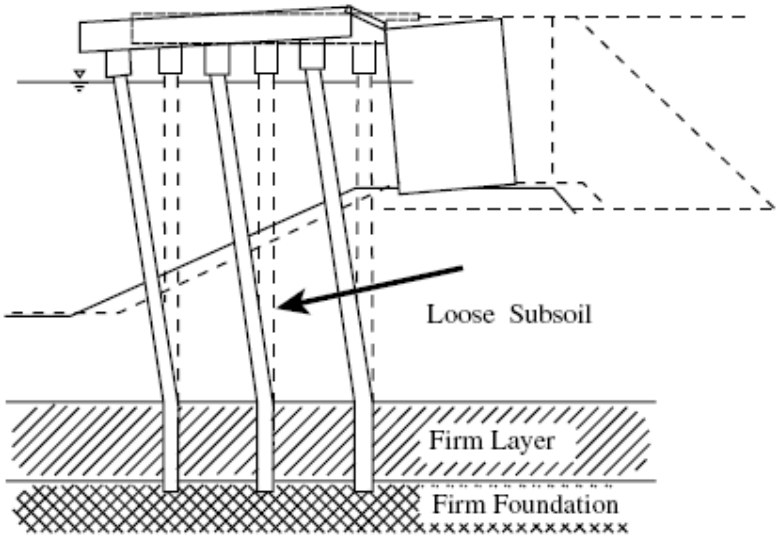

Figure 3.8. Damage due to localized ground movement (Balkema, 2001)

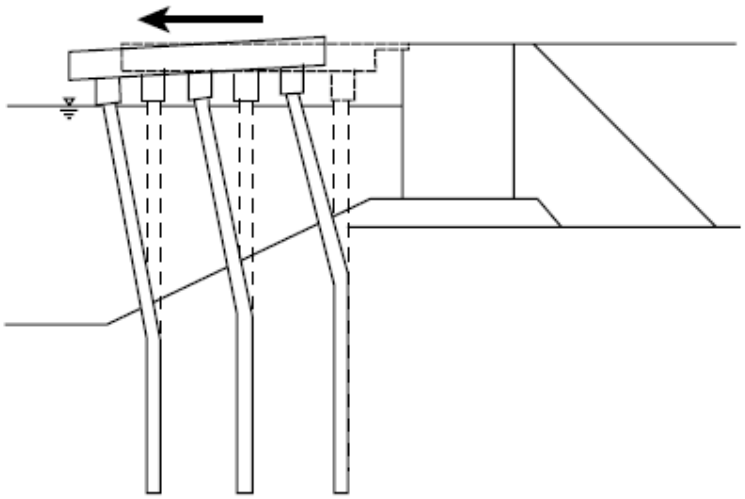

Figure 3.9. Damage due to inertia forces (Balkema, 2001)

Table 3.1. Damage to pile supported marine facilities

Structure	Earthquake	Structural System	Damage	Cause	Ref
7th Street Terminal Wharf	Loma Prieta (1989)	Pile supported Wharf	Tensile failure at top of most batter piles	**B**	Balkema,2001
Goverment Pier No 1	Luzon,Phillippines (1990)	Pile Supported Pier	Extensive opening in pier deck, cracks and chipping at pile cap	A,B	Balkema,2001
B 127 , APL Terminal	Northridge (1994)	Pile Supported Wharf	Pull-out of batter piles at pile cap	D	Balkema,2001
Takahama Wharf	Kobe (1995)	Pile Supported Wharf	Buckling of steel piles at pile cap and below ground level	C	Balkema,2001
Sumiyohimama District	Kobe (1995)	Pile Supported Dolphin	Buckling of Steel Piles, Excessive Lateral deformation	C,D	Balkema,2001
Almirante Port	Costa Rica (1991)	Pile supported Pier	Concrete piled bents severely damaged at railroad trestle, and severe damage to concrete pier	D	Ferrito, 1999
Petkim(Yarimca Petrochemical Complex)	Golcük (1999)	Pile supported Pier	Extensive damage to reinforced concrete batter piles above the water surface due to inadequate shear reinforcing .	D	Boulanger, 2000
Tupras Refinery	Golcük (1999)	Pile supported Pier	Steel piles were buckled at/above the water surface.	C,D	Boulanger, 2000
Shell Oil Piers	Golcük (1999)	Pile supported Pier	The piers were extensively damaged and largely collapsed below water.	*	Boulanger, 2000
Klor Alkali	Golcük (1999)	Pile supported Pier	The pier largely collapsed below water	B	Boulanger, 2000
Transturk	Golcük (1999)	Pile supported Pier	One of the piers largely collapsed below water.	*	Boulanger, 2000
UM Shipyard	Golcük (1999)	Pile supported Pier	The pier was completely damaged and collapsed .	B	Boulanger, 2000
Golcuk Naval Base	Golcük (1999)	Pile supported Pier	Extensive damage due to surface rupture and ground failure, or a combination of both		Boulanger, 2000
Aksa Piers	Golcük (1999	Pile supported Pier	Severe displacement and collapse in piers	D	Boulanger, 2000
Petrol Ofisi	Golcük (1999	Pile supported Pier	The pier was tilted and displaced laterally (away from the new one),	D	Boulanger, 2000

A: Large lateral pressure from backfill B: Liquefaction C: Localized ground movement D: Inertia Forces

* No information

4. STRUCTURAL CHARACTERISTICS AND COMPONENTS

Structural components of pile supported marine structures mainly consist of the following:

a) Prestressed or steel pipe piles as vertical and lateral load carrying elements,

b) Pile-caps as the elements transferring vertical and horizontal loads from the deck to the piles,

c) The deck as the vertical load carrying and in-plane lateral load transferring unit and,

d) Pile-to-pile-cap connections.

4.1. Piles

Piles are the single most important structural elements in marine structures. They carry not only the gravity loads, but at the same time they are major seismic lateral load resisting elements, which are allowed to undergo significant plastic deformations.

4.1.1. Types of Piles

With respect to their construction method, piles are classified mainly into two groups, namely, driven piles and cast-in-situ piles. Driven piles are consisted of precast concrete piles, steel piles, timber piles and composite piles. Cast-in-situ-piles are all reinforced concrete piles. The classification is given in Figure 4.1 where certain types of composite piles are also indicated.

4.1.1.1. Driven piles. Driven piles are the most frequently used piles in marine structures. These types of piles are often constructed in factory in large amounts and have the advantage of shortening the construction period. Driven piles are classified based on their material: Precast concrete piles, steel piles and composite piles.

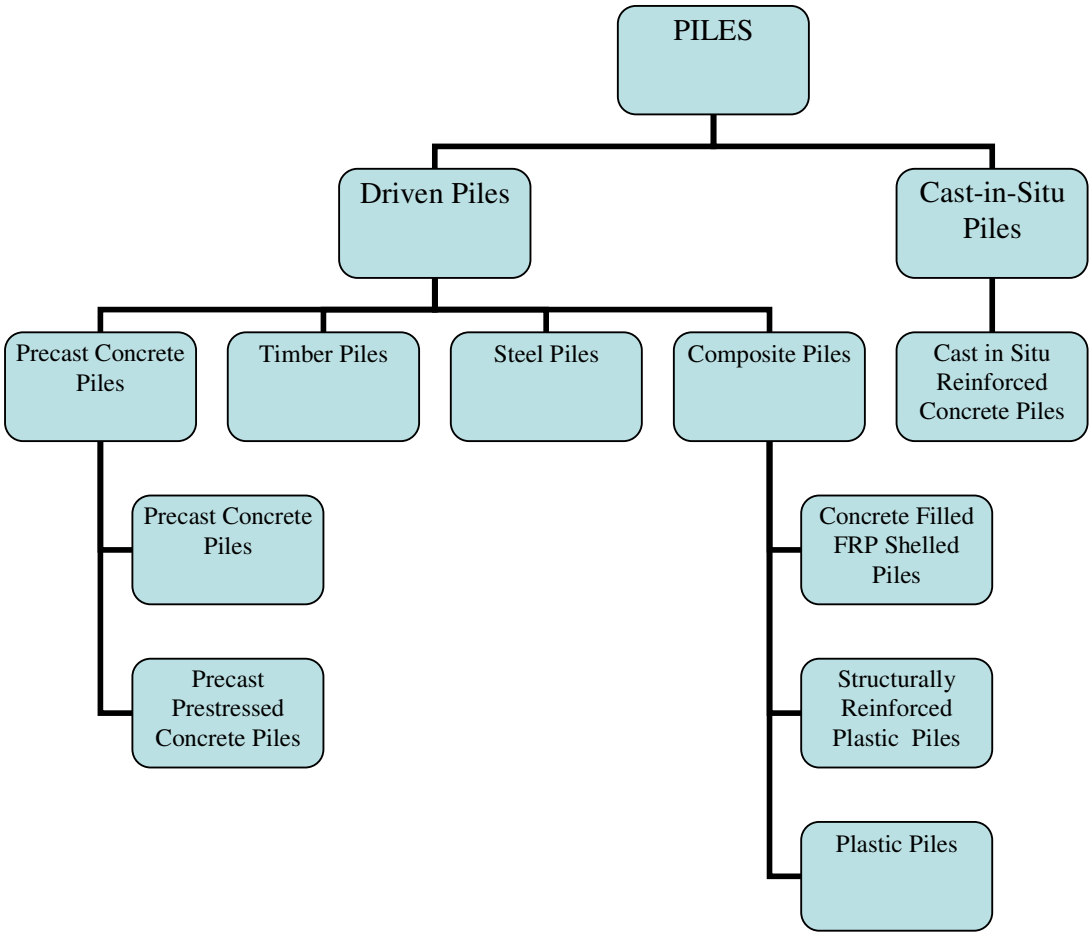

Figure 4.1. Classification of pile types

4.1.1.1.1. Precast concrete piles. Piles in this category are formed in a central casting yard to the specified length, cured, and then shipped to the construction site. If space is available and a sufficient quantity of piles needed, a casting yard may be provided at the site to reduce transportation costs. Precast piles can either produced by using ordinary reinforcement as in Figure 4.2 or they may be prestressed as in Figure 4.3. Precast piles using ordinary reinforcement are designed to resist bending stresses during lifting and transportation to the site in addition to design loading.

Precast concrete piles have their principal use in marine and river structures where the savings in cost due to the rapidity of driving achieved may outweigh the cost of other alternatives. Even though precast prestressed concrete piles are more common in marine

structure practice there are rare occasions where precast reinforced concrete piles have been used.

Precast concrete piles with ordinary reinforced concrete are usually square or hexagonal and of solid cross-section for units of short or moderate length, but for saving weight long piles are usually manufactured with a hollow interior in hexagonal, octagonal or circular sections. The interiors of the piles can be filled with concrete after driving. This is necessary to avoid bursting where piles are exposed to severe frost action.

Ordinary reinforced concrete pile is likely to be preferred for a project requiring a fairly small number of piles, where the cost of establishing a production line for prestressing work on site is not justifiable and where the site is too far from an established factory to allow the economical transportation of prestressed units from the factory to the site. Ordinary reinforced precast piles should be designed with a 28-day cube strength no less than 40 MPa in marine environment.

Because of problems related to driving forces and durability, precast reinforced concrete piles are not preferred in current practice in marine structures.

Prestressed concrete piles require high-strength concrete (28-day cube strength of 40 MPa or more) and careful control during manufacture. Casting is usually carried out in a factory, where the curing conditions can be strictly regulated. Special manufacturing processes, such as compaction by spinning or autoclave curing, can be adopted to produce high strength concrete.

Precast prestressed concrete piles have the most extensive use in marine related structures especially in the USA. They are usually either of solid square or octagonal cross section or hollow cylindrical. The large octagonal or square piles are usually cast with hollow circular core to reduce weight.

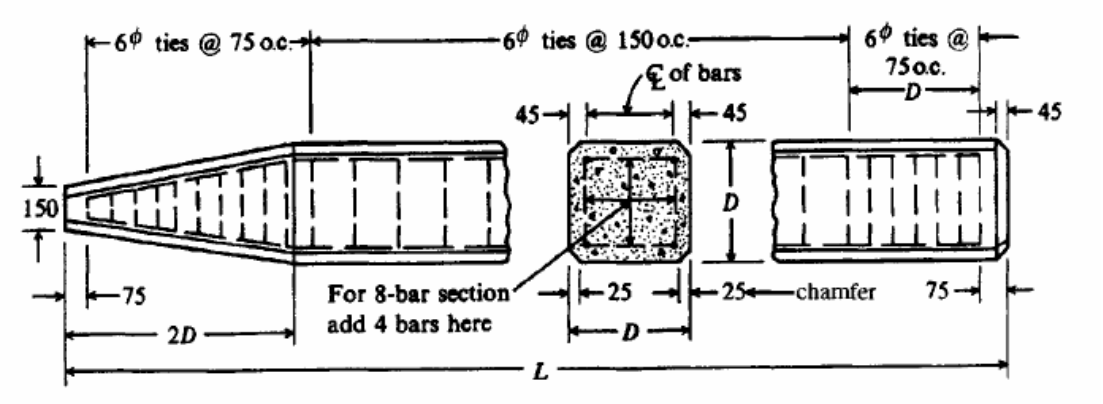

Figure 4.2. Precast concrete piles (Foundation analysis and design, 1997)

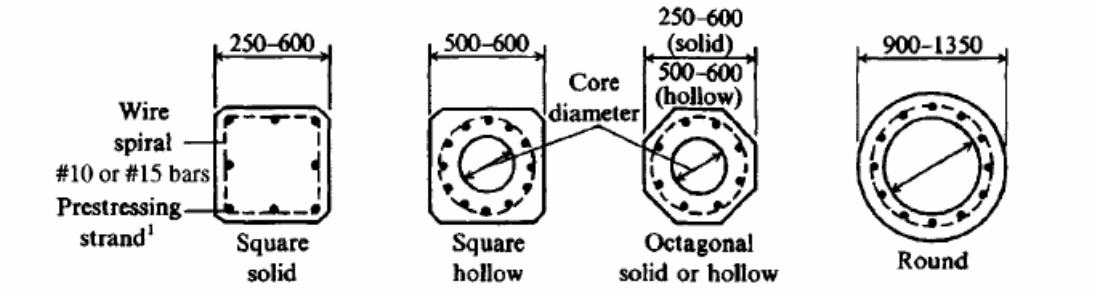

Figure 4.3. Precast prestressed concrete piles (Foundation analysis and design, 1997)

Precast prestressed concrete piles have many advantages when compared to other pile types:

- When compared to precast concrete piles, tensile stresses to be developed during driving can be better resisted and the pile is less likely to be damaged during handling. Bending stresses, which can occur during driving, are also less likely to produce cracking.
- This type of pile is generally less permeable than reinforced concrete piles and may be expected to exhibit superior performance in a marine environment.
- Compared to steel piles, handling and driving of prestressed concrete piles are relatively maintenance free even in severe marine environment.
- Material cost of the precast prestressed concrete piles is comparatively lower than for equivalent steel or composite piles.

The disadvantages of precast prestressed piles are:

- When compared to steel piles the major disadvantage of precast prestressed pile is its weight and its difficulty in splicing.
- In precast prestressed piles the ultimate strength in axial compression decreases as the level of prestressing increases. Therefore, prestressed piles are more vulnerable to damage from striking obstructions during driving.
- They are also difficult to cut after installation, and special techniques have to be employed. They are most suitable for applications where the pile length is predictable and constant.

Even though precast concrete piles are extensively used in many countries their design and construction practice in Turkey is limited and therefore they are not preferred in marine structures.

4.1.1.1.2. Timber piles. Timber piles are not used in modern design practice and therefore are not explained.

4.1.1.1.3. Steel piles. Steel piles are fabricated either in H section or pipe section. Pipe sections are usually preferred to minimize the surface area exposed to corrosion and eliminate corners where the coatings are thin and subjected to damage. H sections are avoided in marine environments unless there is a compelling reason to use. Typical sections are illustrated in Figure 4.4.

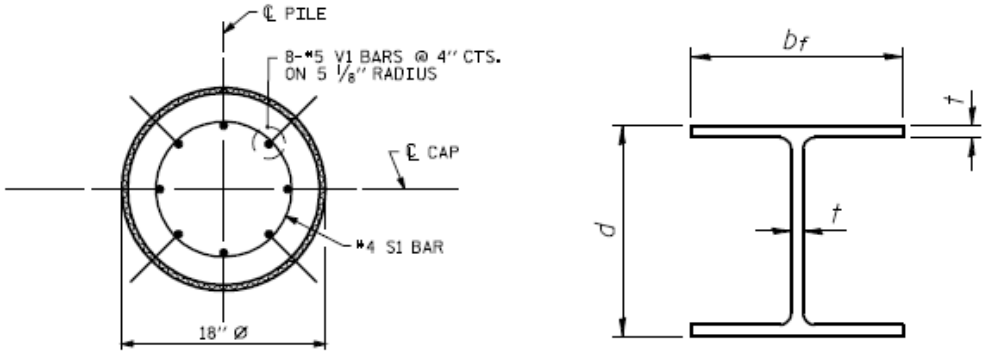

Figure 4.4. Typical section of steel piles

The steel pipe piles are driven either closed ended or open ended. When driven open ended an internal soil plug will develop once the internal skin friction exceeds the end bearing of the plug. When a plug is fully developed an open ended pile has the same capacity as a closed ended pile however, the base resistance of open-end piles can be low in loose to medium dense granular soils. Excessive penetration depth can be avoided by welding H- or T-sections to the circumference.

Hollow steel piles may be driven closed-ended through cohesive soil containing cobbles and small boulders, but heave is then more likely to occur. This pile type performs well in resisting impact and bending loads, and large-diameter sections can be used to carry considerable loads. This has led to their extensive use for marine structures, where long, unsupported pile elements are commonly used at large water depth.

The piles can be manufactured of material with different strength properties: the upper part and the lower section in mild steel, and the center section in high tensile steel. Thus the more expensive high tensile steel is used in the highly stressed zone close to the sea bed.

Most of the closed ended piles and some of the open ended piles are filled with concrete after they are driven in to the ground mostly to protect steel piles from corrosion and sometimes to improve its strength and stability. If there is enough friction between the

pile and the fill concrete these piles can be classified as composite piles. These piles are built with or with out mild steel. A typical section of each type is illustrated in Figure 4.5.

Since piles are expected to undergo plastic deformations during earthquakes steel piles in marine structures, like steel bridge piers, should be designed with compact sections to ensure stability in the post yield zone. Although detailed definitions and limitations exists in both building and bridge design codes, most of the marine structure codes have not prevented the use of non-compact sections. Such definitions exist in Technical Standards for Ports, Harbor Facilities, Railroads, and Airports in Turkey (2007), The Standards for Ports and Harbor Facilities of Japan (1999) and API (1994) recommendations.

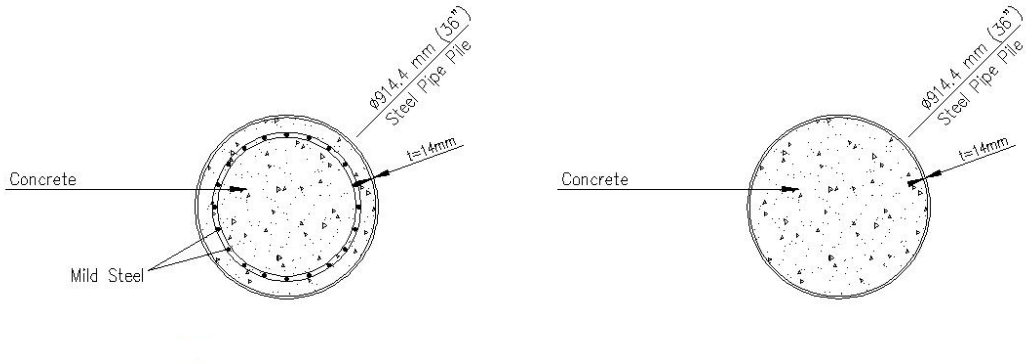

Figure 4.5. Concrete-filled steel piles

Technical Standards for Ports, Harbor Facilities, Railroads, and Airports in Turkey (2007) have limited the diameter-to-wall-thickness ratio of steel piles to

$$\frac{D}{t} \leq 0.08 \frac{E_s}{\sigma_y} \tag{4.1}$$

where D is the diameter , t is the wall thickness of the section, E_s is modulus of elasticity of steel and σ_y is the yield strength of steel. Piles with smaller diameter-to-wall-thickness ratio is accepted to be compact and allowed to yield. Piles with higher diameter-to-wall-thickness ratio are accepted to be non-compact and forbidden to be used as seismic load resisting elements.

The Standards for Ports and Harbor Facilities of Japan (1999) have limited diameter-to-wall-thickness ratio of steel piles to

$$R_t = \frac{D}{2t}\frac{\sigma_y}{E}\sqrt{3(1-\nu^2)} \le 0.08 \tag{4.2}$$

where R_t is the diameter-to-wall-thickness ratio defined by the Japanese specification and ν is the Poisson's ratio.

The same code also limits the allowable ductility of the pile and the maximum allowable strain of a steel pile based on section depth to thickness ratio with following relationships

$$\mu_a = 1.25 + 62.5(t/D) \le 2.5 \tag{4.3}$$

$$\varepsilon_{max} = 0.44t/D \tag{4.4}$$

where μ_a is the allowable ductility of the pile and, ε_{max} is the maximum (allowable) strain.

API recommendations (1994) have given empirical formulae to evaluate the inelastic buckling stress of a steel pile for both bending and axial compression. For axial compression, steel piles with a diameter-to-wall-thickness ratio smaller than 60 is accepted to be compact and inelastic buckling stress is equated to yield stress of the pile. For piles with diameter-to-wall-thickness ratio more than 60, the inelastic buckling stress is evaluated with the following empirical formula:

$$F_{xc} = F_y\left[1.64 - 0.23(D/t)^{0.25}\right] \tag{4.5}$$

where F_{xc} is the inelastic local buckling stress, F_y is the yield stress of steel and D/t is the diameter-to-wall-thickness ratio of the section.

In building codes such as EN-1993 the steel sections are classified into 4 groups based on their diameter-to-wall-thickness ratio:

i. Class 1 cross-sections are those which can form a plastic hinge with the rotation capacity required from plastic analysis without reduction of the resistance.
ii. Class 2 cross-sections are those which can develop their plastic moment resistance, but have limited rotation capacity because of local buckling.
iii. Class 3 cross-sections are those in which the stress in the extreme compression fibre of the steel member assuming an elastic distribution of stresses can reach the yield strength, but local buckling is liable to prevent development of the plastic moment resistance.
iv. Class 4 cross-sections are those in which local buckling will occur before the attainment of yield stress in one or more parts of the cross-section.

In EN-1993 the diameter-to-thickness ratio for each group is limited by

$$D/t = 50\varepsilon^2 \tag{4.6}$$

$$D/t = 70\varepsilon^2 \tag{4.7}$$

$$D/t = 90\varepsilon^2 \tag{4.8}$$

$$\varepsilon = \sqrt{235/F_y} \tag{4.9}$$

where a steel section with a diameter-to-wall-thickness ratio value below Equation 4.6 is classified as class 1, values between Equation 4.6 and 4.7 is classified as class 2, values between Equation 4.7 and 4.8 is classified as class 3 and any value above Equation 4.8 is classified as class 4.

In the case of a concrete filled steel pile there are no limitations defined in marine structure codes but such limitations exists in building codes like EN-1993,AISC LRFD 1994 or CAN/CSA-S16.1-M94

In EN-1993 the diameter-to-thickness ratio is limited by

$$\frac{D}{t} \leq 90(235/F_y) \tag{4.10}$$

In AISC LRFD 1994 it is limited by

$$\frac{D}{t} \leq \sqrt{\frac{8E_s}{F_y}} \tag{4.11}$$

In CAN/CSA-S16.1-M94 it is limited by

$$\frac{D}{t} \leq \frac{28000}{F_y} \tag{4.12}$$

Steel piles and concrete filled steel piles have many advantages compared to other types of piles:

- When compared to precast concrete piles, steel piles are easier to handle and not subjected to cracking during handling or driving.
- They can be cut-off readily if they can not be driven to the anticipated tip elevation or they can be lengthened with a welded splice if driven to a greater embedment than anticipated.
- When driven open ended they cause relatively small soil displacements.
- They can withstand hard driving without the risk of damage.
- They can be driven to sloping bedrock without the risk of deviation or with little deviation.

The disadvantages of steel piles are:

- The major disadvantage of steel piles without concrete infill is their susceptibility to corrosion in marine environment therefore they are not as durable as prestressed concrete piles.
- Compared to precast concrete piles they are more expensive in terms of material cost.

4.1.1.1.4. Composite piles. Composite piles refer to alternative pile foundations composed of fiber reinforced polymers (FRPs), recycled plastics to support axial and/or lateral loads. These piles have been available in the North American market since the late 1980s; their use has been limited mainly to marine fender piles, load-bearing piles for light structures, and experimental test piles. Composite piles have not yet gained wide acceptance in the civil engineering industry, primarily due to the lack of a long track record of performance, and the scarcity of well-documented field load tests.

Several composite pile products are available in the market today, such as steel pipe core piles, structurally reinforced plastic matrix piles, concrete-filled FRP pipe piles, fiberglass pultruded piles, and plastic lumber piles. Of these five pile types, the first three are considered to be better suited for load-bearing applications. These three pile types are shown in Figure 4.6.

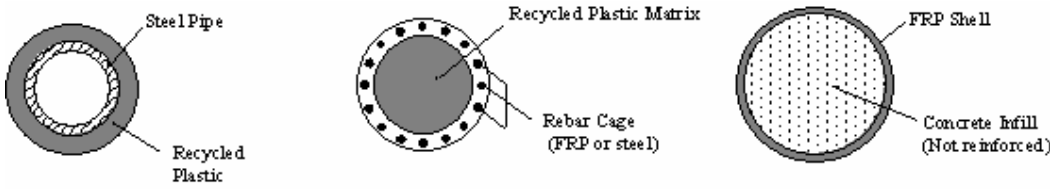

Figure 4.6. Typical composite section piles

Steel pipe core piles consist of a recycled plastic shell with a steel pipe core interior, as shown in Figure 4.6(a) the steel core provides the structural strength while the plastic shell protects the pile from degradation. The plastic shell can be omitted below the portion

of the pile exposed to water. If the plastic shell is used only in the upper portion of the pile that is exposed to water, the design procedure for this pile would be essentially the same as for a conventional steel pipe pile. The plastic shell does not come into play structurally, since its only function is to protect the steel pipe along the exposed portion of the pile.

Structurally reinforced plastic matrix piles consist of a recycled plastic matrix structurally reinforced with FRP rods or a welded steel rebar cage. The typical configuration of this type of pile is shown in Figure 4.6(b).

Concrete-filled FRP composite piles have two main structural components: an FRP shell or tube, and a concrete infill without steel reinforcement. The FRP shell provides, among other things, a stay-in-place concrete form, confinement to the concrete, tensile reinforcement, and corrosion protection. The concrete infill provides compressive load capacity.

Hardcore piles can be installed by driving the empty FRP shell and then filling it with concrete, although they are also installed by filling with concrete and then driving after the concrete has cured.

The composite piles are most advantages in harsh marine environments where traditional pile materials like steel, concrete and timber have limited service life. Potential disadvantage of these piles is their cost and low pile driving efficiency. Also piles with a composite exterior have low friction capacity therefore most suitable to end bearing piles.

4.1.1.2. Cast-in-situ concrete piles. Cast-in-situ reinforced concrete piles are rarely used in marine structures. They can be constructed almost in any reasonable size and in most soils. They are usually installed by the use of steel casing and mainly preferred in locations where pile driving noise or vibration can not be tolerated. Sometimes steel casing is left with the pile, when there is enough shear friction between the steel shell and the concrete they work as a composite pile. These types of piles are called Cast in Shelled Steel Piles. Figure 4.8 illustrates both bare reinforced concrete and steel shelled piles.

Cast in place reinforced concrete piles are comparatively cheaper than the precast concrete or steel piles but the issue of quality control and longer construction time at site puts them second to precast concrete or steel piles in design.

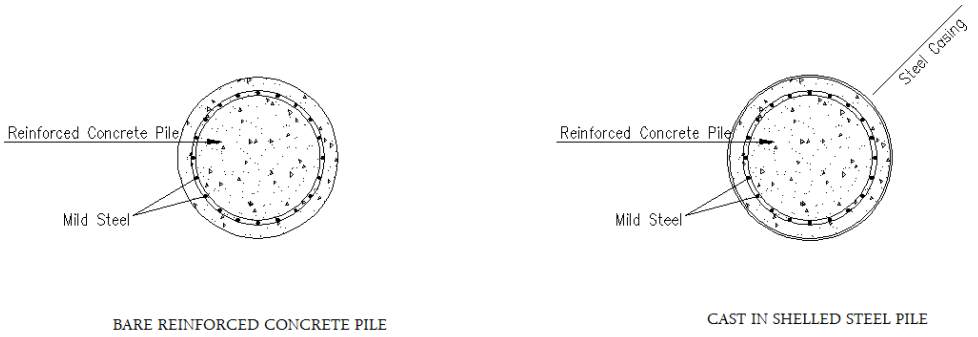

Figure 4.7. Cast-in-place reinforced concrete piles

4.1.2. Pile Arrangements

Pile arrangement in pile supported marine structures is the first step to take before starting any design. Most of the times the arrangement is dictated by either site conditions or the magnitude of the design forces (both lateral and vertical) on the marine structure. A successful selection process is important both for economical and structural safety purposes.

The selection process includes both plan lay-out of the piles which is often dictated by the magnitude of the vertical loads and the geotechnical considerations and pile arrangement in section (vertical, batter or both) which is often dictated by the magnitude of the lateral loads like mooring, berthing, earthquake etc...

4.1.2.1. Pile arrangement in plan. The lay-out of piles in plan as stated above is mainly affected by the magnitude of the vertical loads and the geotechnical data. Typical pile lay-out in plan is given for wharfs and piers in the following figures.

Figure 4.8(a) is a typical wharf with vertical piles only, (b) is a wharf with a combination of vertical piles and landward batter piles and (c) is a wharf with a combination of vertical piles and seaward batter piles.

Figure 4.9(a) is a typical pier with vertical pile only, (b) is a pier with a combination of vertical and batter piles, (c) is a pier with batter piles only.

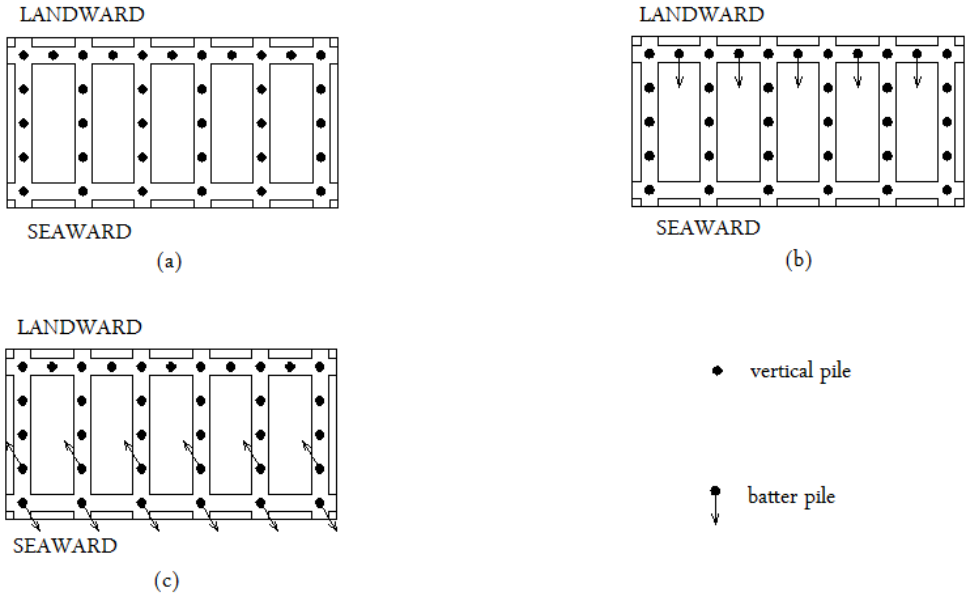

Figure 4.8. Typical wharf pile lay-out

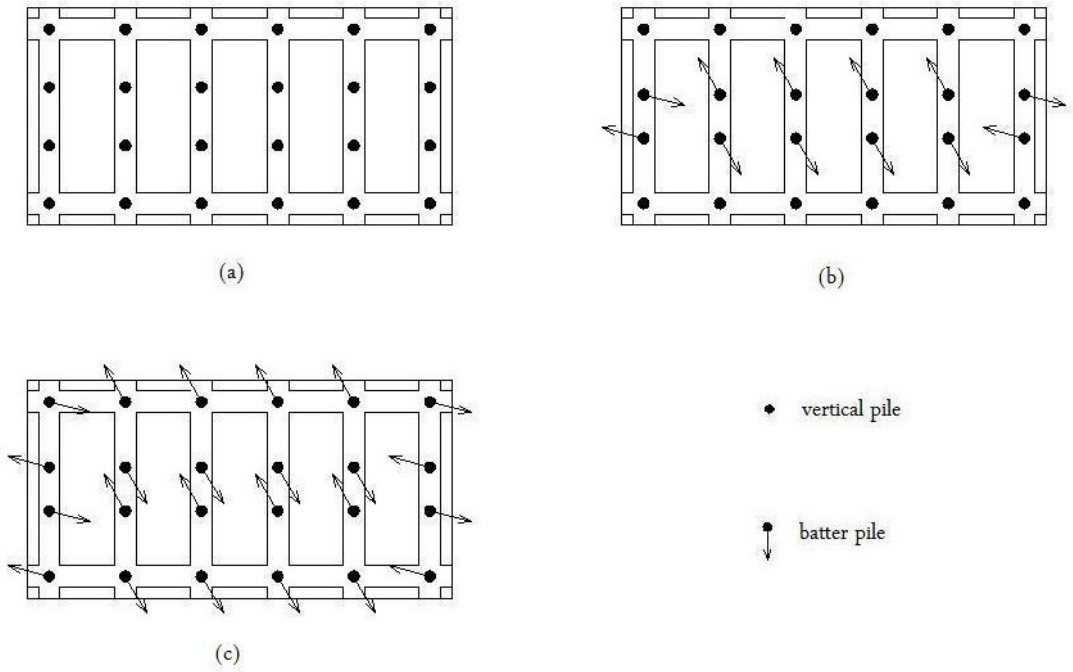

Figure 4.9. Typical pier pile lay-out

4.1.2.2. Pile arrangement in section. Piles in marine structures arranged either as vertical or inclined or both according to the magnitude of the lateral forces such as berthing, mooring or earthquakes. Piles driven vertically are called vertical or plumb piles, piles driven with an inclination angle are called batter or raked piles.

4.1.2.2.1. Vertical piles. Vertical piles are piles that resist lateral loads through bending and shear. Until the early 70's vertical piles remained as vertical load carrying elements mostly due to poor bending capacity of more common types of piles and the difficulties in analyzing vertical piles subjected to lateral loads.

The increased popularity of large diameter drilled piers for bridge foundations in early 70's led to the development of reliable procedures for the design and construction of vertical piles, including the development of p-y analyses for design of piles.

However popular use of vertical piles as lateral load resisting systems was not until the poor performance of batter piles in the 90's. Most of the design codes and guidelines

written after these earthquakes have forbidden the use of batter piles in marine structures which increased the use of vertical piles as lateral load carrying systems.

Vertical piles performed comparatively well compared to batter piles in recent earthquakes. Marine structures with vertical piles showed better performance than the ones with batter piles in similar locations. This is mainly due to their ability to sustain higher plastic deformations.

4.1.2.2.2. Batter piles. Driven piles on an angle are called batter or raked piles. Batter piles carry lateral loads primarily in axial compression and/or tension. Until the 1990s, batter piles were a common means for carrying lateral loads, particularly when the lateral loads were substantial and there was a large unsupported length, or there were weak soils at the ground surface.

In the 1990s, following the poor performance of batter piles in a series of earthquakes, some engineers began advising against the use of batter piles. However, once the reason for the poor performance of batter piles was understood, engineers developed design strategies to address these problems. Some of these strategies included the use of structural fuses and proper detailing of connections, which has been a major source of failure in the past. Also with the introduction of deformation-based design methods in the mid 90's engineers have a better understanding of the post-yield behavior of batter piles which is much different from the elastic behavior.

Batter piles are in principle braces driven in to the ground. Due to their high driving forces and the simplicity of their connection such piles almost always have more capacity in compression than in tension. Per design axial capacity of the pile in tension or compression should be larger than the capacity of the soil or the connection, which means yielding is concentrated in the tension connection or the tensile force is limited by pile pullout in the soil (Harn, 2004).

In contrast, in concentric braces of buildings, compression brace buckles before the tension brace yields and the compression forces are carried by the columns. Consequently,

buildings move horizontally during earthquakes both in elastic and inelastic range as shown in Figure 4.10.

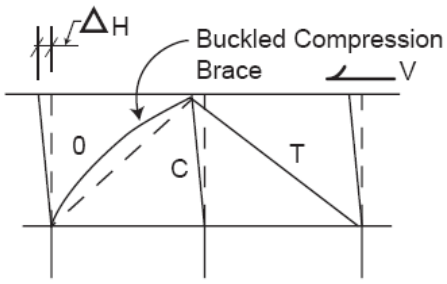

Figure 4.10. Building bracing system (Harn, 2004)

In a pier, once the tension batter piles 'fail,' or 'yield' by any means, including yielding of the connection or pullout in the soil, the structure will "pole vault" over the compression piles and the structure will move vertically as well as horizontally in an earthquake (Harn,2004), as shown in Figure 4.11. As the structure attempts to rise, large tension forces are developed in the remaining vertical piles as well as batter piles in the orthogonal direction, causing their connections to yield or fail.

If the earthquake demand is high enough, the dead load of the structure plus the tension forces in the yielded pile connections will be delivered to the compression piles. During this process, large compatibility forces may also be induced in the pile caps or deck system. These compatibility forces can be multiples of the evaluated elastic design forces with increased batter.

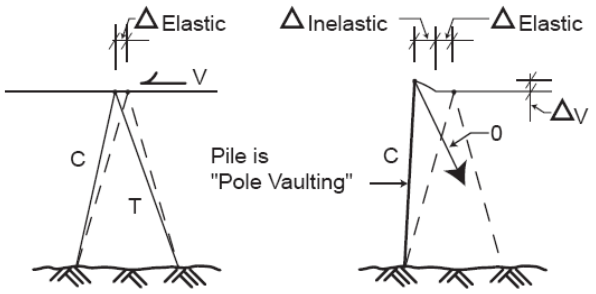

Figure 4.11. The pole vaulting phenomenon (Harn, 2004)

Pole vaulting can not be quantified unless an inelastic time history or inelastic pushover analysis is performed. Consequently, the use of force-based methods, where elastic forces are divided by a response modification factors to account for ductility in the system, will result in a structural behavior much different from what the designer intended.

4.2. Pile Caps

Pile-cap is the structural element that transfers the vertical and horizontal loads from the deck to the pile. There are generally three practical alternatives which are:

- Cast in place concrete pile caps.
- Precast concrete pile caps
- Precast/cast in place combined pile caps

4.2.1. Cast in Place Concrete Pile-Caps

Cast in place concrete pile caps are the most preferred type of pile caps used in practice mainly due to the fact that they are better in tolerating pile driving tolerances. They are formed either as inverted T or rectangular sections. A typical section is shown in Figure 4.12.

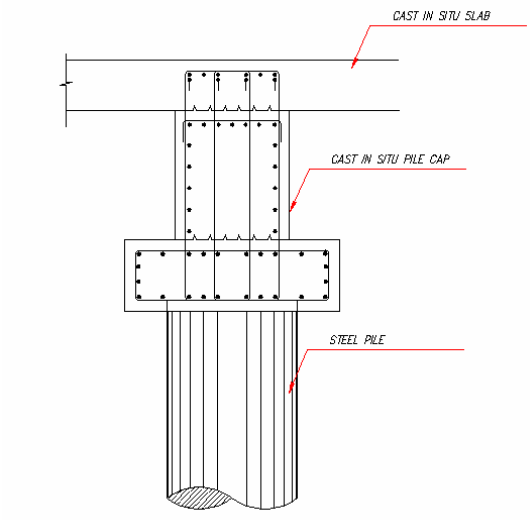

Figure 4.12. Cast-in-situ reinforced concrete pile-cap

4.2.2. Precast Concrete Pile-Caps

Precast concrete pile caps are used mainly to shorten construction time. They can be in any shape and size and when needed can be prestressed to improve the strength of the section. Their major advantage is that the precasting process provides better concrete curing and quality control ensuring consistent concrete cover, which provides a considerably durable structure in harsh marine environment. However they are extremely sensitive to pile driving tolerances which is why they are used in locations where small deviations are expected. A typical precast pile cap is shown in Figure 4.13.

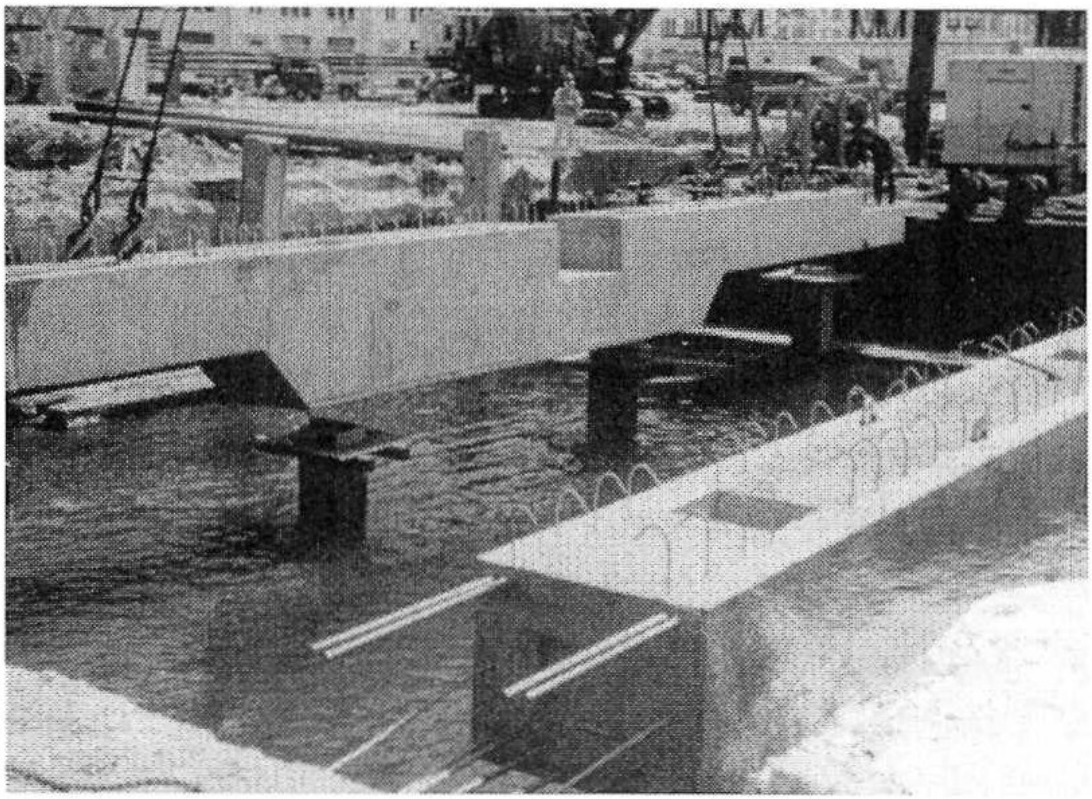

Figure 4.13. Precast concrete pile-cap (Port Engineering, 2004)

4.2.3. Precast /Cast in Place Concrete Pile-Caps

This type of pile caps are consisted of a U shaped precast shell filled with cast in place concrete. The major advantage of precast /cast in place pile cap is that they eliminate the costly formwork over water and they are durable against the adverse effects of sea

water. Casting in place to the interior of the pile cap reduces the lifting weight and permit simple connection between the pile and the pile cap. A typical precast /cast in place pile cap is shown in Figure 4.14.

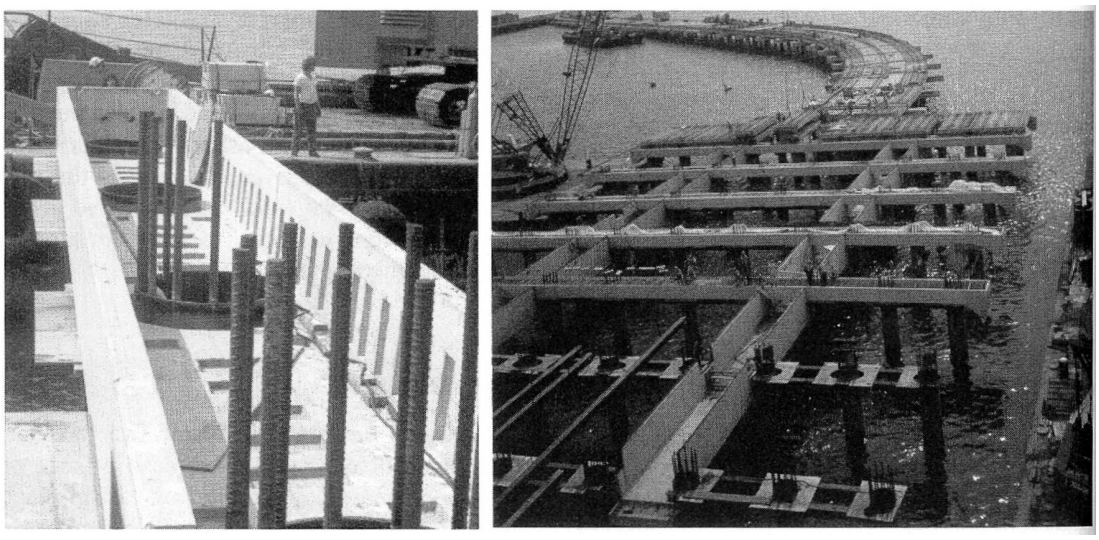

Figure 4.14. Precast /Cast in place concrete pile-cap (Port Engineering, 2004)

4.3. Decks

The decks in modern marine structures are constructed of concrete, either cast in place or precast, or some combination of cast in place and precast.

For cast in place concrete decks the design should be robust, featuring thick slabs with few, if any, beams or girders. Many modern cast in place concrete decks completely eliminate the use of pile caps, beams and girders, and are based on flat slab design principles.

The individual elements of precast concrete decks may be simple solid planks, prestressed or non prestressed or hollow elements of various configurations usually prestressed. Often times standard precast, prestressed concrete bridge deck sections may prove cost effective.

Probably the most widely used deck construction consists of precast concrete elements with a cast in place concrete topping. The cast in place topping distributes concentrated loads among adjacent individual precast elements and over the thinner portion of the hollow elements, ties the entire structure together and provides a convenient location for installing negative moment reinforcing steel to create continuous structure. Each type of deck is illustrated in Figure 4.15. The number of expansion joints should be kept to minimum because historically expansion joints have resulted in maintenance problems.

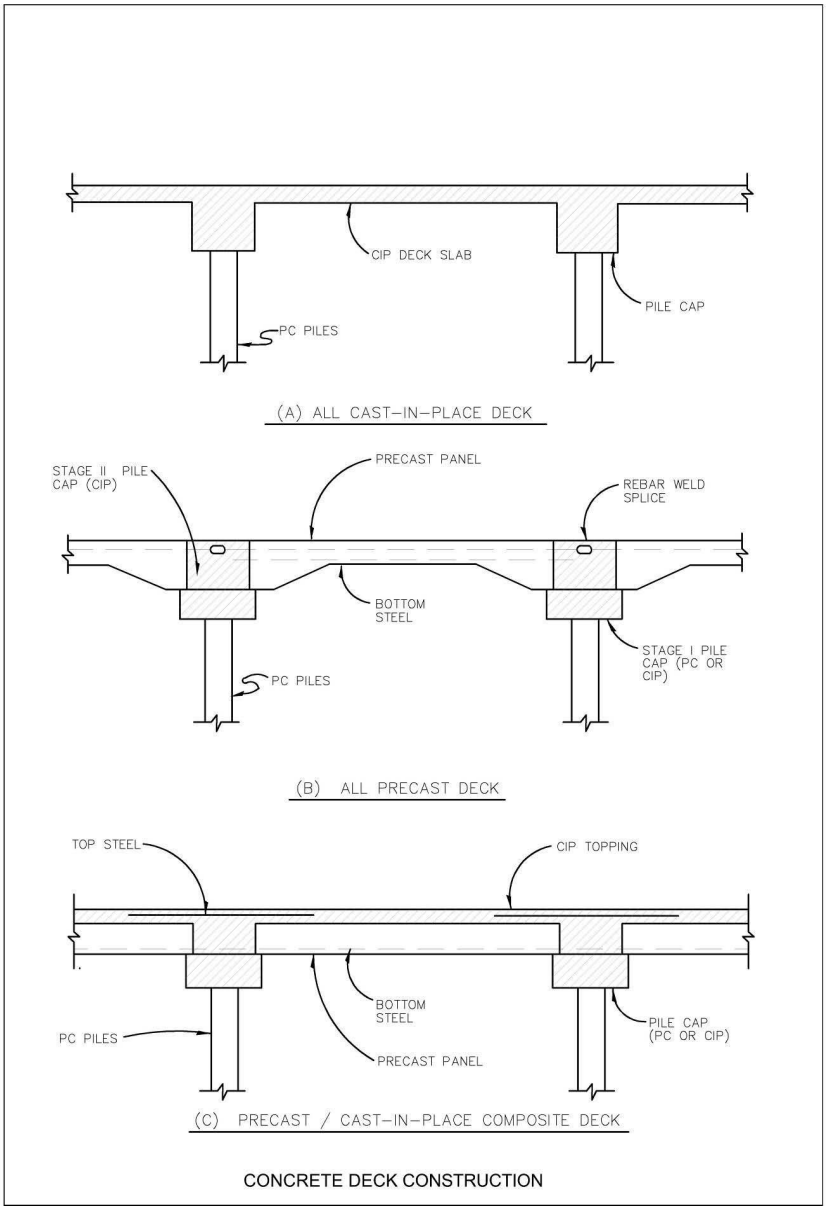

Figure 4.15. Concrete deck sections (UFC, 2005)

4.4. Pile-to-Deck or Pile-to-Pile-Cap Connections

The pile-pile cap/ deck connection is one of the most important structural elements since piles are the sole support for the large gravity loads, and they are also needed to assure the lateral stability of the structural system. If the piles or connections are unable to sustain the seismic movements, the piers or wharfs may collapse or lose the ability to perform their service function.

Detailing of the pile-pile cap/deck connection must be sufficient to develop necessary pile forces and to assure adequate inelastic deformation during large earthquakes. It is also desirable that the connection remains undamaged (other than minor flexural cracking) under small or moderate seismic events because it is necessary that the port remain in service under these conditions. Further, the connections are difficult to inspect and repair, and premature damage may go undetected (Roader, 2002).

Since modern construction practice uses steel and precast prestressed piles only steel pile and precast prestress pile connection will be discussed in this chapter. Variation of connection types to pile configuration (vertical or batter) will also be discussed in this chapter.

4.4.1. Steel Pile-to-Pile-Cap/Deck Connections

Steel pipe piles are normally connected to the pile-cap via reinforcing bars and a concrete plug. When the plug is only placed in the vicinity of the connection it has to be ensured that shear transfer exists between the concrete and the steel shell. This is often done by the use of a weld metal laid on the inside surface of the steel shell in a continuous spiral in the connection region. It has been found that this type of connections could achieve extremely large ductility and strength. An example of force-displacement hysteresis is shown in Figure 4.16. It can be observed that the flexural strength considerably exceeds the nominal strength denoted by H_{ACI}. This is partly a result of enhanced concrete strength resulting from very effective concrete confinement by the steel shell, and partly a result of steel shell acting as compression reinforcement by bearing against concrete pile cap. A typical detail is shown in Figure 4.17.

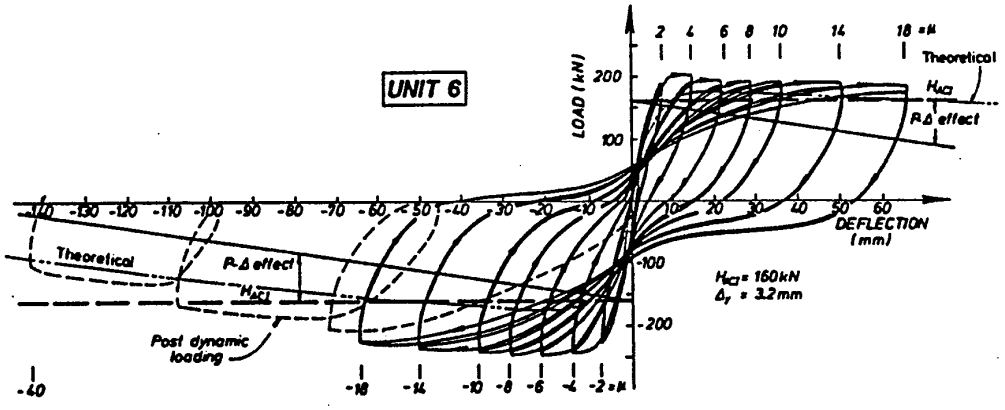

Figure 4.16. Hysteresis of a mild steel pipe to concrete pile-cap connection (Roader, 2002)

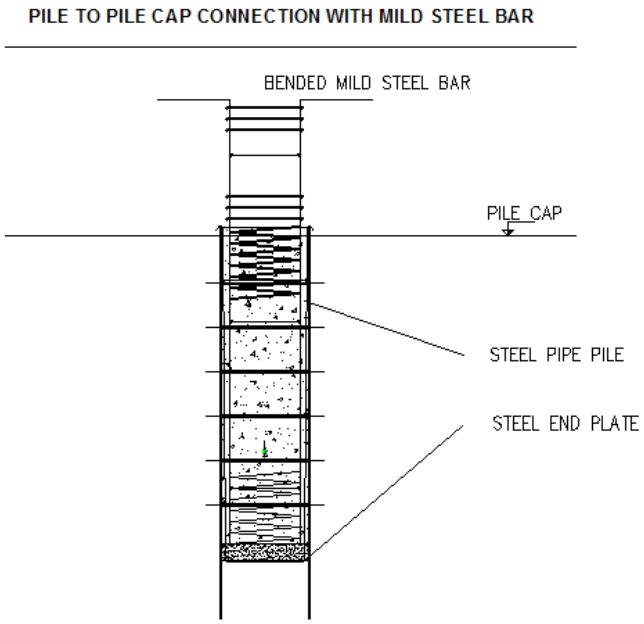

Figure 4.17. A typical mild steel connection to concrete pile-cap

There are also alternative connection details available for steel batter piles as shown in Figure 4.18 to Figure 4.20.

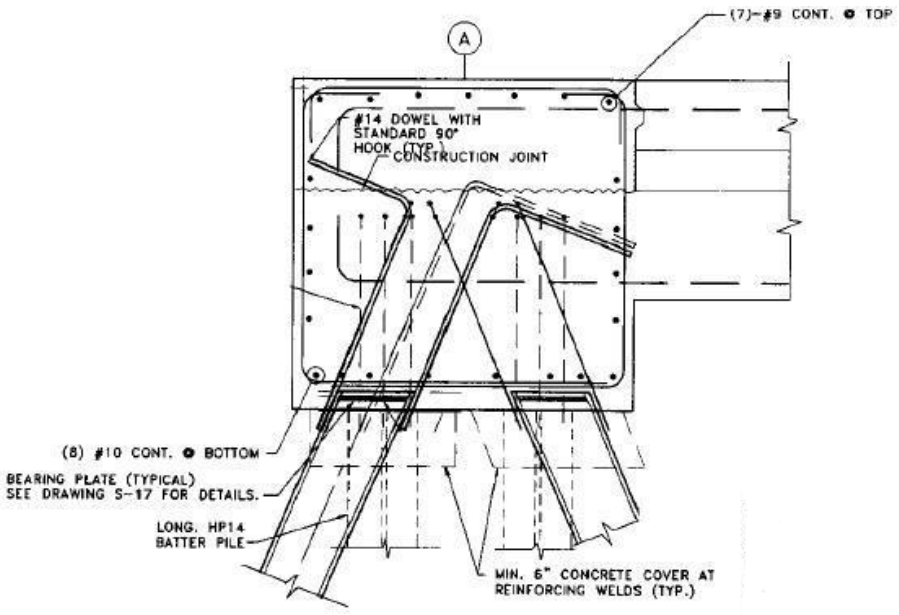

Figure 4.18. Alternative steel pile connections of a H-section pile (Roader, 2002)

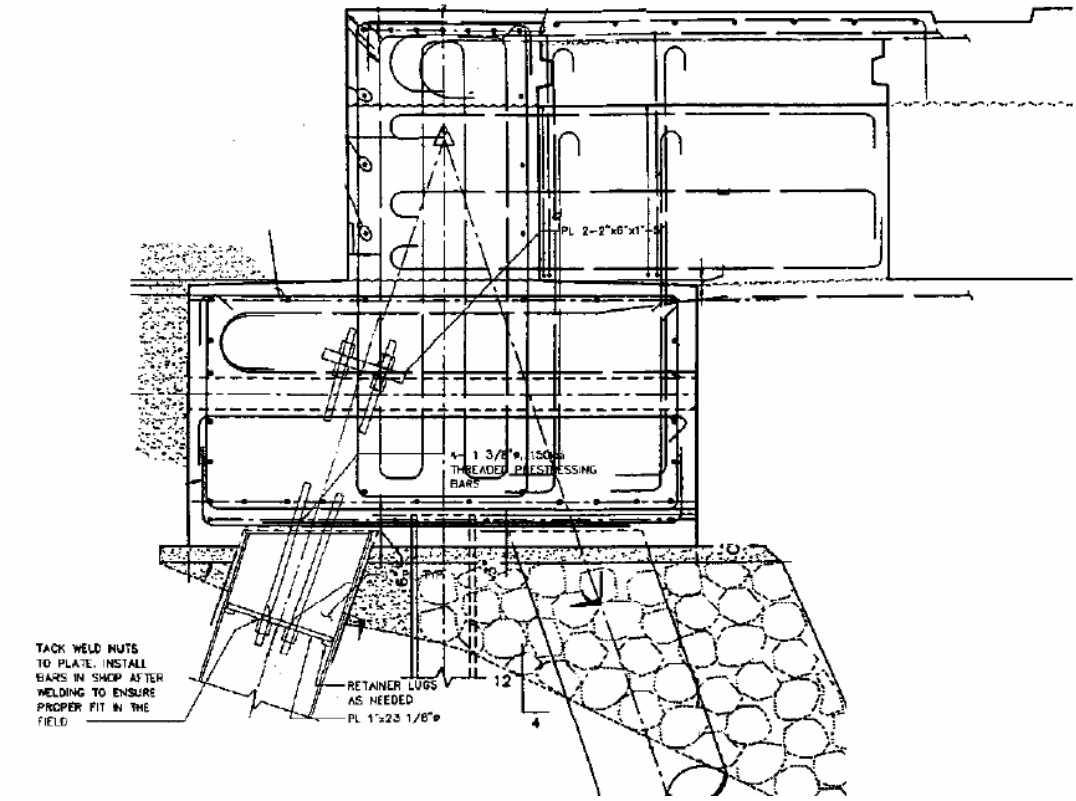

Figure 4.19. Alternative steel pile connections of a pipe-section pile (Roader, 2002)

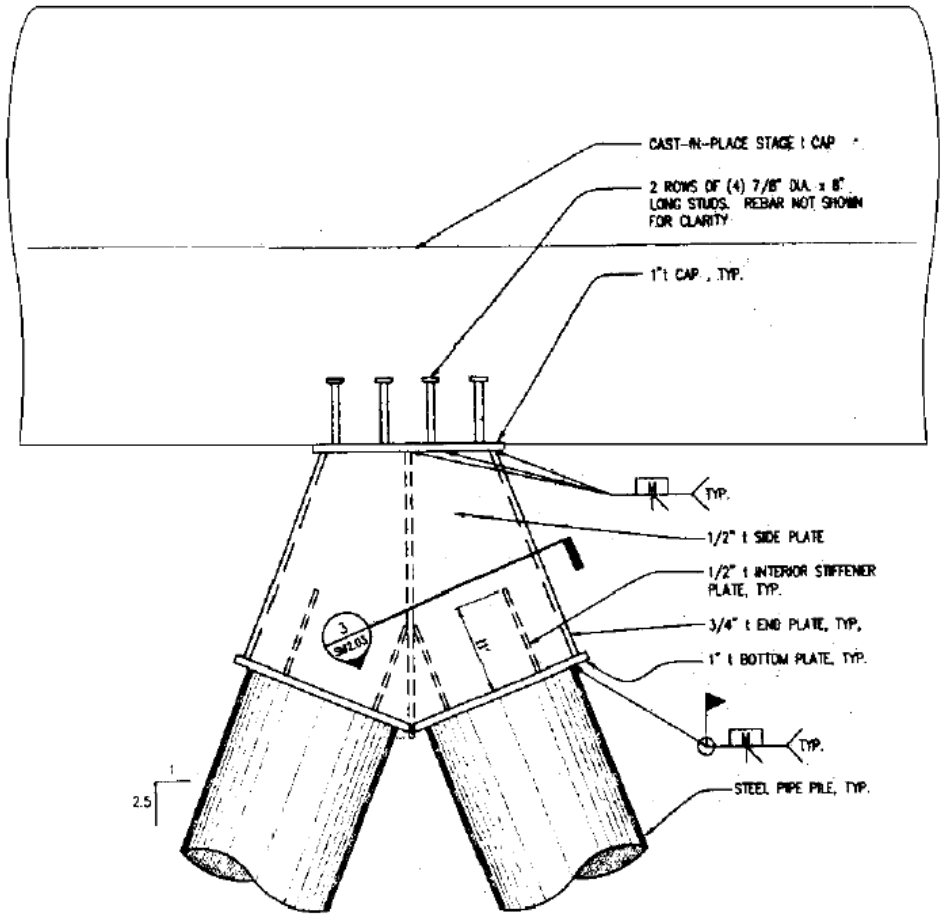

Figure 4.20. Alternative steel pile connections of a pipe-section pile with high inclination(Roader, 2002)

Figure 4.18 shows a detail where H-piles are embedded into the cap beam of the wharf deck. The H-pile has a cap plate to provide end bearing and a limited pullout cone for tensile resistance. However, the embedment length is relatively short. Eight dowel bars are welded to the pile flange and anchored into the concrete with a bent bar detail.

Figure 4.19 shows a relatively complex anchorage arrangement where the tubular steel pile is cast into the concrete wharf deck beams, and the pile bears on the concrete through an internal steel plate. The internal steel seat plate is anchored into the concrete wharf deck girder by high-strength steel bars for tensile resistance. Figure 4.20 shows another detail that utilizes shear connectors and bent bars to transfer the nominal shear force and resultant tensile force into the wharf deck. The pile connection directly balances the bulk of the axial pile force by direct connection of the two batter piles.

4.4.2. Precast Pile-to-Pile-Cap/Deck Connections

Precast piles with moment-resisting connections are commonly used in marine structures. There are three main configurations used for this purpose which are:

- Outward bend dowel connections.
- Inward bend dowel connections.
- Bond bar or T headed dowel bar connections.

Typical details of outward bend connection are illustrated in Figure 4.21 to Figure 4.23.

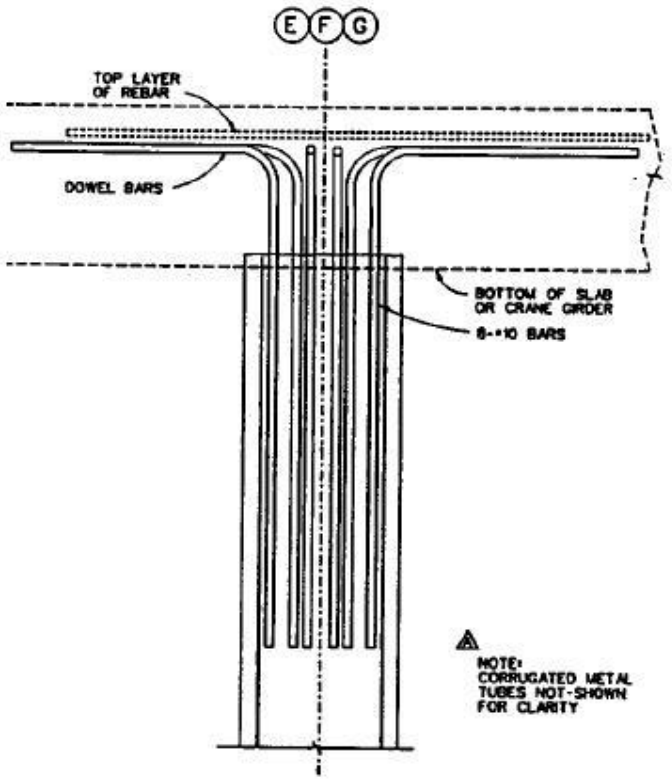

Figure 4.21. Typical prestressed concrete pile moment connections with outward bent dowel connection (Roader, 2002)

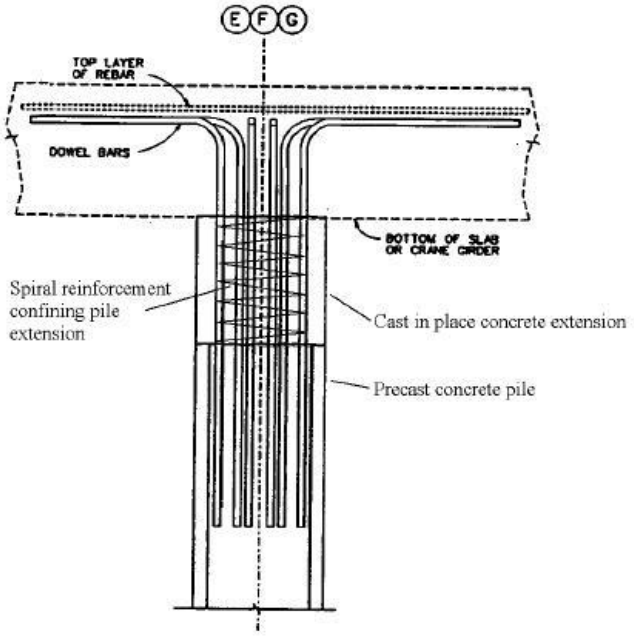

Figure 4.22. Typical prestressed concrete pile moment connections with extended outward bent dowel connection (Roader, 2002)

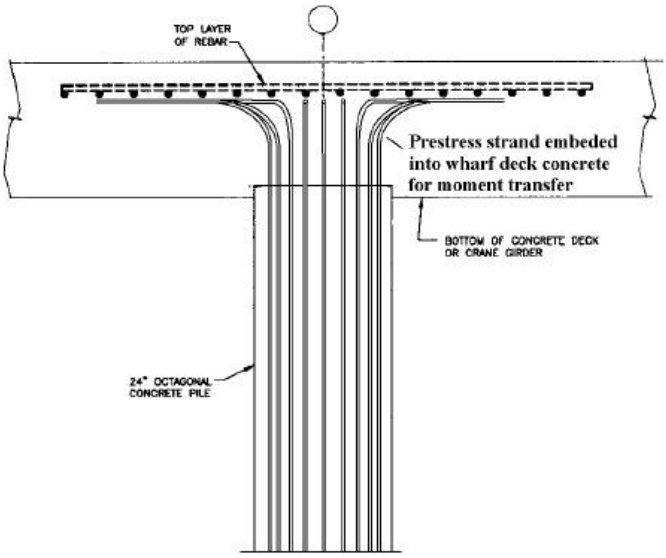

Figure 4.23. Typical prestressed concrete pile moment connections with extended strand connections (Roader, 2002)

Typical details of inward bend connection and bond bar and T headed dowel bar connection are illustrated in Figure 4.24 to Figure 4.26.

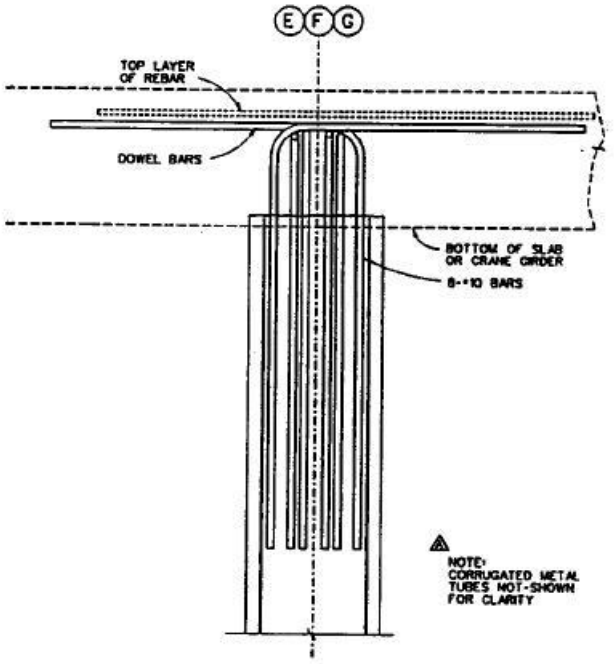

Figure 4.24. Typical prestressed concrete pile moment connections with inward bent dowel (Roader, 2002)

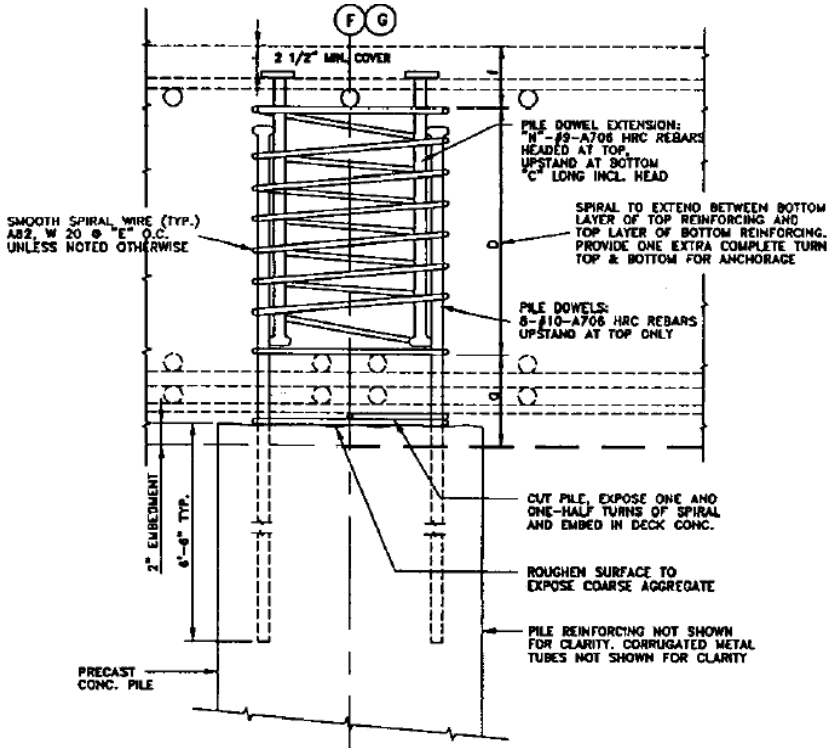

Figure 4.25. Typical prestressed concrete pile moment connections bond bar (Roader, 2002)

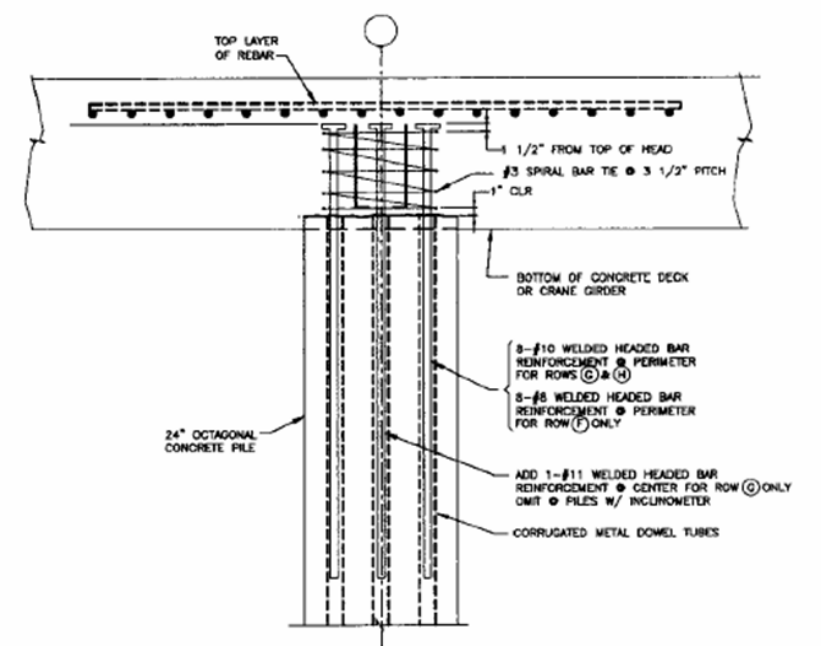

Figure 4.26. Typical prestressed concrete pile moment connections T-Headed dowel bar (Roader, 2002)

In addition, there are also pin connections available for hollow section pile. Such a connection detail is shown in Figure 4.27.

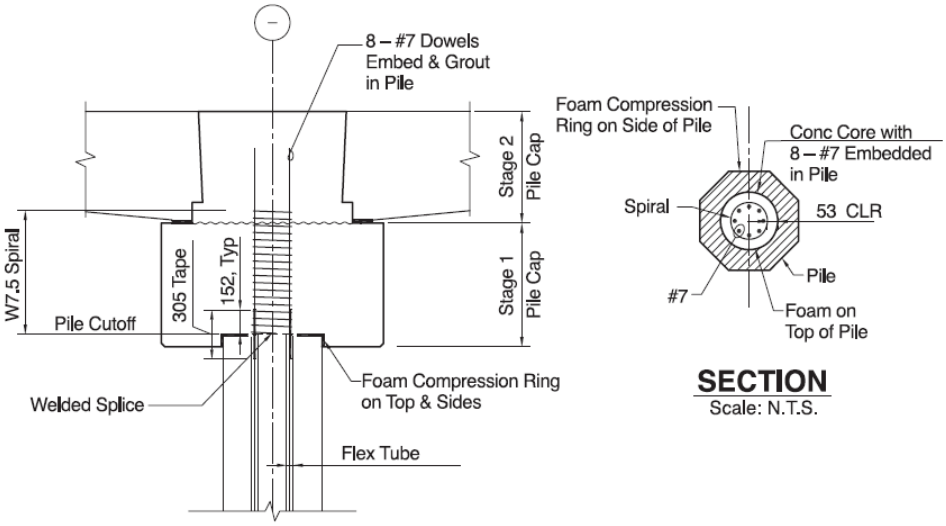

Figure 4.27. A typical pin connection for hallow section piles (Klusmeyer, 2004)

5. STRUCTURAL MODELING

As it is stated in Chapter 4, pile supported marine structures, *i.e*., wharves and jetties, are consisted of piles, pile-cap, deck, pile-to-pile-cap connections as structural elements. The structural modeling concepts of each will be explained in this chapter.

In general, a structural model should include the following:

- Soil structure-foundation system.
- Structural components and elements.
- P-Delta effects.
- Realistic representation of inelastic behavior.

5.1. Modeling of Deck

The decks of wharves and jetties, in principle, should remain elastic during an earthquake event since they carry high gravity loads as well as transfer lateral loads to the pile-caps. Typically they are modeled as rigid diaphragms with total mass and mass moment of inertia of the system assigned to the center of gravity of the structure.

5.2. Modeling of Pile-Caps and Piles

5.2.1. Modeling of Pile caps

Pile caps are also structural elements that have to stay elastic during an earthquake event. For this reason they are modeled as linear frame elements.

5.2.2. Modeling of Piles

Piles and the pile-to-pile-cap connections are the only structural elements that are allowed to experience substantial plastic deformation. For this reason great care should be

given to their structural modeling and modeling assumptions. The structural model above the soil level at pile-to-pile cap interface is shown in Figure 5.1.

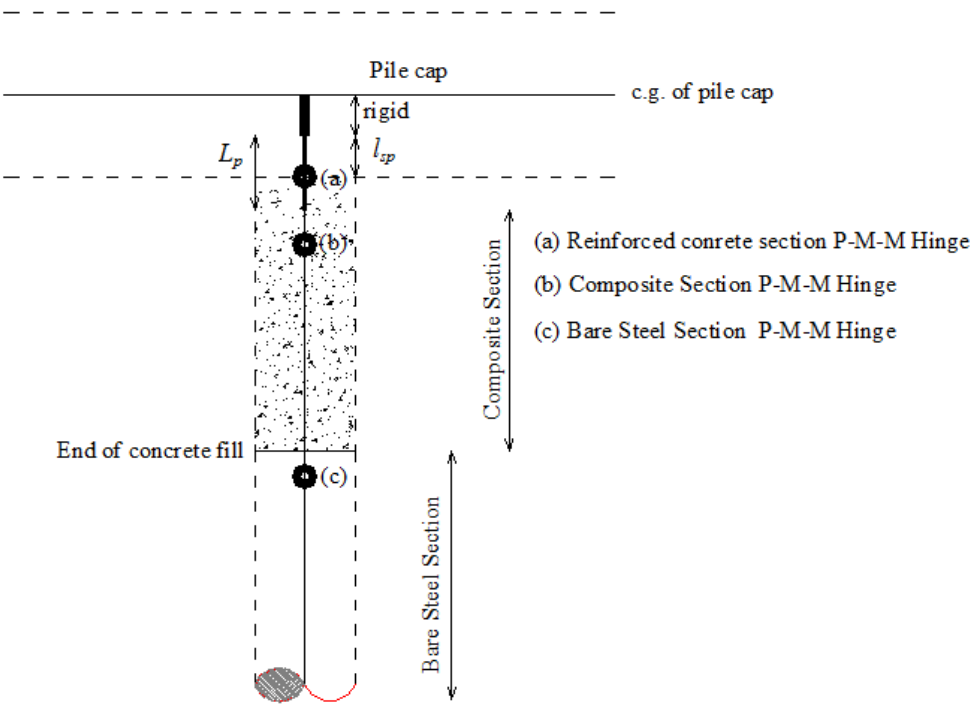

Figure 5.1. Structural model at the pile top

In the case of a typical pile-to-pile-cap connection with reinforcing bars as explained in Chapter 4, top of the piles are modeled at three different sections as shown in Figure 5.2. The first element that connects the pile to the pile-cap is basically a reinforced concrete section. The hinge at this region is defined through a reinforced concrete section with a plastic hinge length of L_p ,which also penetrates in to the pile-cap with a strain penetration length of l_{sp} :

$$L_p = 0.044 d_b f_y \tag{5.1}$$

$$l_{sp} = 0.022 d_b f_y \tag{5.2}$$

The next element is a fully composite segment extending down from the concrete section to the end of the concrete fill in pile. The hinge at this section has the capacity of a

full composite section. The following element is bare steel section, where the plastic hinge is represented by a steel section.

At the pile bottom, the first plastic hinge is defined just above the soil. Other plastic hinges are placed with spacing equal to the diameter of the pile. Inelastic p-*y* curves are modeled with compression-only nonlinear uniaxial springs on both sides of the pile shaft to satisfy the hysteresis shape shown in Figure 5.3. The inelastic t-*z* curves are modeled with nonlinear axial springs with equal tension and compression capacities, and finally the inelastic Q-*z* curves are modeled at the pile tip with compression-only nonlinear axial spring elements as shown in Figure 5.2.

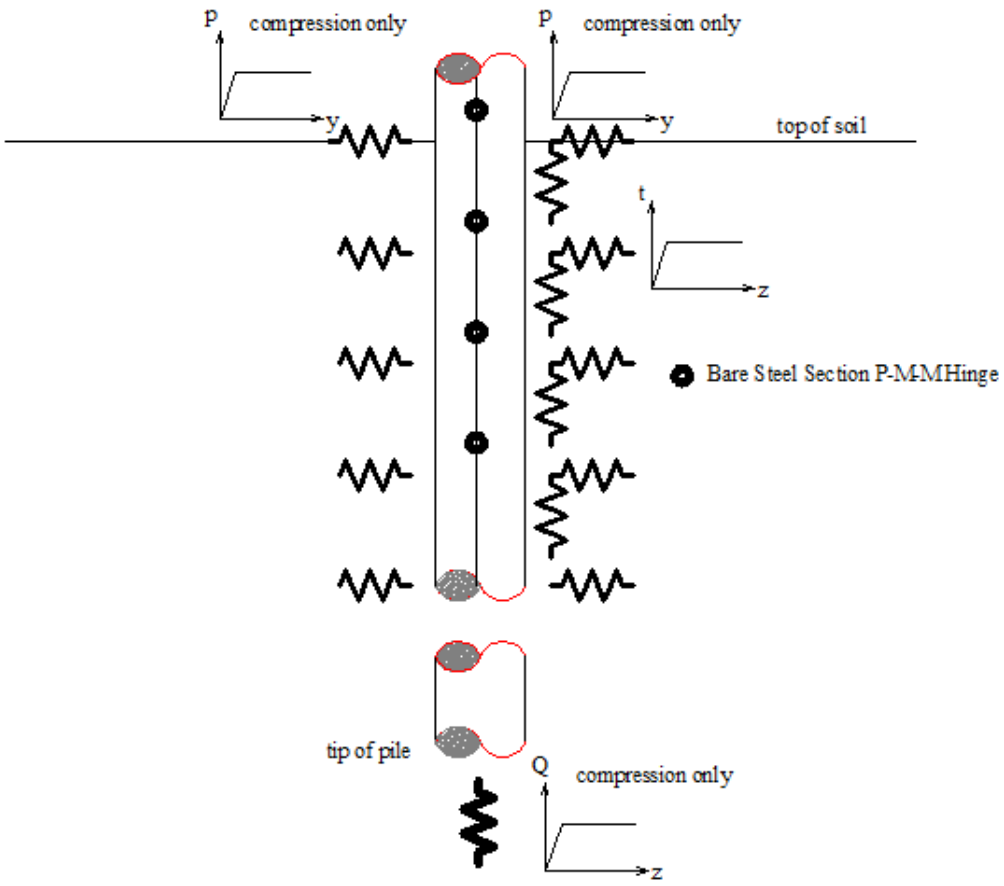

Figure 5.2. Structural model below soil level

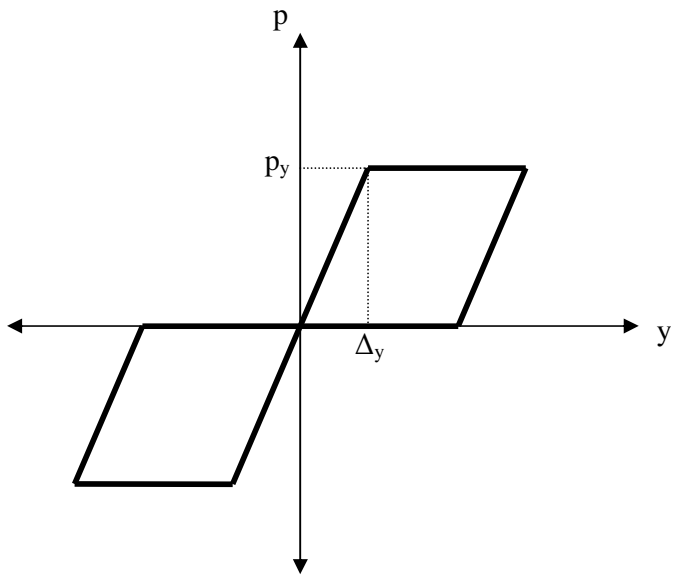

Figure 5.3. Hysteretic behavior of p-y springs

5.2.3. Plastic Hinge Properties

The nonlinear behavior of piles can be represented by lumped plastic hinge model, where the inelastic behavior in the yielding region of the component is lumped into a single location, which can also be used to model axial-flexural interaction. Alternatively, the nonlinear model can be constructed as a macroscopic element model where yielding regions of the component are finely discretized with fibers. In this model inelastic behavior is represented at the fiber level that automatically takes axial-flexural interaction into consideration.

The lumped plastic hinge model is the most frequently used model due to its simplicity and less computational time requirements.

The fiber element method is rarely used due to computational time required to perform the analysis. In general these models are more accurate compared to lumped plastic hinge models. Figure 5.4 illustrates both lumped plastic hinge and fiber element model.

Lumped plastic hinge models can be used to model steel pile section and composite section hinges, the inelastic fiber element models should be used to model reinforced concrete section hinges of batter piles where axial deformations should be more accurately evaluated.

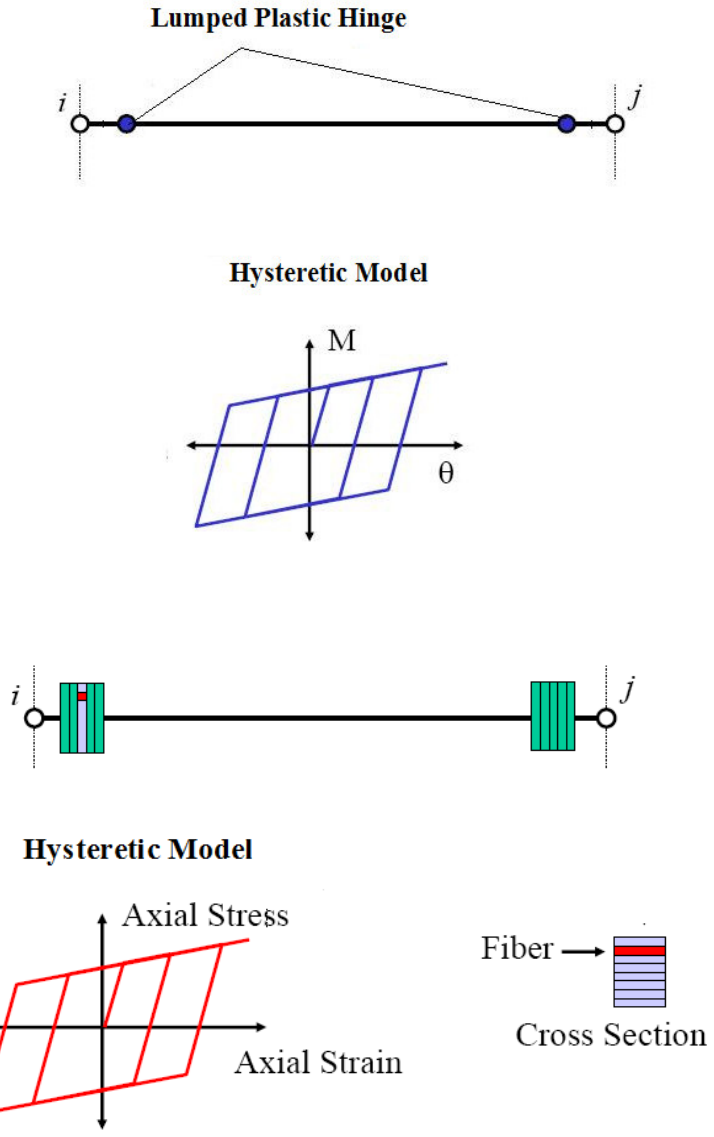

Figure 5.4. Lumped plastic hinge and fiber element model

5.2.4. Material Properties.

5.2.4.1. Concrete. The concrete inside the steel pipe tube is evaluated with Mander's confined concrete model with a confinement steel diameter equal to the thickness of steel tube and a center to center distance of 1 cm. It has been observed that the extraordinary confining pressure at pile to pile cap connection zone increases both capacity and ultimate strain capability of concrete which is also reflected at the experiments mentioned in the 4th chapter. A typical stress strain curve of confined and unconfined concrete is shown in Figure 5.5.

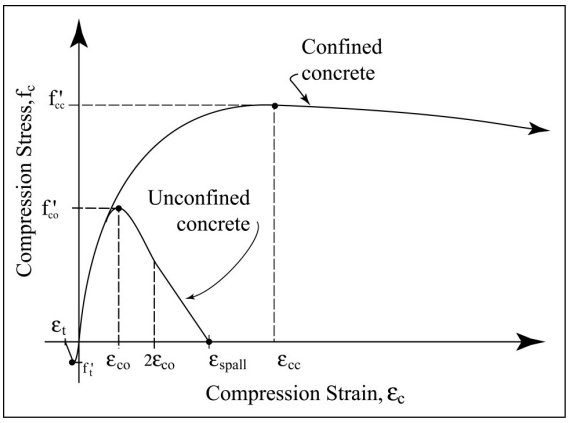

Figure 5.5. Stress-strain curves for confined and unconfined concrete

5.2.4.2. Reinforcing steel and structural steel. The material properties of both reinforcing steel and structural steel are shown in Figure 5.6.

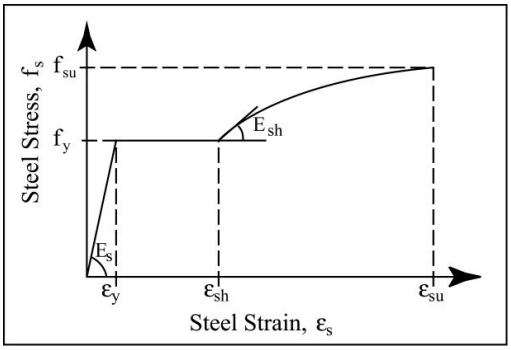

Figure 5.6. Stress-strain curve for reinforcing steel and structural steel

5.3. Modeling of Pile-to-Deck or Pile-to-Pile-Cap Connections

The force and the stress profile of a steel pile-to-pile cap connection with mild steel is shown in Figure 5.7.

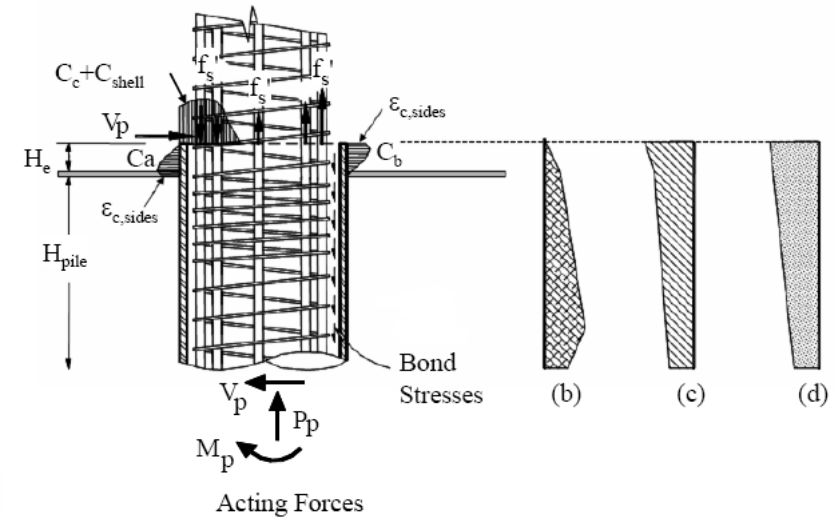

Figure 5.7. Anchorage region force equilibrium relations (Silva, 2001)

In this figure (b) is the tensile stresses distribution in the steel pile, **(c)** is the compressive stress in the steel pile,(d) is the stresses in the longitudinal reinforcement. The section capacity within the anchorage region can be evaluated by the following equation.

$$M_p = M_{pc} + \Delta M_p - V_p H_e \tag{5.3}$$

$$\Delta M_p = C_a \frac{H_e}{3} \tag{5.4}$$

where M_{pc} is the plastic moment capacity of the reinforced concrete section, ΔM_p is the increase in flexural capacity due to contact of steel pipe with pile cap cover concrete, P_p is the axial compression or tension force at the pile section, V_p is the pile shear force, C_a is the compressive stress at the side of the pile embedded in the pile-cap and H_e is the embedding length of the steel pile to the pile-cap.

Since all the secondary terms in Equation 5.3 will disappear once the cover concrete of the pile cap reaches to the crashing strain of 0.004, the capacity of the section simply can be taken equal to the capacity of the reinforced concrete section.

5.4. Modeling of Soil

Piles in groups are often subject to both axial and lateral loads. Designers up to mid-1960s usually assumed piles could carry only axial loads and therefore lateral loads were carried by batter piles, where the lateral load was a component of the axial load in those piles. Graphical methods were used to find the individual pile loads in a group, and the resulting force polygon could close only if there were batter piles for the lateral loads. This was mainly due to poor bending capacity of more common types of piles and the difficulties in analyzing vertical piles subjected to lateral loads. This trend of design has changed in the USA with drilled shaft bridge piers becoming more popular in the early 60's. The improved bending capacity of both drilled and driven vertical piles and the improvements in analysis techniques implemented in early computers have made it possible for design engineers to consider vertical piles as a part of the lateral load resisting system.

Since the behavior of laterally loaded piles depends on stiffness of the pile and the soil, mobilization of resistance in the surrounding soil and at the pile tip is very important in rational modeling of both the soil and the boundary conditions.

Proper modeling of axial pile response is also very important in the analysis of laterally loaded pile groups with batter piles, since the stiffness and capacity of batter piles are different in compression and tension, which could affect the overall response of the structure. One very important consequence of such a modeling is the "pole vaulting" effect caused by the pile pullout from the soil in tension.

Analytical methods for predicting lateral deflections, rotations and stresses in single piles, from the simplest to the most complicated ones, can be grouped under the following four headings:

- Winkler approach.
- p-y , t-z and Q-z curves.
- Elasticity theory.
- Finite element methods.

5.4.1. Winkler Approach

The Winkler approach, also called the subgrade reaction theory, is the oldest method for predicting pile deflections and bending moments. The approach uses Winkler's modulus of subgrade reaction concept to model the soil as a series of unconnected linear springs with a stiffness, E_s, which is called the modulus of soil reaction (or soil modulus):

$$E_s = \frac{-P}{y} \tag{5.5}$$

where p is the lateral soil reaction per unit length of the pile, and y is the lateral deflection of the pile. The behavior of a single pile can be analyzed using the equation of an elastic beam supported on an elastic foundation, which is represented by the 4th order differential beam bending equation:

$$E_p I_p \frac{d^4 y}{dx^4} + Q\frac{d^2 y}{dx^2} + E_s y = 0 \tag{5.6}$$

where E_p is the modulus of elasticity and I_p is the moment of inertia of the pile section, Q is the axial load on the pile and y is the lateral deflection of the pile at point x along the length of the pile.

The governing equation can be simplified by ignoring the axial load as

$$\frac{d^4 y}{dx^4} + \frac{E_s}{E_p I_p} y = 0 \tag{5.7}$$

Solutions to Equation 5.7 have been obtained by making simplifying assumptions regarding the variation of E_s with depth. Generally E_s is taken constant with depth for clays and *varies* linearly with depth in sands.

The Winkler method is widely employed in practice because it has a long history of use, and because it is relatively straightforward to apply using available charts and tabulated solutions, particularly for a constant or linear variation of E_s with depth. Despite its frequent use, the method is often criticized because of its theoretical shortcomings and limitations. The most important shortcoming of this approach is that it assumes a linear load versus deflection relationship for soil.

McClelland and Focht (1956) augmented the subgrade reaction approach using finite difference techniques to solve the beam bending equation with nonlinear load versus deflection curves to model the soil. Their approach is known as the p-y method of analysis. This method has gained popularity in recent years with the availability of powerful personal computers.

5.4.2. P-y Curves

The p-y approach for analyzing the response of laterally loaded piles is essentially a modification or "evolutionary refinement" of the basic Winkler model, where p is the soil pressure per unit length of pile and y is the pile deflection. The soil is represented by a series of nonlinear p-y curves that vary with depth and soil type. A hypothetical p-y curve is presented in Figure 5.8.

Martin and Lam (1986) presented a summary of the design of pile foundations. They showed that a nonlinear soil model is required to capture the lateral behavior of pile and the most efficient method would be using p-y curves as the nonlinear springs. They have concluded that the most reliable procedure for computing required soil load deformation relationship to characterize the spring properties is the API approach, which can be found in guidelines prepared for fixed offshore platforms (American Petroleum Institute - API, 1994).

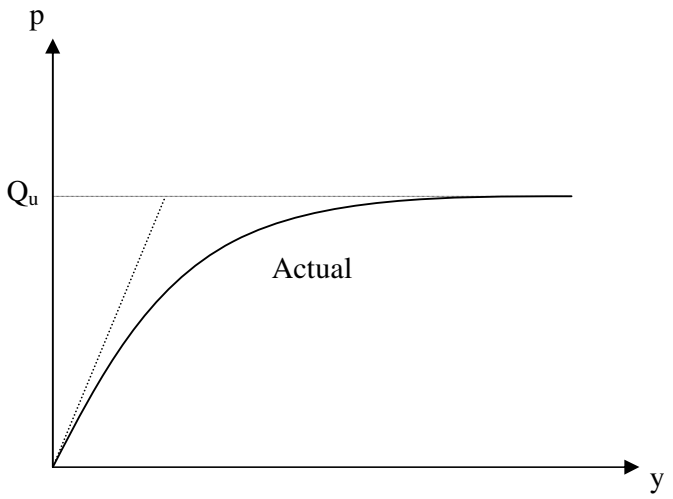

Figure 5.8. Hypothetical p-y curve

The origin of the API equation for sand evolved from the work by Reese, Cox (1974) who established a set of equations based on the forces associated deformation of a soil wedge and the lateral deformation of a rigid cylinder into soil. They established the early shape of the load deflection p-y curve based on soil subgrade modulus. The procedure later modified and simplified by consolidation term.

The American Petroleum Institute (1994) recommended practice for offshore platforms gives detailed guidance for determining p-y curves, which is explained in detail in the following pages.

5.4.2.1. P-y springs in cohessionless soil. The ultimate lateral bearing capacity of sand has been found to vary from a value at shallow depths determined by Equation 5.8 to a value at deep depths determined by Equation 5.9. At any given depth the equation giving the smallest value of Q_u should be used as the ultimate bearing capacity.

$$Q_{us}=(C_1x+ C_2D)\gamma x \tag{5.8}$$

$$Q_{ud}=C_3D\gamma x \tag{5.9}$$

where Q_u is the ultimate resistance [kN/m] (*s* is shallow, *d* is deep), *x* is the depth (m), **γ** is the effective soil weight (kN/m^3), *D* is the pile diameter (m), C_1, C_2, C_3 are coefficients determined from Figure 5.10.

The lateral soil resistance vs deflection (p-y curve) relationship for sand is also nonlinear and the nonlinear curve can be evaluated with the following formula:

$$P = AQ_u \tanh\left[\frac{kxy}{AQ_u} y\right] \tag{5.10}$$

where *A* is a factor to account for loading type, defined as 0.9 for cyclic loading and (3-0.8x/d) ≥0.9 for static loading; Q_u is ultimate load bearing capacity at depth *x*; *k* is the initial modulus of subgrade reaction in force per volume; *y* is lateral deflection.

By substituting *y* with y/y_c, where y_c is the soil displacement at Q_u, the p-y curve for sand can be drawn in the following form shown in Figure 5.9:

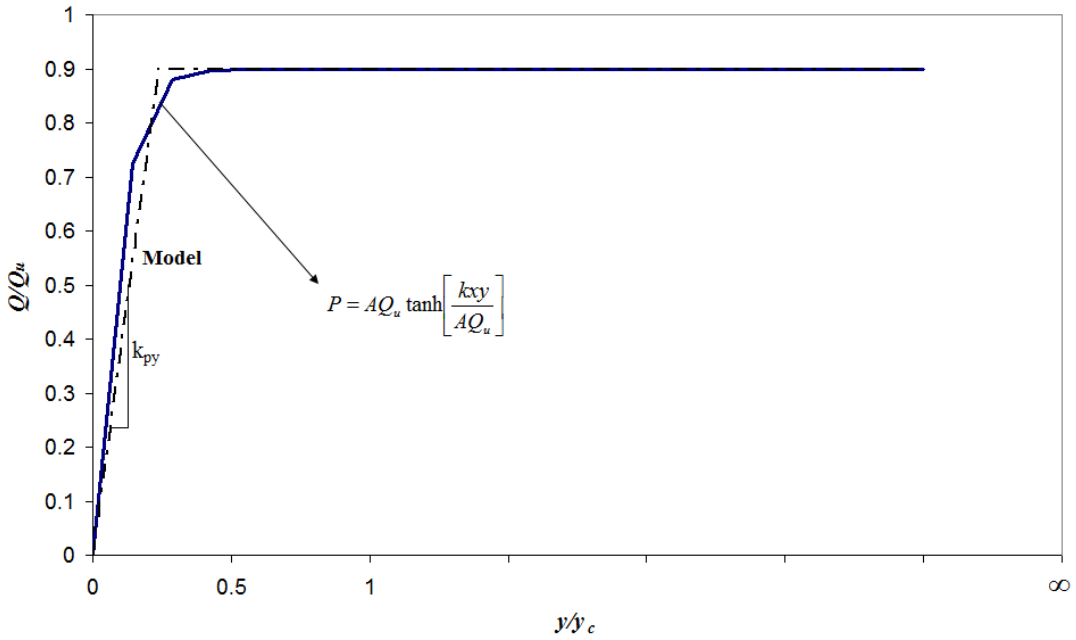

Figure 5.9. Shape of P-y curve of sand for cyclic loading

The nonlinear spring properties can be written as:

Yield force:

$$F_{sy} = Q_u Dh \tag{5.11}$$

where F_{sy} is the yield force of the nonlinear spring, h is the tributary length between the nodes of the pile and D is the diameter of the pile.

Effective elastic stiffness:

$$k_{py} = \frac{F_{sy}}{\delta_y} \tag{5.12}$$

where k_{py} is the effective elastic stiffness and δ_y is the yield displacement of the elasto-plastic nonlinear spring element.

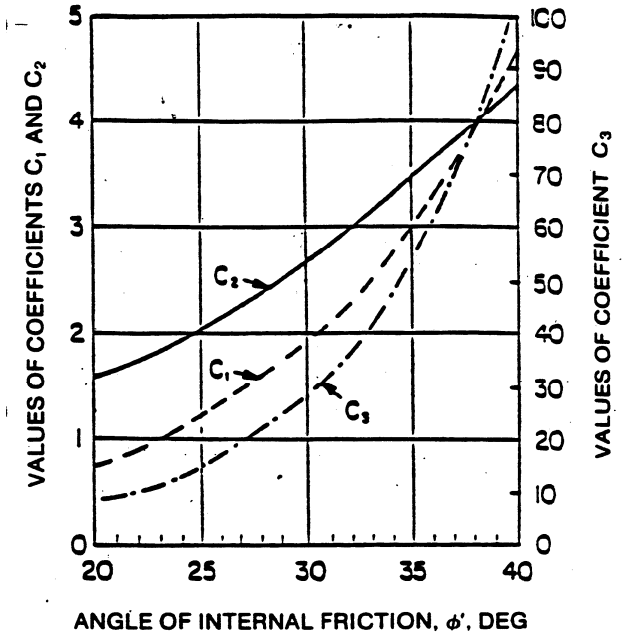

Figure 5.10. API coefficients for sand (API, 1994)

5.4.2.2. P-y springs in cohesive soil. For static lateral loads the ultimate unit load bearing capacity of the soft clay varies between 8*c* to 12c with c being the cohesion value, except shallow depths where failure occurs in a different mode due to minimum overburden pressure. In this region the unit load bearing capacity is assumed to vary between 3*c* to 9*c* and this region is called the wedge action zone.

At the wedge action zone:

$$Q_u=\gamma xD+3C_uD+J\,C_ux \tag{5.13}$$

where Q_u is the ultimate resistance in stress units (kN/m^2), x is the depth (m), γ is the effective soil weight (kN/m^3), D is the pile diameter (m), C_u is the undrained shear strength of undisturbed clay and J is a dimensionless empirical constant varying between 0.25 to 0.5.

At depths where there is no wedge action:

$$Q_u=9C_uD \tag{5.14}$$

$$E_s= Q_u/(5\varepsilon_{50}D) \tag{5.15}$$

where ε_{50} is the soil strain at 50% of maximum stress.

The nonlinear soil resistance vs. deflection relationship for soft clay for static loading can be generated from the following Table 5.1.

Table 5.1. p-y curve for soft clay

Q/Q_u	y/y_c
0	0
0.50	1
0.72	3
1	8
1	∞

where Q is the actual resistance, y is the actual deflection and y_c is equal to 2.5 $\varepsilon_{50}D$. The actual load–deflection curve is shown in Figure 5.11.

The nonlinear soil resistance vs. deflection relationship for soft clay for cyclic loading can be generated from the following Table 5.2.

Table 5.2. P-y curve for soft clay for cyclic loading

Outside wedge action zone		**Wedge action zone**	
Q/Q_u	y/y_c	Q/Q_u	y/y_c
0.5	1	0.5	1
0.72	3	0.72	3
0.72	∞	$0.72x/x_r$	15
		$0.72x/x_r$	∞

For static lateral loads, the ultimate unit load bearing capacity of the stiff clay (Q_u>96 kPa) varies between 8c to 12c. Due to rapid deterioration under cyclic loading static resistance should be reduced to recommended values by the geotechnical engineer for cyclic loading. While stiff clays also have nonlinear stress-strain relationship they are generally more brittle than soft clays. In developing stress-strain curves and subsequent p-y curves for cyclic loads a geotechnical consultancy should be taken, which may considers possible rapid deterioration of load capacity at large deflections.

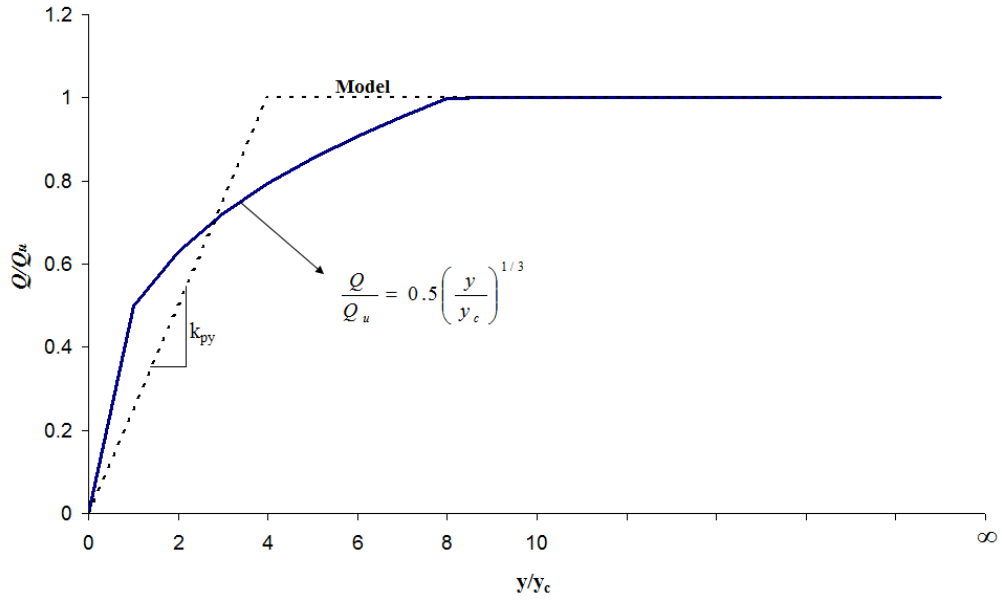

Figure 5.11. Shape of p-y curve of clay for static loading

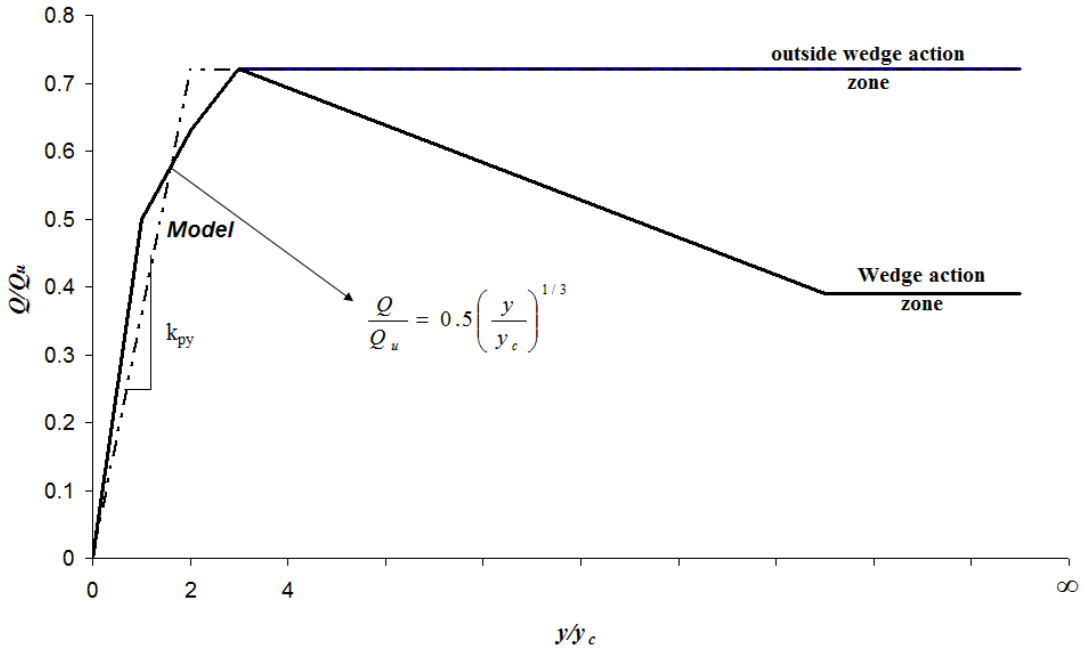

Figure 5.12. Shape of p-y curve of clay for cyclic loading

The nonlinear spring properties can be written as :

Yield force:

$$F_{sy} = Q_u Dh \tag{5.16}$$

where F_{sy} is the yield force of the nonlinear spring, h is the tributary length between the nodes of the pile and D is the diameter of the pile.

Effective elastic stiffness:

$$k_{py} = \frac{F_{sy}}{\delta_y} \tag{5.17}$$

where k_{py} is the effective elastic stiffness and δ_y is the yield displacement of the elasto-plastic nonlinear spring element.

In the absence of relevant geotechnical data, the values given in the following tables can be taken (Table 5.3 and Table 5.4). For cohesionless soil, Φ represents internal friction angle. For cohesive soil, C_u is the undrained shear strength of undisturbed clay soil samples and *J* refers to dimensionless empirical constant with values ranging from 0.25 to 0.5 determined from field test. A value of 0.5 is appropriate to be used in the absence of relevant data. ε_{50} is the soil strain at 50% of maximum stress.

Table 5.3. Properties of cohesionless soil

Type	**Standard Penetration Blow Count, N**	**Φ (Degrees)**	**Relative Density, Dr (%)**
Verly loose to loose	< 10	28-30	0-35
Medium Dense	10-30	30-36	35-65
Dense	30-50	35-42	65-85
Very Dense	50+	40-45	85-100

Table 5.4. Properties of cohesive soil

Type	**Undrained Shear Strength (kN/m^2)**	**ε_{50}**
Unconsolidated Clays	2.5-7	2
Normally Consolidated Clay at depth z	7+0.13	2
Medium stiff	24-48	1
Stiff	48-96	0.7
Very stiff	96-192	0.5
Hard	Over 192	0.4

5.4.2.3. P-y springs in slope. Piles are often installed in sloping rock fill for the construction of marginal wharves. To examine the effect of a slope on *p-y* curves, curves were developed at various depths using standard procedures for sand for a horizontally layered profile (Reese et al. 1974) and for a profile sloped at 1.5V:1H (Wang and Reese 1993) . The soil was assumed to have typical rock fill properties (effective friction angle, φ' = 45 deg; total unit weight, γ = 20.4 kN/m3; soil modulus parameter, *k* = 24430 kN/m3), and the procedure for developing sand *p-y* curves was utilized with a pile diameter of 610 mm (24 in). The resulting down slope and horizontal *p-y* curves were then compared using

a β_c correction factor, which is the ratio of the p resistance in the sloping ground ($p_{sloping}$) to the p resistance in the horizontal ground ($p_{horizontal}$).

$$\beta_c = \frac{p_{sloping}}{p_{horizontal}} \tag{5.18}$$

The resulting β_c correction factors comparing the down slope of horizontal p-y curves are shown in Figure 5.13.

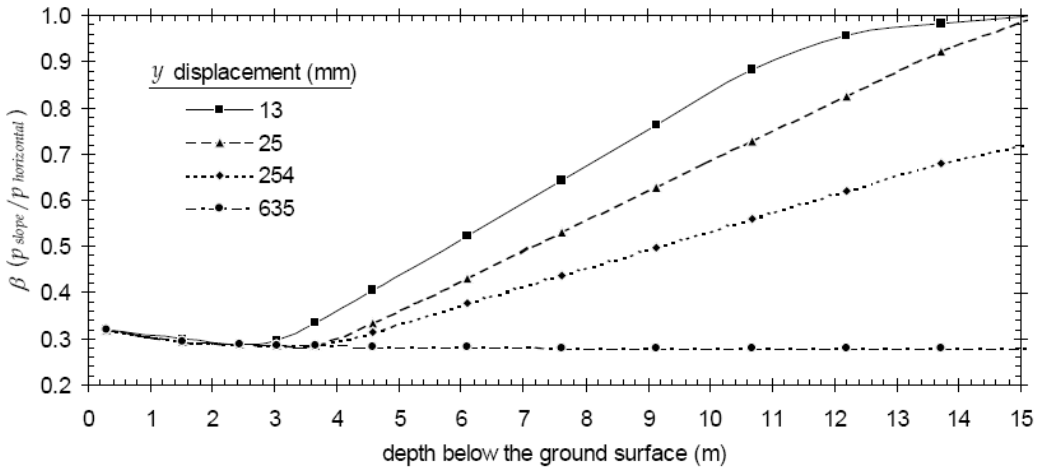

Figure 5.13. Lateral resistance β_c correction factors for down slope movements (McCullough *et al*, 2001)

5.4.2.4. Pile group effects. Measurements of displacements and stresses in full-scale and model pile groups indicate that piles in a group carry unequal lateral loads, depending on their location within the group and the spacing between piles. This unequal distribution of load among piles is caused by "shadowing", which is a term used to describe the overlap of shear zones and consequent reduction of soil resistance. A popular method to account for shadowing is to incorporate p-multipliers into the p-y method of analysis. The p-multiplier values depend on pile position within the group and pile spacing.

The concept of p-multipliers (also called f_m) were described by Brown et al. (1988) as a way of accounting for pile group effects by making adjustments to p-y curves. The multipliers are empirical reduction factors that are experimentally derived from load tests

on pile groups. Because they are determined experimentally, the multipliers include both elasticity and shadowing effects. This eliminates the need for a separate y-multiplier, which is found in many elasticity-based methods. The procedure follows the same approach used in the *p-y* method of analysis, except that a multiplier, with a value less than one, is applied to the p-values of the single pile *p-y* curve. This reduces the ultimate soil resistance and softens the shape of the p-y curve, as shown in Figure 5.14.

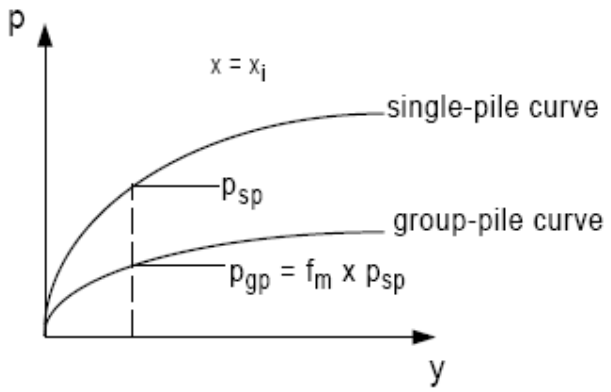

Figure 5.14. P-multiplier concept for lateral group analysis

R.L Mokwa (2001) performed an extensive study recently on the pile group behavior and compared all past tests performed for this purpose and proposed a *p-multiplier* chart to be used for design. This chart can be seen in Figure 5.15.

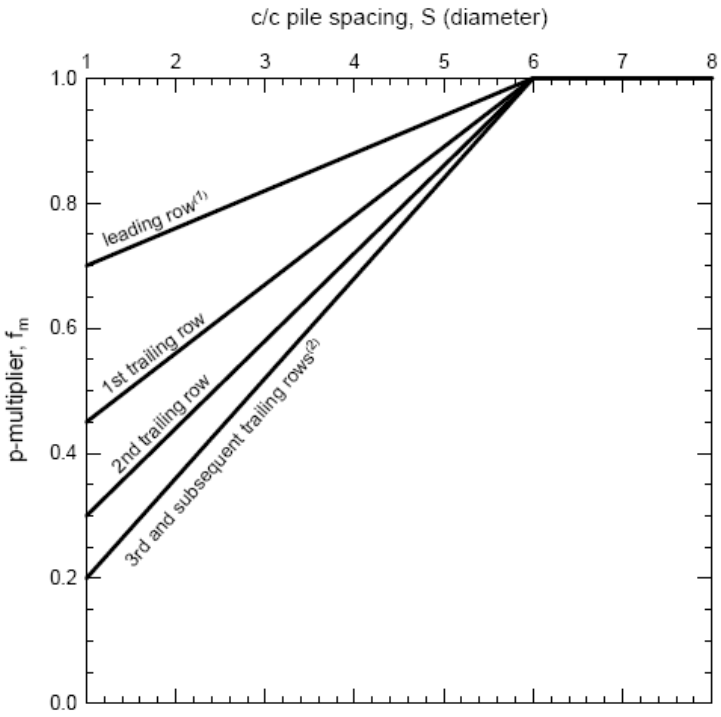

Figure 5.15. p-multiplier design curves (Mokwa et al, 2001)

This chart is proposed for pile groups in the line of loading direction with pile spacing more than three pile diameters normal to the direction of loading. For pile spacing more than three pile diameters normal to the direction of loading pile group effects need not to be taken account for this direction.

5.4.2. T-z and Q-z Curves

Since batter piles resist lateral loads mainly through their axial stiffness, it is important to model the axial stiffness of the batter pile system. The axial stiffness of the pile is a function of pile stiffness as well as the axial resistance components of the soil, which is provided by axial soil-pile adhesion or load transfer along the sides of the pile and the end bearing resistance. An analytical modeling for determining the axial stiffness of a pile is provided, which make use of axial pile shear transition vs. local pile deflection, namely, *t-z* curves and end bearing vs. tip deflection response, namely, *Q-z* curves to model the axial support provided by the soil along the full length of the pile.

This method simply divides pile in to many short elements each connected to a nonlinear spring in depended of each other with a nonlinear spring attached to the tip of the pile. Various empirical and theoretical methods are available for developing *t-z* and *Q-z* curves. The most common ones are the methods defined in API recommendations (American Petroleum Institute 1994), which is based on studies by Kraft et al (1981).

5.4.3.1. T-z and Q-z springs for cohesionless soil. For cohesionless soil the shaft friction *f* may be calculated by the equation:

$$f=K\sigma_0 tan\ \delta \tag{5.19}$$

where K is the coefficient for lateral earth pressure (ratio of horizontal to vertical normal pressure), σ_o is the effective overburden pressure at the point in question (kPa), δ is the friction angle between the soil and pile according to Table 5.6.

For open ended pipe piles driven unplugged, it is appropriate to assume K as 0.8 for both tension and compression loading. Values for full displacement piles may be assumed to be 1. For long piles friction may not indefinitely increase linearly with the overburden pressure. In such cases it is appropriate to limit friction values with those given in Table 5.6.

For piles end bearing in cohesionless soils, the unit end bearing Q_p can be computed by the following equation:

$$Q_p = \sigma_0 N_q A_p \tag{5.20}$$

where Q_p is the total end bearing, A_p is the area of cross section of the pile, σ_o is the effective overburden pressure at the point in question (kPa), N_q is a dimensionless bearing capacity factor.

Recommended values of N_q and limiting end bearing capacities are given in Table 5.7. For piles considered to be plugged, the end bearing pressure may be assumed to act over the entire cross section the pile.

In the absence of more definitive criteria the following t-z curve in Figure 5.16 is recommended for sands and other cohesionless soil.

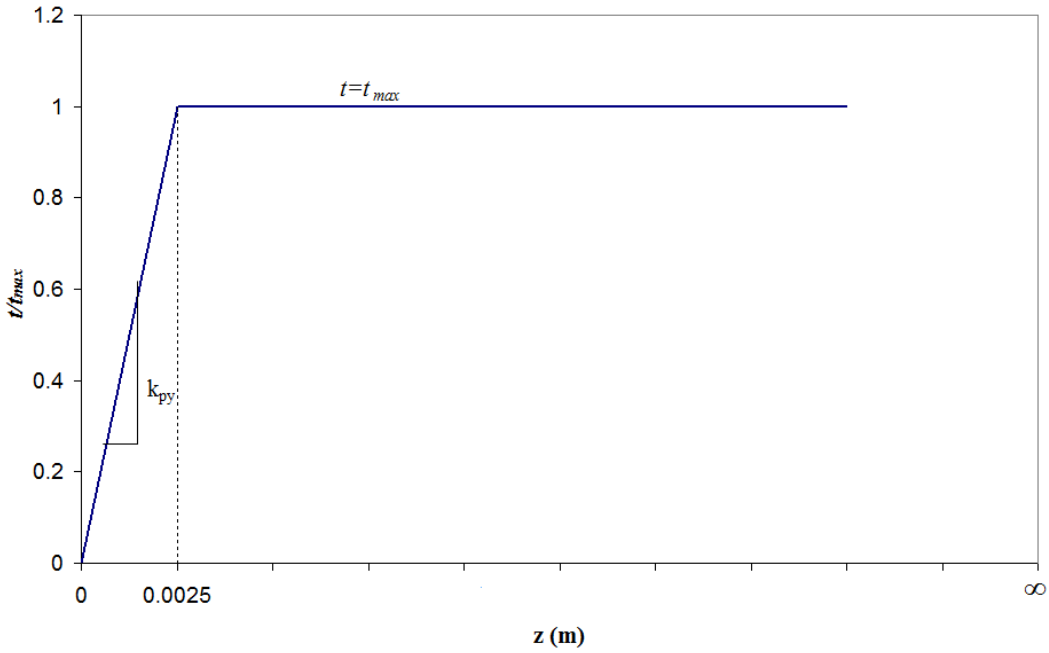

Figure 5.16. T-z curve for cohessionless soil

In Figure 5.16, t_{max} represents the maximum unit skin friction capacity of the soil, z is the local pile deflection. The effective elastic stiffness of the nonlinear t-z spring can be defined as

$$k_{py} = \frac{t_{\max}}{\delta_y} \tag{5.21}$$

where k_{py} is the effective elastic stiffness and δ_y is the yield displacement of the nonlinear spring element, which is taken equal to 0.0025 m for cohesionless soils .

Relatively large pile tip movements are required to mobilize the full end bearing resistance. A pile tip displacement up to 10% of the pile diameter may be required to fully mobilize cohesionless soils. In the absence of more definitive criteria the following curve defined in Table 5.5 is recommended for cohesionless soils. The actual and the idealized bilinear Q-z curve is shown in Figure 5.17.

Table 5.5 Q-z curve for cohesionless soil

z/D	Q/Q_p
0.002	0.25
0.013	0.50
0.042	0.75
0.073	0.90
0.10	1
∞	1

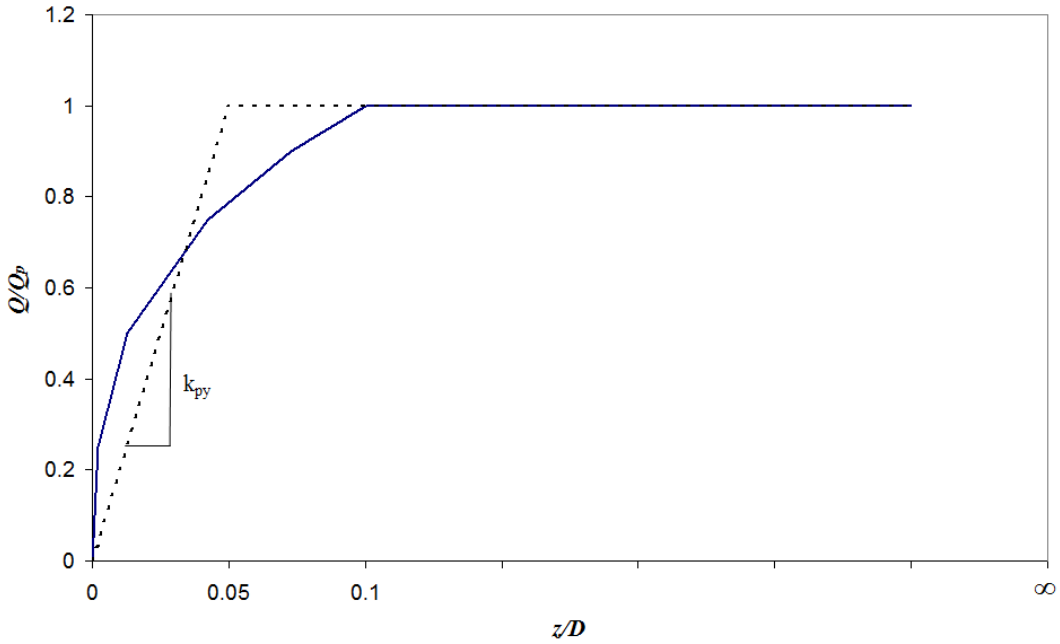

Figure 5.17. Q-z curve for cohessionless soil

In Figure 5.19, z represents the axial tip deflection, D is the pile diameter, Q is the mobilized end bearing capacity , Q_p is the total end bearing capacity. The effective elastic stiffness of the nonlinear Q-z spring can be defined as

$$k_{py} = \frac{Q_p}{\delta_y} \tag{5.22}$$

where k_{py} is the effective elastic stiffness and δ_y is the yield displacement of the nonlinear spring element.

Table 5.6. API recommendations for side friction in siliceous soil

Density	Soil Description	Soil-Pile Interface Friction Angle, δ [2] (degrees)	Limiting Shaft Friction, f_s	
			(kips/ft^2)	(kPa)
Very loose	Sand	15	1.0	47.8
Loose	Sand-silt [3]			
Medium	Silt			
Loose	Sand	20	1.4	67.0
Medium	Sand-silt			
Dense	Silt			
Medium	Sand	25	1.7	81.3
Dense	Sand-silt			
Dense	Sand	30	2.0	95.7
Very dense	Sand-silt			
Dense	Sand	35	2.4	114.8
Very dense	Sand-silt			

Table 5.7. API recommendations for tip resistance in siliceous soil

Density	Soil Description	N_q	Limiting Tip Resistance, q_b	
			(kips/ft^2)	(MPa)
Very loose	Sand	8	40	1.9
Loose	Sand-silt			
Medium	Silt			
Loose	Sand	12	60	2.9
Medium	Sand-silt			
Dense	Silt			
Medium	Sand	20	100	4.8
Dense	Sand-silt			
Dense	Sand	40	200	9.6
Very dense	Sand-silt			
Dense	Sand	50	250	12.0
Very dense	Sand-silt			

5.4.3.2. T-z and Q-z springs for cohesive soil. For piles in cohesive soil the shaft friction f at any point along the pile can be calculated by the equation:

$$f=\alpha\, C_u \tag{5.23}$$

where α is a dimensionless factor, and C_u is the undrained shear strength of the soil at the point in question.

The factor α can be calculated by the following equations:

$$\alpha=\psi^{0.5} \qquad \psi \le 1.0 \tag{5.24}$$

$$\alpha=\psi^{0.25} \qquad \psi \ge 1.0 \tag{5.25}$$

with the constraint that $\alpha \le 1$ where :

$$\psi = C_u/\sigma_0 \tag{5.26}$$

and σ_0 is the effective overburden pressure at the point in question (kPa)

For piles end bearing in cohesive soil, the unit end bearing may be computed by the equation :

$$Q_p=9*Cu*A_p \tag{5.27}$$

where Q_p is the total end bearing, C_u is the undrained shear strength of the soil at the point in question and A_p is the cross section area of the pile.

In the absence of more definitive criteria the following t-z curve in Table 5.8 is recommended for clays and other cohesive soil. The actual t-z and the idealized tri-linear t-z curve is shown in Figure 5.18.

Table 5.8. t-z curve of cohesive soil

z/D	t/t_{max}
0.0016	0.30
0.0031	0.50
0.0057	0.75
0.0080	0.90
0.0100	1
0.0200	0.7-0.9
∞	0.7-0.9

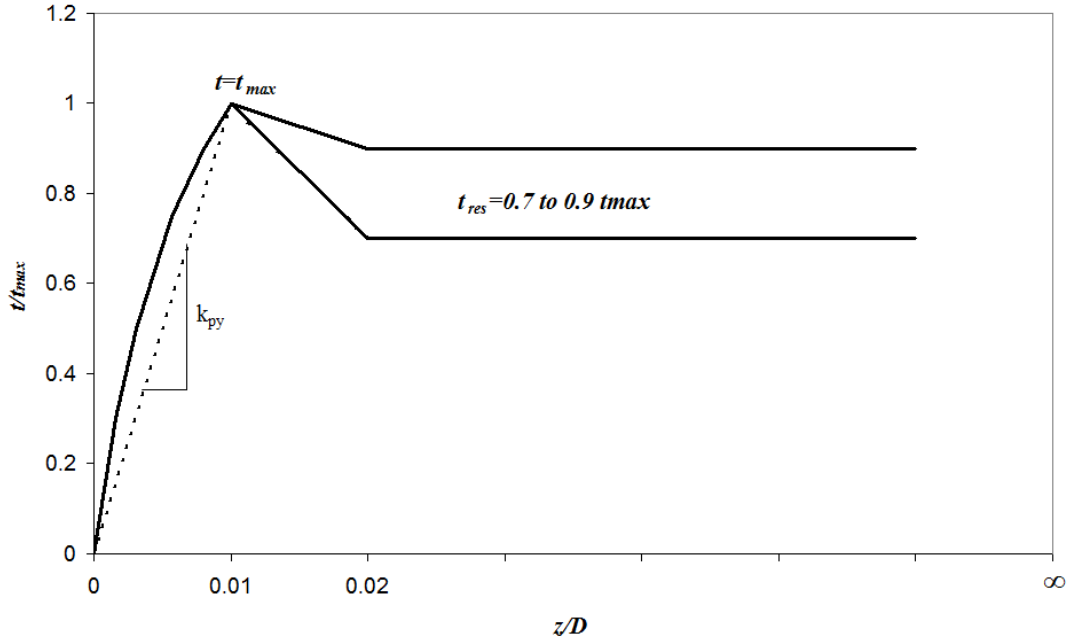

Figure 5.18. T-z curve for cohesive soil

In Figure 5.18, $t_{max}=f$ is the maximum unit skin friction capacity of the soil, z is the local pile deflection and D is the pile diameter. The elastic stiffness of the nonlinear t-z spring can be defined as

$$k_{py} = \frac{t_{\max}}{\delta_y} \tag{5.28}$$

where k_{py} is the elastic stiffness nonlinear spring element, δ_y is the yield displacement of the nonlinear spring element ,which is equal to 0.01 D for cohesive soils. The nonlinear soil spring can either be in the form of elasto-plastic nature with t=0.70 or 0.90 times t_{max} or in the form of tri-linear curve as shown in Figure 5.20.

Unless test data indicate otherwise f should not exceed c or the following limits:

For high plasticity clays f may be equal to C_u for unconsolidated and normally consolidated clays. For over consolidated clays f should not exceed 48 kPa for shallow penetrations or C_u equivalent to a normally consolidated clay for deeper penetrations, whichever is greater.

For other types of clays f should be taken equal to C_u for C_u less than 24 kPa . For C_u in excess of 24 kPa but less than 72 kPa the ratio of f to C_u should decrease linearly from unity to 0.5. For C_u in excess of 72 kPa f should be taken 0.5 C_u.

Relatively large pile tip movements are required to mobilize the full end bearing resistance. A pile tip displacement up to 10% of the pile diameter may be required to fully mobilize cohesive soils. In the absence of more definitive criteria the following curve defined in Table 5.9 is recommended for cohesive soils. The actual Q-z and the idealized bilinear t-z curve is shown in Figure 5.19.

Table 5.9. Q-z Curve for Cohesive soil

z/D	Q/Q_p
0.002	0.25
0.013	0.50
0.042	0.75
0.073	0.90
0.10	1
∞	1

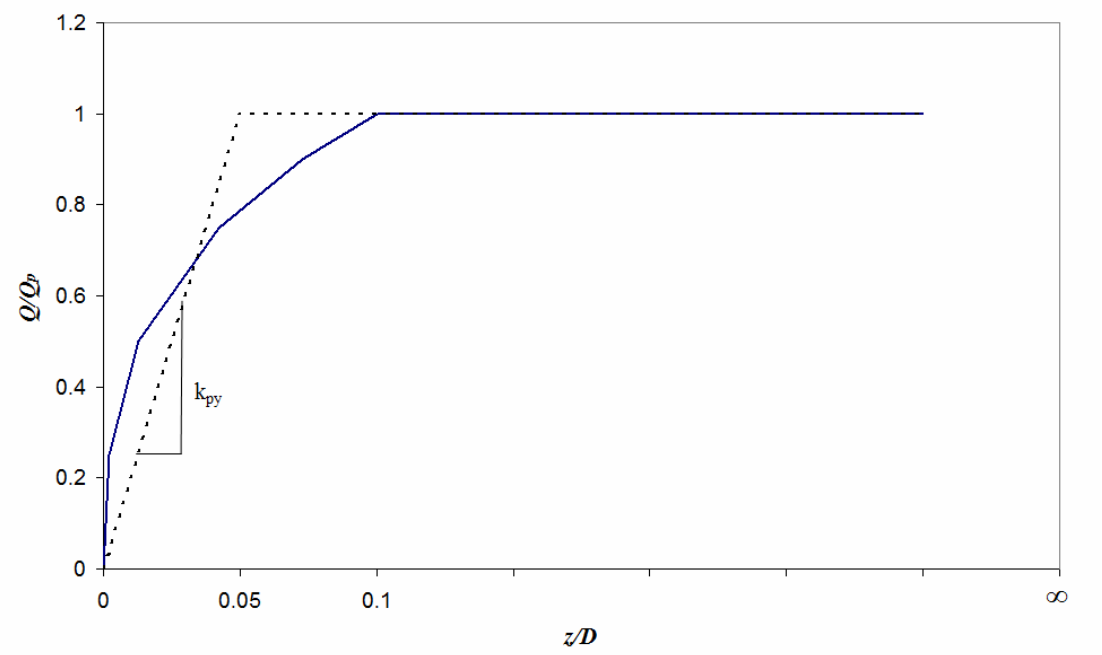

Figure 5.19. Q-z curve for cohesive soil

In Figure 5.19, z represents the axial tip deflection, D is the pile diameter, Q is the mobilized end bearing capacity , Q_p is the total end bearing capacity. The effective elastic stiffness of the nonlinear Q-z spring can be defined as

$$k_{py} = \frac{Q_p}{\delta_y} \tag{5.29}$$

where k_{py} is the elastic stiffness nonlinear spring element and δ_y is the yield displacement of the elasto-plastic nonlinear spring element

5.4.4. Elasticity Method

Poulos (1971) presented the first systematic approach for analyzing the behavior of laterally loaded piles and pile groups using the theory of elasticity. Because the soil is represented as an elastic continuum, the approach is applicable for analyzing battered piles, pile groups of any shape and dimension, layered systems, and systems in which the soil modulus varies with depth. The method can be adapted to account for the nonlinear

behavior of soil and provides a means of determining both immediate and final total movements of the pile (Poulos 1980).

Poulos's (1971) method assumes the soil is an ideal, elastic, homogeneous, isotropic semi-infinite mass, having elastic parameters E_s and ν_s. The pile is idealized as a thin beam, with horizontal pile deflections evaluated from integration of the classic Mindlin equation for horizontal subsurface loading. The Mindlin equation is used to solve for horizontal displacements caused by a horizontal point load within the interior of a semi-infinite elastic-isotropic homogeneous mass. Solutions are obtained by integrating the equation over a rectangular area within the mass. The principle of superposition is used to obtain displacement of any points within the rectangular area.

The pile is assumed to be a vertical strip of length L, width D (or diameter, D, for a circular pile), and flexural stiffness E_pI_p. It is divided into $n+1$ elements and each element is acted upon by a uniform horizontal stress p. The horizontal displacements of the pile are equal to the horizontal displacements of the soil. The soil displacements are expressed as:

$$\{y_s\} = \frac{d}{E_s}[I_s]\{p\} \tag{5.30}$$

where $\{y_s\}$ is the column vector of soil displacements, $\{p\}$ is the column vector of horizontal loading between soil and pile, and $[I_s]$ is the $n+1$ by $n+1$ matrix of soil displacement influence factors determined by integrating Mindlin's equation, using boundary element analyses (Poulos 1971).

The finite difference form of the beam bending equation is used to determine the pile displacements. The form of the equation varies depending on the pile-head boundary conditions. Poulos and Davis (1980) present expressions for free-head and fixed-head piles for a number of different soil and loading conditions.

5.4.5. Finite Element Method

The finite element method is a numerical approach based on elastic continuum theory that can be used to model pile-soil-pile interaction by considering the soil as a three-dimensional, quasi-elastic continuum. Finite element techniques have been used to analyze complicated loading conditions on important projects and for research purposes.

Salient features of this powerful method include the ability to apply any combination of axial, torsion, and lateral loads; the capability of considering the nonlinear behavior of structure and soil; and the potential to model pile-soil-pile-structure interactions. Time dependent results can be obtained and more intricate conditions such as battered piles, slopes, excavations, tie-backs, and construction sequencing can be modeled. The method can be used with a variety of soil stress-strain relationships, and is suitable for analyzing pile group behavior.

6. SEISMIC ISOLATION AND SEISMIC FUSES IN PILE SUPPORTED MARINE STRUCTURES

In the 1990s, following the poor performance of batter piles in a series of earthquakes, some engineers began advising against the use of batter piles. However, once the reason for the poor performance of batter piles was understood, engineers started developing new design strategies to address these problems. One very important strategy developed for the purpose of dissipating energy and preventing extend of damage to batter piles is the application of structural fuse concept or seismic isolation.

6.1. Seismic Isolation in Marine Structures

Though seismic isolation is very widely used in engineering structures its application in water front structures is quite limited. This is mainly due to maintenance issue of isolation devices in harsh marine environment and cost of isolation devices.

The first design example of a isolated waterfront structure was presented by Zmuda *et al* at the Port of Los Angeles in 1995. They designed an extension of a wharf at berth 136 to resist a MCE earthquake without structural or nonstructural damage. The wharf was isolated with sliding friction isolators with four physical barriers to prevent damage to both deck and its support pilings which are:

- A force barrier that strong enough to resist lateral forces exerted by berthing, mooring, etc. and well below the earthquake forces that otherwise induce damage to decks or supporting piles.
- An energy barrier that throws off an earthquake's energy by friction rubbing, turning it into heat discharge to the surrounding air without any part of the friction system breaking or rupturing.
- A vibration barrier that prevents seismic vibrations from tuning in and causing resonant build up of horizontal forces in the structure.

- A displacement barrier of soft springs that exert a biasing force to pull the deck back to its initial position on the piling.

A detail of the isolators and barrier system with a section drawing of the system can be seen in Figure 6.1 ,6.2 and 6.3.

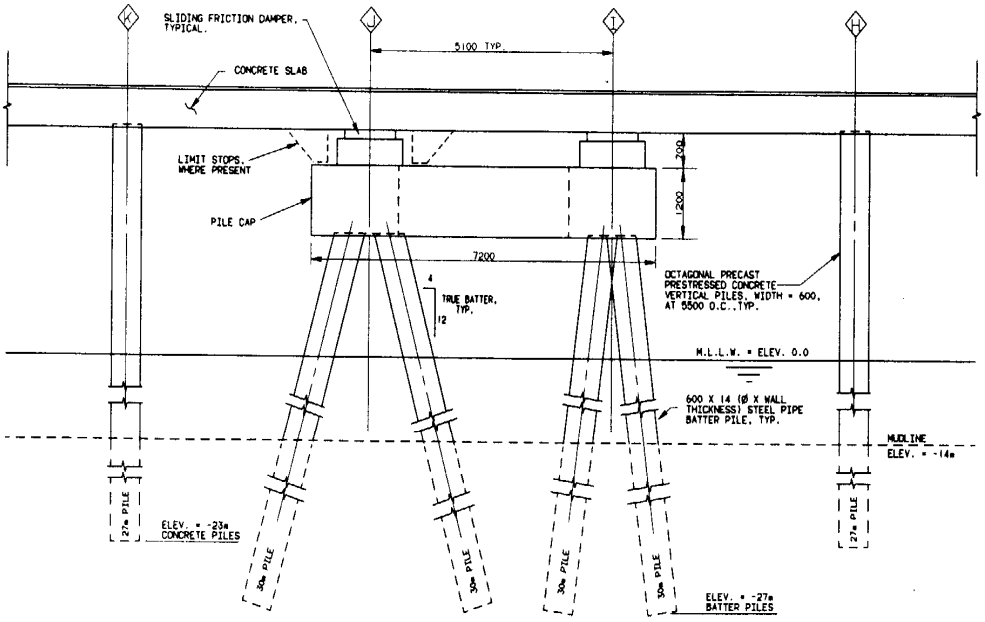

Figure 6.1. Partial wharf cross section (Zmuda *et al,* 1995)

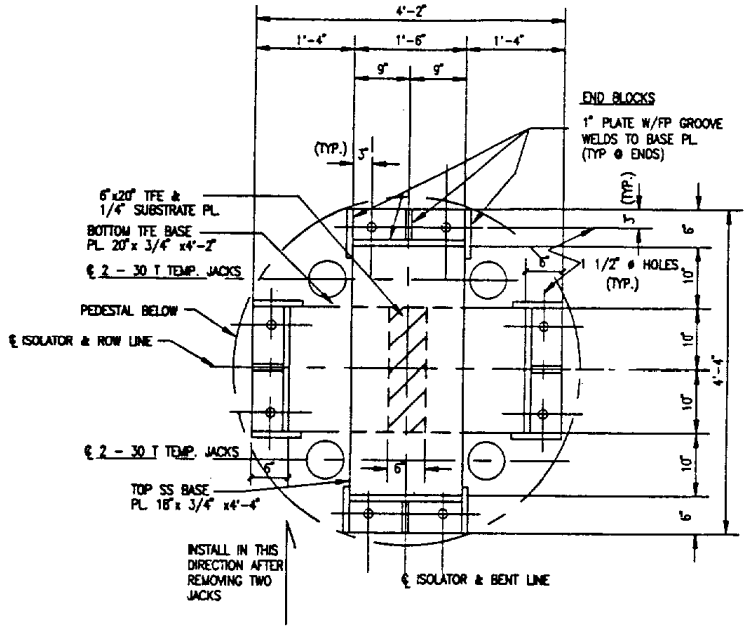

Figure 6.2. Plan view of the isolation system (Zmuda *et al,* 1995)

.

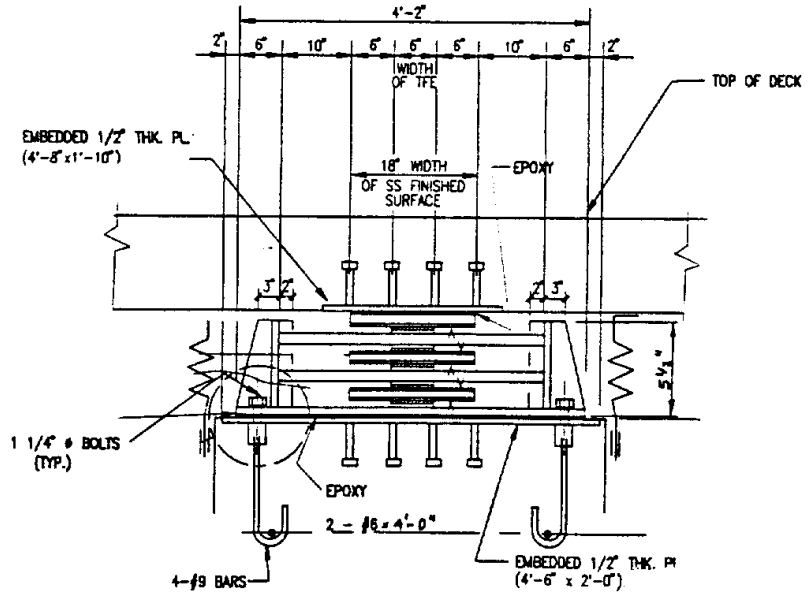

Figure 6.3. Elevation view of the isolation system (Zmuda *et al,* 1995)

There is one other example of isolated wharf in literature which is the retrofit of a large wharf structure by Davidson *et al* (1988) in New Zealand which was done by a series of batter piles fastened to a wharf with post tensioned lead rubber bearing acting as energy absorbers.

Other than these two design examples the application of seismic isolation in waterfront structures is very much limited to isolation of crane legs from the wharf or pier deck to prevent tilting of cranes or damage to the carne legs due to seismic forces transmitted from the deck to the crane structure.

6.2. Structural Fuses

The use of structural fuse to limit forces transmitted to structural elements and dissipate energy with yielding of the fuse element has been a major design tool in engineering structures over the last two decades. An example to a widely accepted fuse is the use of shear link beams in eccentric brace frame structures where the force at any story is limited with the yielding force of shear link beam. Unfortunately engineers who are dealing with waterfront structures hesitated to use such elements until the end of 90's. With the overwhelming data provided in recent earthquakes about the behavior of traditionally designed batter piles engineers are more and more discouraged to use batter piles in marine structures. Even some codes like POLA (2002) has forbidden the use of batter piles in waterfront structures.

Johnson et al proposed a structural fuse system for the first time in 1998 to limit the transmitted inertia forces to the landside batter piles of a wharf designed at the port of long beach where two battered pile rows are interconnected at the top with a continuous thrust beam which is connected to the fuse beam at certain intervals utilizing concrete piers. The fuse beam is also connected to the deck structure via drag members spaced with certain center to center distance and centered between the piers. Therefore the fuse beam forms a link via which transverse lateral loads from wharf structure can be delivered to the batter piles. The fuse beam was designed to form a plastic hinge at a lower load level required to fail batter piles and prevent damage extending to structure (Johnson *et al*, 1998) .A figure of the structural fuse system is shown in Figure 6.4.

A similar fuse system was also used at the same port Pier A where the prestressed concrete piles were connected to a steel beam below deck that is designed to yield and rotate after the pile undergo 1 inch of elastic compression. This system is shown in Figure 6.5

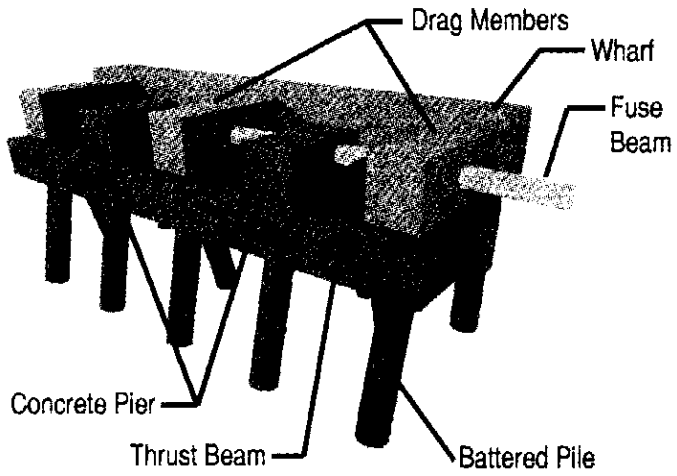

Figure 6.4 Fuse beam system used at Los Angeles Port (Johnson *et al,* 1998)

.

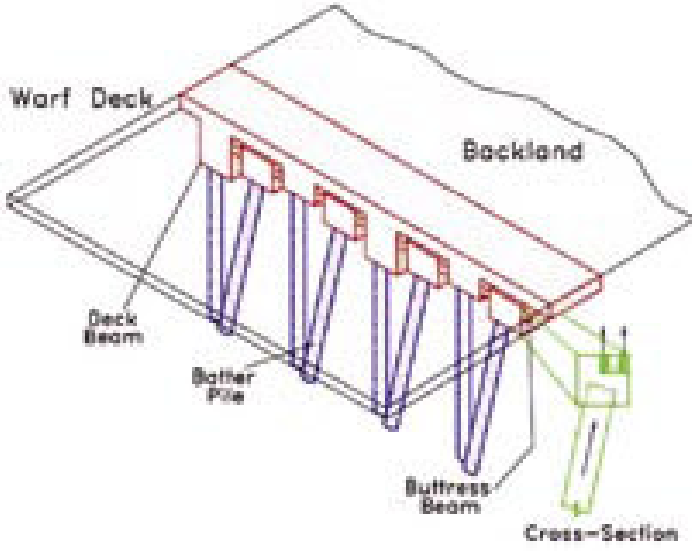

Figure 6.5. Fuse beam system used at Pier A (Johnson *et al,* 1998)

Though the before mentioned fuses have proven to be efficient with the following tests performed over the years their use in application is not easy. Harn in 2004 proposed a new fuse which works in tension stating that most of the batter piles are more likely to fail in tension either at the pile to pile cap connection or the pull-out of the pile from the soil rather than failing in compression. The fuse was simply consisted of mild steel bars debonded by sleeves penetrating in side the pile to lengthen the plastic hinge length of the connection to reduce or control steel strains at the bar. The biggest advantage of this fuse system is its ease of construction compared to other fuses .A figure and a photo of the fuse system is illustrated at Figure 6.6 and 6.7.

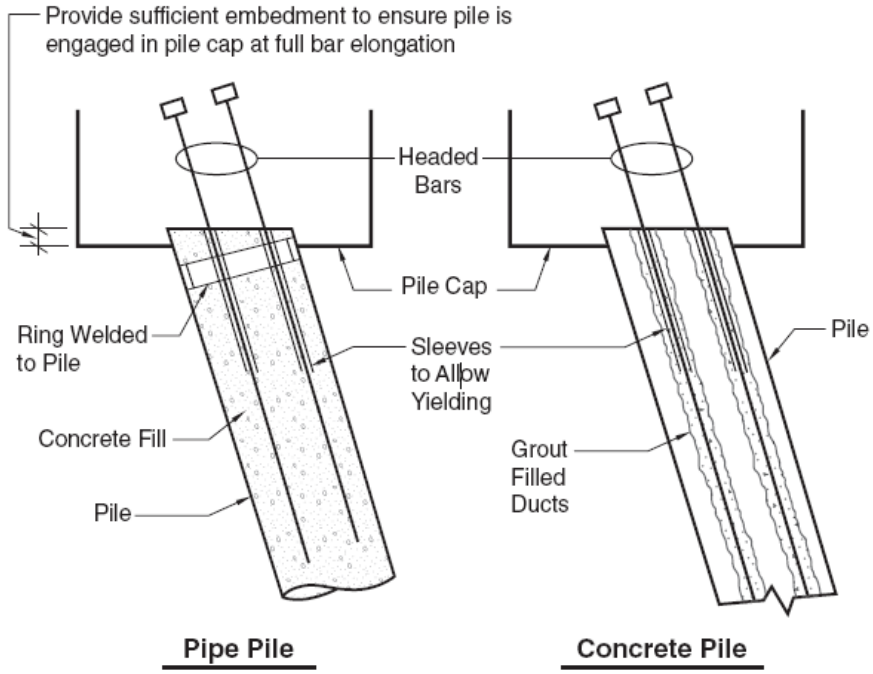

Figure 6.6. Sample tension fuse details for concrete and pipe piles (Harn, 2004)

.

Figure 6.7. Pipe piles with a tension fuse detail under construction (Harn, 2004)

7. SEISMIC ANALYSIS

7.1. Identification of Seismic Input

Traditionally all seismic design codes or guidelines define seismic input through design spectra, which is based to a seismic hazard study at the site of interest. The objective of a seismic hazard study is to quantify the characteristics of ground shaking and reoccurrence of potential damaging ground motions that pose a risk at the site of interest. Seismic input at a given site is related to:

- Regional tectonics and geological setting
- Seismic sources in the region of interest
- Seismic slip rates along the faults in the region
- Data base of historical earthquakes in the region
- Earthquake recurrence models
- Ground motion attenuation relationship
- Source contribution of all faults
- Local site conditions
- Local site response

Technical Standards for Ports, Harbor Facilities, Railroads, and Airports in Turkey (2007) has defined seismic hazard maps for the whole Turkey. Three separate earthquake risk levels with relevant performance levels depending on the structure type are defined in the code

- Earthquake Level 1 which has a 50 % probability of exceedence in 50 years
- Earthquake Level 2 which has a 10% probability of exceedence in 50 years
- Earthquake Level 3 which has a 2% probability of exceedence in 50 years

7.1.1. Design Spectra

The new Turkish code defines the design spectra with two main parameters which are short period (0.2 sec) spectral acceleration value S_s and spectral acceleration value at 1.0 sec period S_1 for class B soil .The spectral acceleration values for other types of soils are calculated by the following formulas:

$$S_{MS} = F_a S_s \tag{7.1}$$

$$S_{M1} = F_v S_1 \tag{7.2}$$

Later the design spectrum is defined with the following equations:

$$\begin{aligned}
&S_{ae}(T) = 0.4\,S_{MS} + 0.6\,\frac{S_{MS}}{T_o}T && (T_o \le T)\\
&S_{ae}(T) = S_{MS} && (T_o \le T \le T_S)\\
&S_{ae}(T) = \frac{S_{M1}}{T} && (T_S \le T \le T_L)\\
&S_{ae}(T) = \frac{S_{M1}T_L}{T^2} && (T_L \le T)
\end{aligned} \tag{7.3}$$

$$T_S = \frac{S_{M1}}{S_{MS}} \quad ; \quad T_o = 0.2T_S \tag{7.4}$$

where F_a is the short period amplification factor, F_v is the amplification factor for 1 sec period spectral acceleration, T_s the characteristic period of the spectrum, T_o is the shorth perios and T_L is the long period values of the design spectrum.

A typical design spectrum curve is shown in Figure 7.1. The design spectrum for the three levels of earthquake used in this study is shown in Figure 7.2. Values of F_a and F_v is given in Table 7.1 and 7.2 respectively

Table 7.1. Short period spectral amplification factors.

Soil Class	Short Period Spectral Acceleration (g)[a]				
	$S_S \leq 0.25$	$S_S = 0.50$	$S_S = 0.75$	$S_S = 1.0$	$S_S \geq 1.25$
A	0.8	0.8	0.8	0.8	0.8
B	1.0	1.0	1.0	1.0	1.0
C	1.2	1.2	1.1	1.0	1.0
D	1.6	1.4	1.2	1.1	1.0
E	2.5	1.7	1.2	0.9	0.9
F	–	–	–	–	–

Table 7.2. Spectral amplification factors at 1.0 sec.

Soil Class	Spectral Acceleration Values at 1.0 sec (g)[a]				
	$S_1 \leq 0.1$	$S_1 = 0.20$	$S_1 = 0.3$	$S_1 = 0.4$	$S_1 \geq 0.5$
A	0.8	0.8	0.8	0.8	0.8
B	1.0	1.0	1.0	1.0	1.0
C	1.7	1.6	1.5	1.4	1.3
D	2.4	2.0	1.8	1.6	1.5
E	3.5	3.2	2.8	2.4	2.4
F	–	–	–	–	–

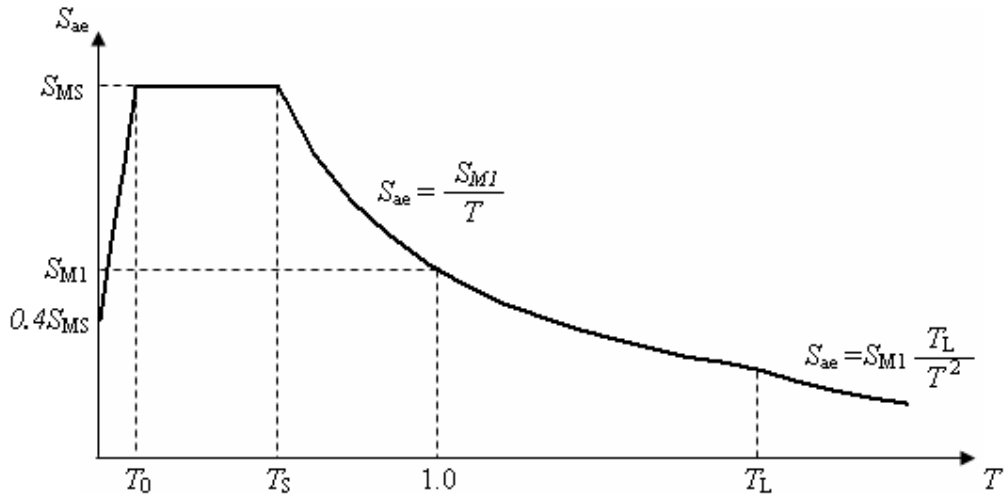

Figure 7.1. Design spectrum

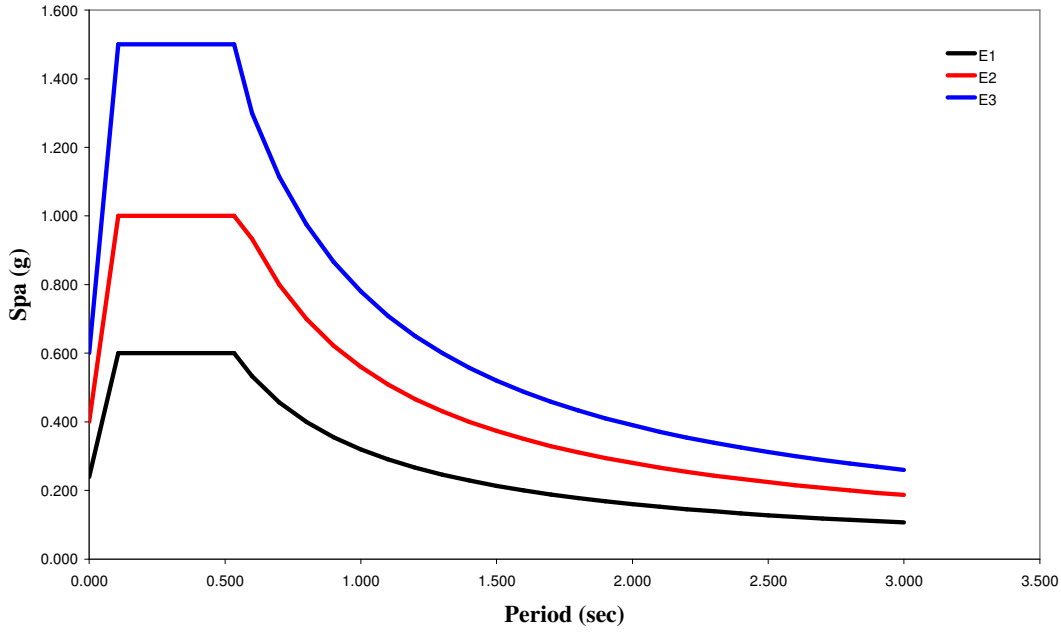

Figure 7.2. Design spectra used in this study

7.1.2. Selection and Scaling of Ground Motion Time Histories

Since the introduction of performance based design concepts and based isolated structures nonlinear time analysis has become a common method of analysis. Some code provisions governing design of seismic isolated structures have included nonlinear time history provisions for more than a decade. Modern performance based design codes and guidelines such as FEMA, IBC etc contain detailed provisions for performing nonlinear time history analysis.

Virtually all codes and guidelines require scaling of selected ground motion time histories so that they match or exceed the controlling design spectrum with in a period range of interest. A typical code or guideline provision would require scaling of the two horizontal component of each ground motion such that the average square root of the sum of squares of the 5% damped response spectra of the ground motion used does not fall below α times the 5% damped design spectrum for periods between T_0 and T_n . Typical values of α is either 1.3 or 1.4 and T_0, T_n are usually assigned values such as 0.2T and 1.5T where T is the fundamental period of the structure.

In literature, there are three sources of acceleration time histories: design response spectrum compatible artificial records, synthetic records obtained from seismological models and accelerograms recorded in real earthquakes. Generally, two methods for scaling actual time histories to match a given design spectrums are used: scaling in time domain and frequency domain. Selection criteria of proper time history records to fit the design code spectrum account for geological and seismological conditions at specific site.

There are three types of accelerograms used in practice which are :

- Real Accelerograms
- Artifical Accelerograms
- Synthetic Accelerograms

7.1.2.1. Methods of ground motion scaling of real accelerograms. There are two methods for modifying actual time histories to match a given design spectrum: Ground motion simulation in time domain and frequency domain.

7.1.2.1.1. Ground motion scaling in time domain. In this approach, recorded motion is simply scaled up or down uniformly to best match the target spectrum within a period range of interest, without changing the frequency content. It could be stated that the accelerograms should only be scaled in terms of amplitude. Nevertheless, scaling on the time axis has been used to modify the frequency content of real ground-motion records. The procedure is based on minimizing the differences between the scaled motion's response spectrum and target spectrum in a least-square sense.

7.1.2.1.2 Ground motion scaling in frequency domain. This method is based on the concept of using actual records to generate time histories that fit a given target response spectrum. The physical characteristics of the earthquake motion are retained throughout the procedure, which makes the technique powerful in comparison with the classical artificial record generation. A frequency domain scaling methodology uses an actual record to produce a similar motion that matches almost perfectly a target (design) spectrum. In this method, an actual motion is filtered in frequency domain by its spectral ratio with the design target spectrum. The Fourier phases of the motions remain unchanged during the

entire procedure. The technique is repeated iteratively until the desired matching is achieved for a certain range of periods

The earthquake ground motions used in this study are scaled with the use of time domain scaling process. The names and the other properties of the earthquakes are given in the table below. The elastic response spectrums of the earthquakes are given in Figure 7.3 with respect to design spectra.

Table 7.3. Earthquake records used in this study

Record No	Earthquake	Time	Station	Distance	Record
P0012	Imperial Valley	15.10.1979	El Centro Array #12 USGS	18	H-E12140
P0013	Imperial Valley	15.10.1979	Delta UNAM/UCSD	31.7	H-DLT262
P0164	Taiwan SMART1(45)	14.11.1986	SMART1 O01 N.A.	-	45O01EW
P0752	Loma Prieta	18.10.1989	Anderson Dam (L Abut)	20	ADL340
P0778	Loma Prieta	18.10.1989	Salinas - John & Work	31.4	SJW160
P0843	Landers	28.06.1992	LA - W 70th St USC	-	W70000
P0967	Northridge	17.01.1994	LA - Pico & Sentous	29	PIC090

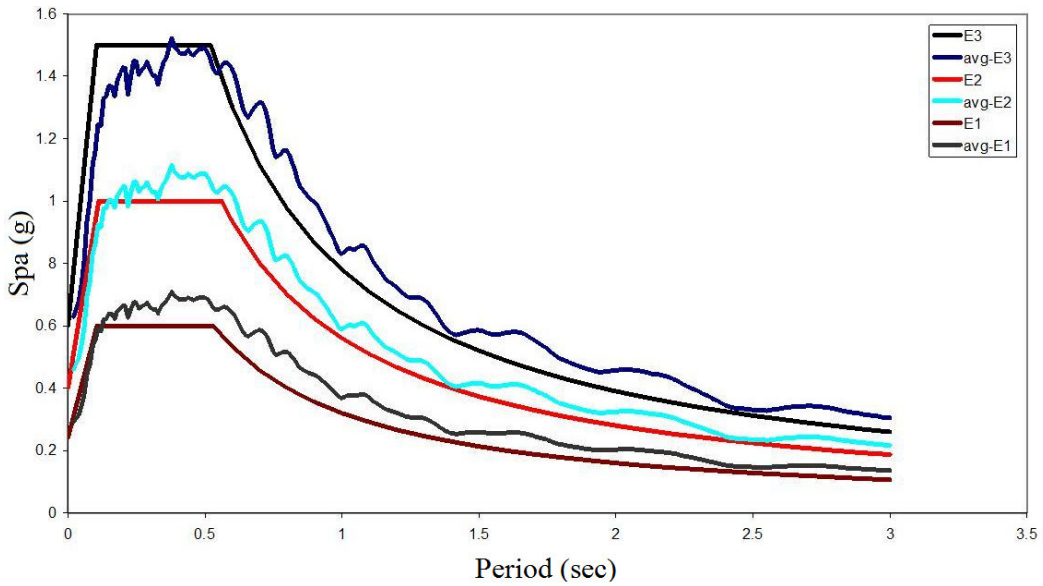

Figure 7.3. Comparison of design spectrum to average response spectrum of data sets

Also the inelastic response properties of each data set have been evaluated to see whether or not they satisfy the equal displacement approximations. Below figures explains the inelastic to elastic deformation ratios for each data sets average for constant R values from 1 to 5. As the figures show the average $d_{inelastic}/ d_{elastic}$ values approaches to 1 in long periods which indicates that the data sets satisfy the equal displacement approximation.

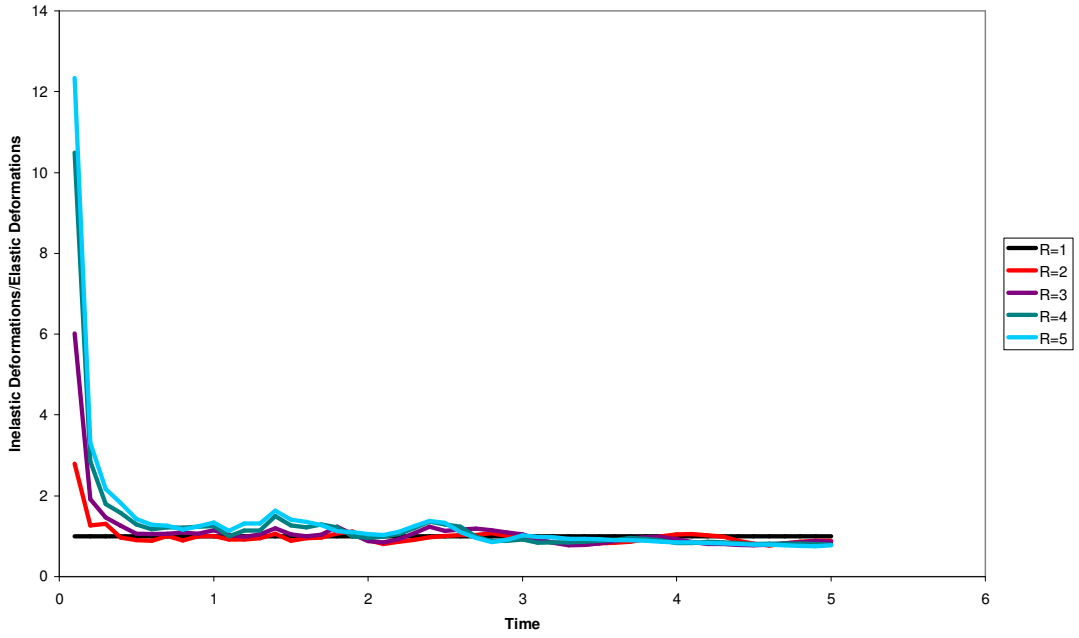

Figure 7.4. Inelastic deformation demands/elastic deformation demands for constant R values for E1 earthquake set of data

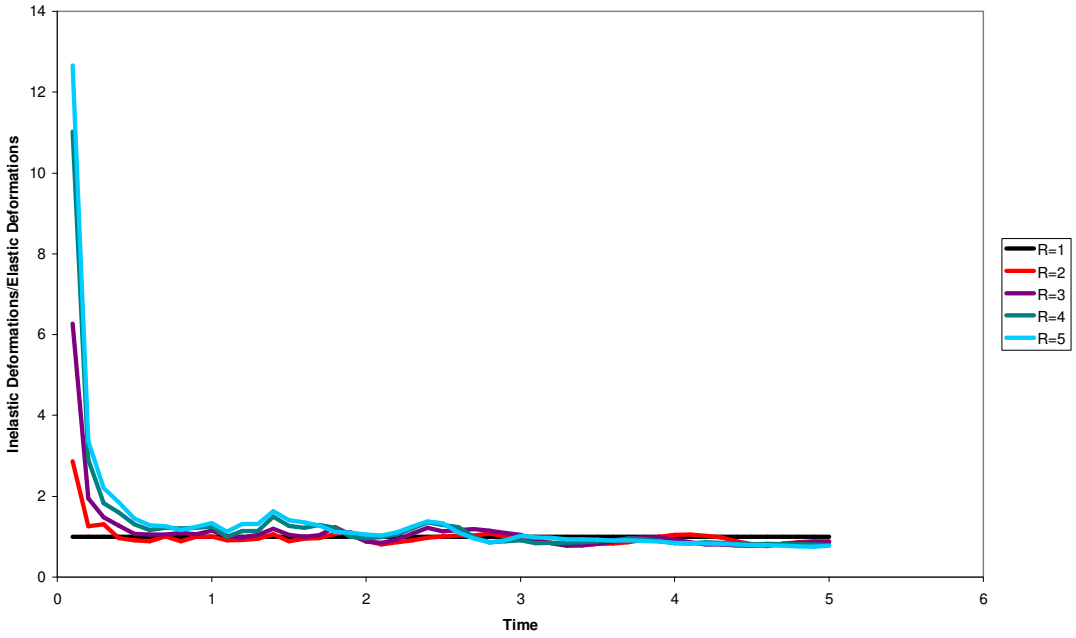

Figure 7.5. Inelastic deformation demands/elastic deformation demands for constant R values for E2 earthquake set of data

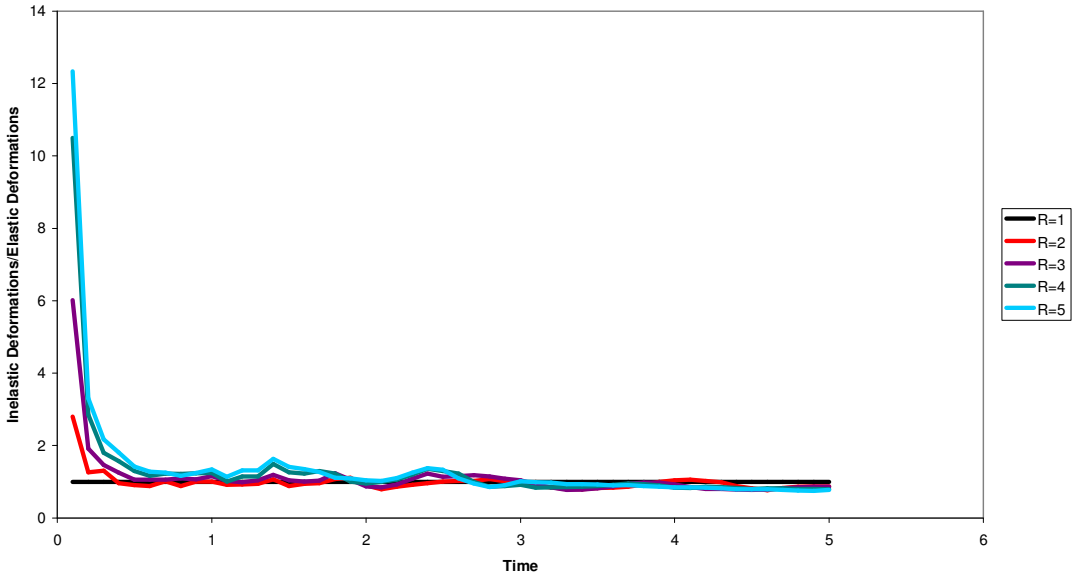

Figure 7.6. Inelastic deformation demands/elastic deformation demands for constant R values for E3 earthquake set of data

7.2. Analysis Procedures

7.2.1. Non Linear Response History Analysis

Once a structural model is formed and a set of realistic strong ground motion data is selected performing a nonlinear response history analysis is as straight forward as a nonlinear static analysis with the exception of a reasonable representation of inherent damping. In nonlinear static procedures the structural damping is represented at the demand side of the procedure which is the spectral displacements of a single degree of freedom system evaluated with the relevant damping ratios. In nonlinear response history analysis however selection of damping is important to evaluate response of the structure with reasonable accuracy.

Since the computer programs available for nonlinear response history analysis uses direct integration of the equation of motion at each sides the most common form of damping used is the Rayliegh damping which is a function of both stiffness and mass.

Rayleigh damping assumes that the structure has a damping matrix given by :

$$C = \alpha_i M + \beta_i K \tag{7.5}$$

where C is the damping matrix, M is the mass matrix and K is the initial elastic stiffness matrix. The relevant coefficients of α_i and β_i can be evaluated by the following formulas:

$$\alpha_i = \frac{T_i}{4\pi\xi} \tag{7.6}$$

$$\beta_i = \frac{T_i \xi}{\pi} \tag{7.7}$$

where the summation of α_i and β_i is equal to ξ_i variation of damping with respect to period is shown in Figure 7.7.

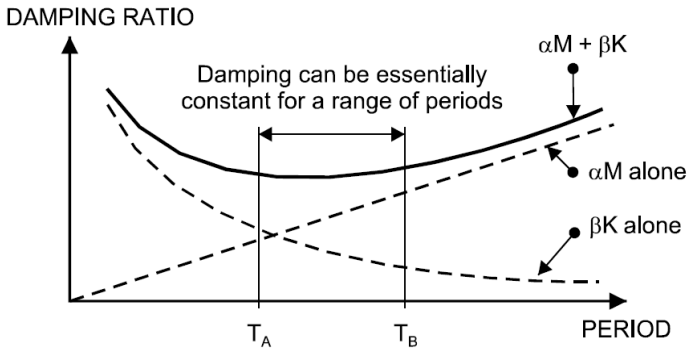

Figure 7.7. Variation of damping ratio with period (Perform 3-D)

When this type of damping is used it should be noted that after the structural elements yield it will soften therefore as shown in Figure 7.5, the damping can be over estimated when the elastic periods are used. For this reason the damping term should be defined for a period reasonable higher than the period of interest.

Some commercial programs update the damping matrix in each step of the analysis with the change in the stiffness matrix in order to keep the damping constant through the nonlinear response history analysis. In this case definition of damping will only be constrained to the periods of interest. It should also be noted that this type of analysis is highly time consuming and most likely diverge, offering no solution, therefore is not advised.

7.2.2. Spectrum Based Approximate Nonlinear Analysis Methods

For decades the inelastic time history analysis has been the only tool of predicting inelastic deformation demands of structures. The difficulty of performing such an analysis have led to codes which are based ductility of the structure that ignores the fact that the structural response is nonlinear by using response modification coefficients applied to a force-based design procedure with an elastic force demand.

With the recent earthquakes in mid 90's in USA and JAPAN the huge amount of economic loss have led the engineering community to come out with new codes or guidelines which have multiple performance definitions. The guidelines and codes developed in this era promoted deformation based methods instead of force-based methods

(FEMA 273,ATC 40). The before mentioned complexity of performing inelastic time history analysis forced the structural engineering society to look for simpler analysis methods which then led to Nonlinear Static Procedure (NSP). In this method seismic demands are computed by nonlinear static analysis of structure subjected to monotonically increasing lateral force with an invariant height-wise distribution until a predetermined target displacement is reached. Two of the most common methods used for this purpose are the Capacity Spectrum Method (CSM) and Displacement Coefficient Method (DCM) which are based on the previous studies of Freeman (1975) and Fajfar (1988). These two methods introduced a two stage procedure where in the first stage a nonlinear capacity curve of an equivalent SDOF system is provided and in the second stage seismic demands are evaluated through nonlinear analysis of this equivalent SDOF system under a given inelastic response spectrum. The major drawback of these methods is that the force distribution and the seismic demand evaluation is controlled by the fundamental mode. The assumption of controlling response by a single mode is satisfactory for regular and low-rise structures however it fails to predict seismic demands for irregular structures with a reasonable margin. To overcome this limitation many researchers have made studies to include more than the fundamental vibration mode. Unfortunately all but two have failed to satisfy the second stage of NSP. The methods proposed by Chopra (Modal Pushover Analysis, 2003) and Aydınoğlu (Incremental Response Spectrum Analysis, 2003) successfully conform the above definitions. In this study MPA has been used as a prediction tool and its ability to predict deformation demands have been tested for pile supported marine structures.

7.3. Modal Pushover Analysis

7.3.1. Theory

The classical modal analysis procedure for elastic systems may be interpreted as finding the response of the structure to $\mathbf{p}_{\text{eff},n}(t)$ for each n and superposing the responses for all n. The response of the system to $\mathbf{p}_{\text{eff},n}(t)$ is entirely in the nth mode, with no contribution from other modes, which implies that the modes are uncoupled. Then the floor displacements are given by

$$u_n(t) = \Phi_n q_n(t) \tag{7.8}$$

where the modal coordinate is governed by

$$\ddot{q}_n = 2\xi_n \omega_n \dot{q}_n + (\omega_n)^2 q_n = -\Gamma_n \ddot{u}_g \text{ (t)} \tag{7.9}$$

$$q_n(t) = \Gamma_n d_n(t) \text{ (t)} \tag{7.10}$$

Substituting Equation 7.10 into Equation 7.8 gives the lateral displacements in the *x* and *y* directions and torsional rotations of the floors:

$$u_{xn}(t) = \Phi_{xn}\Gamma_{xn} d_n(t) \; u_{yn}(t) = \Phi_{yn}\Gamma_{xn} d_n(t) \; u_{\theta n}(t) = \Phi_{\theta n}\Gamma_{xn} d_n(t) \tag{7.11}$$

Equations 7.10 represent the response of the MDF system to $\mathbf{p}_{\text{eff,n}}(t)$. Therefore, the response of the system due to total excitation $\mathbf{p}_{\text{eff,n}}(t)$is

$$r_t = \sum_{n=1}^{3N} r_n(t) \tag{7.12}$$

This is the UMRHA procedure for exact analysis of elastic systems, which is identical to the classical modal RHA. However, these standard equations have been derived in an unconventional way to rational basis for the Modal Pushover Analysis (MPA) procedure.

Although modal analysis is not valid for an inelastic system, its response can be usefully discussed in terms of the modal coordinates of the corresponding elastic system. Each structural element of this elastic system is defined to have the same stiffness as the initial stiffness of the same structural element of the inelastic system. Both systems have the same mass and damping. Therefore, the natural vibration periods and modes of the corresponding elastic system are the same as the vibration properties—referred to as natural "periods" and "modes"—of the inelastic system undergoing small oscillation.

The response of an inelastic system to excitation $\mathbf{p}_{\text{eff,n}}(t)$ will no longer be described by Equation 7.8 because "modes" other than the *n*th "mode" will also contribute to the response, implying that the vibration modes of the corresponding elastic system are now coupled; thus the floor displacements are given by the first part of Equation 7.13:

$$u_n(t) = \sum_{n=1}^{3N} \Phi_r q_r(t) \approx \Phi_n q_n(t) \tag{7.13}$$

This is based on the assumption that even after the yielding of an element the coupling of the modes is very small and the predefined mode for the response history is still dominant. Thus the structural response due to excitation $\mathbf{p}_{\text{eff,n}}(t)$ by the second half of Equation 7.13 where is governed by

$$\ddot{q}_n = 2\xi_n \omega_n \dot{q}_n + \frac{F_{sn}}{M_n} = -\Gamma_n \ddot{u}_g \text{ (t)} \tag{7.14}$$

and F_{sn} is a nonlinear hysteretic function of q_n :

$$F_{sn} = F_{sn}(q_n, sign\dot{q}_n) = \Phi_n^T f_s(q_n, sign\dot{q}_n) \tag{7.15}$$

If the contributions of other modes had not been neglected, F_{sn} would depend on all modal coordinates, implying coupling of modal coordinates because of yielding of the structure. With the above-stated approximation, the solution of Equation 7.14 can be expressed as Equation 7.10 where $\mathrm{d}_n(t)$ is governed by

$$\ddot{d}_n = 2\xi_n \omega_n \dot{q}_n + \frac{F_{sn}}{M_n} = \ddot{u}_g \tag{7.16}$$

d_n (*t*)may be interpreted as the deformation response of the *n*th-"mode" inelastic SDF system, an SDF system with small-oscillation vibration properties—natural frequency and damping ratio ξ *n* —of the *n*th mode of the corresponding linear system; and (2) $F_{sn}/L_n - \mathrm{d}_n$ relation between resisting force and deformation, where

$$F_{sn} = F_{sn}(d_n, sign\dot{d}_n) = \Phi_n^T f_s(d_n, sign\dot{d}_n) \tag{7.17}$$

which will be determined by nonlinear static or pushover analysis of the system using a modal force distribution. Introducing the *n*th mode inelastic SDF system permitted extension of the well-established concepts for elastic systems to inelastic systems; compare Equation 7.9 to 7.14, Equation 7.11 to 7.17, and note that Equation 7.9 applies to both systems.

Solution of the nonlinear Equation 7.17 provides $d_n\ (t)$, which substituted into Equations. 7.11 and 7.12 gives floor displacements and story drifts. Equations 7.11 and 7.12 approximate the response of the inelastic MDOF system to $\mathbf{p}_{\text{eff,n}}\ (t)$, the *n*th-mode contribution to $\mathbf{p}_{\text{eff,n}}\ (t)$. The superposition of responses to $\mathbf{p}_{\text{eff,n}}\ (t)$, according to Equation 7.13 to obtain the total response to $\mathbf{p}_{\text{eff,n}}\ (t)$, is strictly valid only for linearly elastic systems; however, it is assumed to be valid for symmetric-plan inelastic systems. This is the UMRHA procedure for approximate analysis of inelastic systems. When specialized for linearly elastic systems, it becomes identical to the rigorous classical modal RHA described earlier.

7.3.2. Procedure

In the MPA procedure, the peak response *rn* of the inelastic building to effective earthquake forces **p**eff,n (t) is estimated by a nonlinear static analysis of the structure subjected to lateral forces and torques distributed over the building height with the forces increased to push the structure up to roof displacements u_{rxn}, u_{ryn}, $u_{r\theta n}$.

$$u_{rxn}(t) = \Gamma_n \Phi_{rxn} d_n \ ; \ u_{ryn}(t) = \Gamma_n \Phi_{ryn} d_n \tag{7.18}$$

These values of the roof displacement components are determined from Equation 7.18, as for elastic systems, but d_n is now the peak deformation of the *n*th-"mode" inelastic SDF system, determined by solving Equation 7.17 for $d_n\ (t)$. Alternatively, d_n can be determined from inelastic response (or design) spectrum or the elastic response (or design)

spectrum in conjunction with empirical equations for inelastic deformation ratio. At this roof displacement, nonlinear static analysis provides an estimate of the peak value r_n of response quantity $r_n(t)$: floor displacements, story drifts, and other deformation quantities.

For an inelastic system, no invariant distribution of forces will produce displacements proportional to the *n*th elastic mode. Therefore, the three components of roof displacement of an inelastic system will not simultaneously reach the values given by Equation 7.18. One of the two lateral components will be selected as the controlling displacement; the choice of the component would be the same as the dominant motion in the mode being considered. Nonlinear static analysis using force distribution leads to the *n*th-"mode" pushover curve, a plot of base shear V_{bn} versus roof displacement u_{rn} in the appropriate (x or y) direction. At the yield point the base shear is V_{bn}^{y} and the roof displacement is u_{rn}^{y} Figure 7.8 shows properties of the *n*th mode inelastic SDOF system pushover curve.

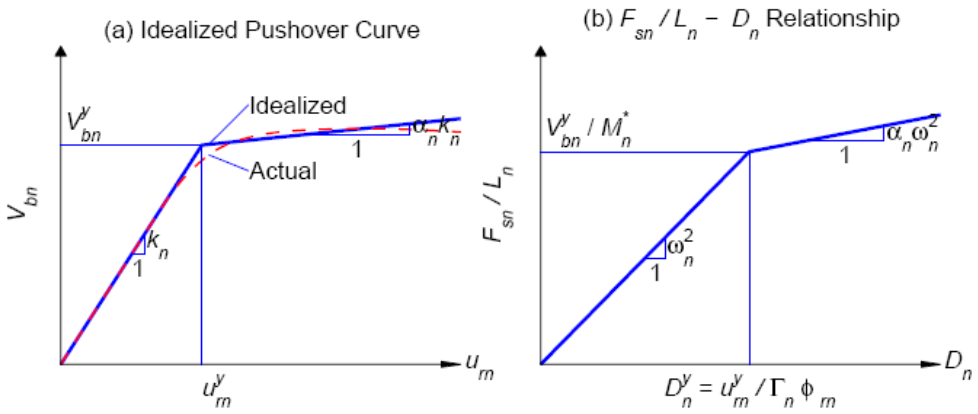

Figure 7.8. Properties of the *n*th mode inelastic SDOF system from the pushover curve

The nonlinear capacity curve of *n*th mode inelastic SDOF system is required to determine d_n In an unsymmetrical-plan building the nonlinear static procedure leads to two pushover curves corresponding to the two lateral directions, x and y. In principle, both

pushover curves will lead to the same nonlinear capacity curve thus either one may be used.

MPA procedure contains a different source of approximation, which does not exist in UMRHA. The peak "modal" response r_n , each determined by one pushover analysis, are combined by the CQC rule, just as for elastic systems. This application of modal combination rules to inelastic systems obviously lacks a rigorous theoretical basis, but seems reasonable because the modes are assumed to be weakly coupled.

A step-by-step summary of the MPA procedure to estimate the seismic demands for an unsymmetrical-plan multistory building is presented as a sequence of steps :

1. Compute the natural frequencies, ω_n and modes, Φ_n , for linearly elastic vibration of the building.
2. For the *n*th-mode, develop the base shear-roof displacement, V_{bn} -u_{rn} , pushover curve by nonlinear static analysis of the building using the force distribution. Between the two pushover curves obtained corresponding to two lateral directions, *x* and *y*, preferably choose the pushover curve in the dominant direction of motion of the mode. Gravity loads, including those present on the interior (gravity) frames, are applied before pushover analysis. Note the value of the lateral roof displacement due to gravity loads, u_{rg} .
3. Idealize the pushover curve as a bilinear curve. If the pushover curve exhibits negative post yielding stiffness, the second stiffness (or post-yield stiffness) of the bilinear curve would be negative.
4. Convert the idealized V_{bn}-u_{rn} pushover curve to the force-displacement, F_{sn} /L_n-d_n relation for the *n*th-"mode" inelastic SDOF system.
5. Compute the peak deformation d_n of the nth-"mode" inelastic single-degree-of-freedom (SDOF) system defined by the force-deformation relation developed in Step 4 and damping ratio ξ_n .
6. Calculate peak roof displacement u_{rn} in the direction of the selected pushover curve associated with the *n*th-"mode" inelastic SDOF system from $u_{rn}(t) = \Gamma_n \Phi_{rn} d_n$.

7. From the pushover database (Step 2), extract values of desired responses r_{n+g} due to the combined effects of gravity and lateral loads at roof displacement equal to $u_m + u_{rg}$
8. Repeat Steps 3-7 for as many modes as required for sufficient accuracy.
9. Compute the dynamic response due to nth-"mode": $r_n = r_{n+g} - r_g$, where r_g is the contribution of gravity loads alone.
10. Determine the total response (demand) by combining gravity response and the peak "modal" responses using the CQC or SRSS rule. (Chopra, 2003)

8. SEISMIC BEHAVIOR OF BATTER PILE SYSTEMS

The general design hypothesis for pile supported marine structures is to ensure that the cap-beam and the deck system will remain elastic and the yielding will occur either at pile-to-cap-beam connection or the pile itself. Traditionally the design is usually performed with force-based design methods, where the structure is expected to withstand elastic seismic design forces divided by response modification factors. Having a brace frame characteristics pile supported marine structures with batter piles have certain post-yield behavior modes that may produce a structural behavior much different than the above-mentioned design concept.

In this chapter possible post-yield behavior modes and their relation to structural performance have been investigated through nonlinear analysis of generic pier structures. The investigated post-yield modes are:

- Pile pull-out in the soil and the effect of soil nonlinearity to structural elements.
- Pile-to-cap-beam connection yielding and its contribution to pole vaulting effect.
- The fragile behavior of batter piles with non-compact steel sections.

Over the last ten years the use of structural fuses to control section forces transmitted to batter piles have been very popular. The use and applicability of such a fuse system have also been investigated.

Pier structures are usually consisted of long and regular segments, where a two dimensional frame as shown in Figure 8.1 will be sufficient to reflect the structural characteristic of the system. Based on this fact, in order to investigate seismic behavior of batter pile systems, two dimensional generic frame models with a lumped mass at cap-beam level are used in this study. Also to simplify and reduce the amount of data to work with, a single mode pushover analysis is performed for structures where no strength deterioration is expected. The structural deformation demands are calculated by taking advantage of equal displacement approximation. For structures where severe strength deterioration is observed due to connection fracture or inelastic local buckling of steel

piles, structural deformation demands are calculated through a series of inelastic response history analysis with the time history records explained in Chapter 7.

The cap-beams in these generic frames are modeled with non-yielding frame elements, consistent with the previously explained design philosophy. In a typical modern pier construction, the steel pipe piles are usually cut below the bottom reinforcement bar of the cap-beam. The full-moment connection of the steel pile to the-cap beam is provided by mild steel bars extending from the concrete fill of the steel pipe-pile to cap-beam (Figure 8.3 and 8.4). The pile in this zone has the strength and stiffness properties of a reinforced concrete section with a length equal to twice the strain penetration length of the reinforcing bar, which is also equal to the plastic hinge length of the section. The pile-to-cap-beam elements are modeled with fiber elements to reflect a more accurate axial vs. flexural deformation interaction (Figure 8.6).

From the pile-to-cap-beam connection to the end of the concrete fill, the pile has the stiffness and strength properties of a full composite section (Figure 8.3 and 8.4). In this zone, the pile is modeled with elastic beam elements and lumped plastic P-M-M hinges, located under the pile-to-cap-beam element.

From the concrete fill to the tip, the pile has the stiffness and strength of the bare steel section properties (Figure 8.3 and 8.4). The pile is modeled with elastic beam elements. Above the pile-soil interface, the inelastic behavior is modeled with lumped plastic P-M-M hinges located under the concrete fill and just over the pile-soil interface. Once the pile penetrates into the soil, a plastic P-M-M hinge which has a length equal to the depth of the pile section is lumped to each pile element. The plastic hinge length of steel pipe section is assumed to be one half of the section depth above the pile-soil interface and one section depth below the soil level.

The stiffness and strength of the soil surrounding the piles are modeled with nonlinear axial spring elements connected to each pile element. A section view of the pile-cap and the deck is shown in Figure 8.2. Detailed explanation of the two-dimensional structural models is illustrated in Figure 8.5.

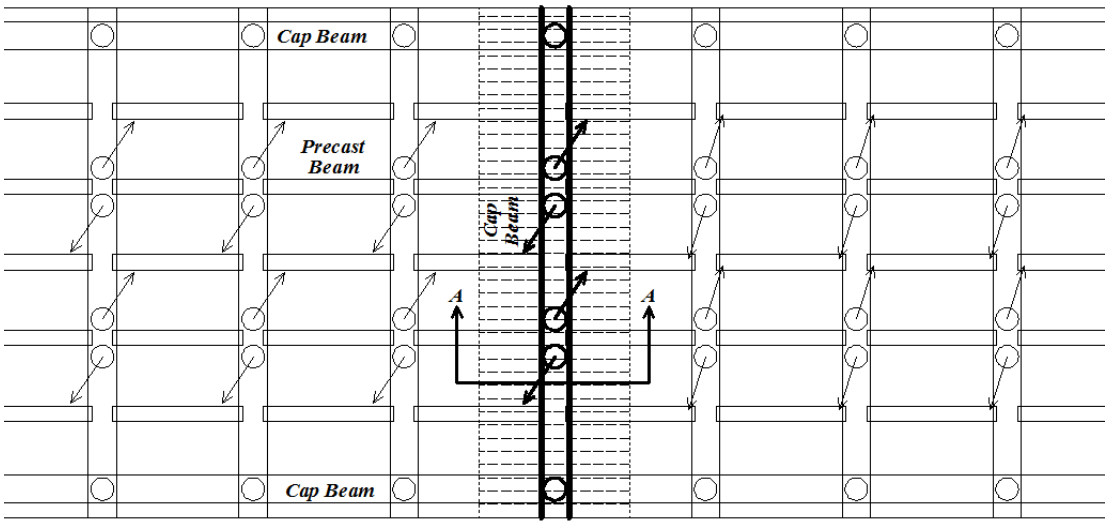

Figure 8.1. Structural system of a typical pier

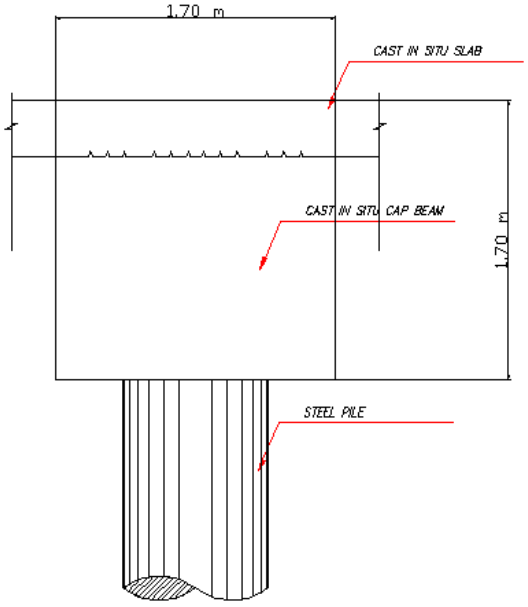

Section A-A

Figure 8.2. Section view of cap-beam

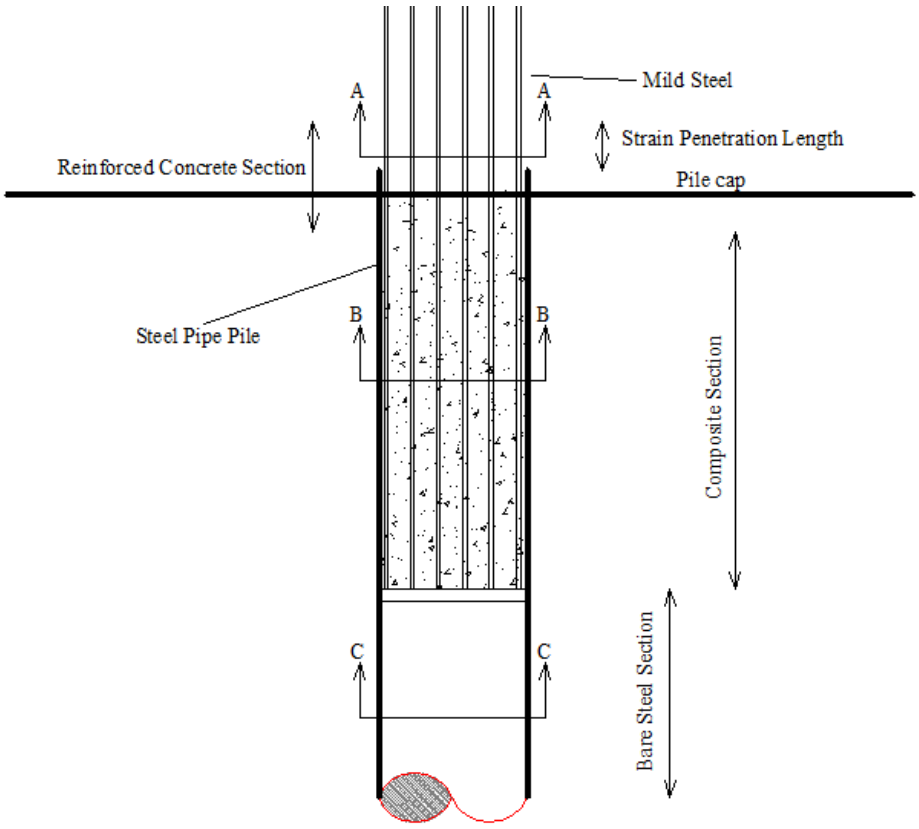

Figure 8.3. Section view of pile-to-cap-beam connection

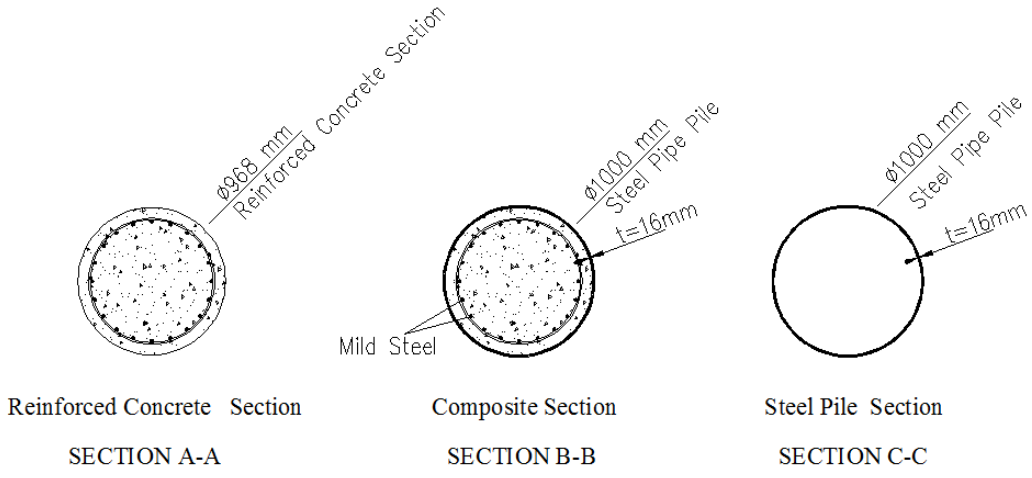

Figure 8.4. Plan view of pile sections

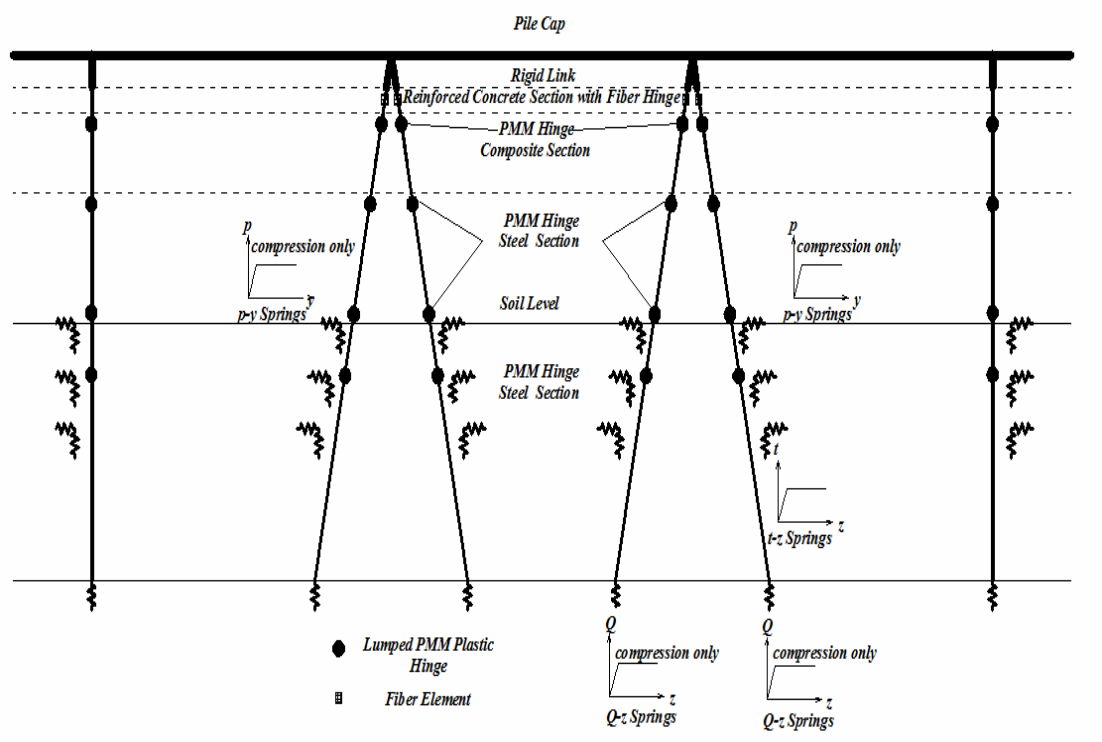

Figure 8.5. 2-Dimensional analysis model of generic pier

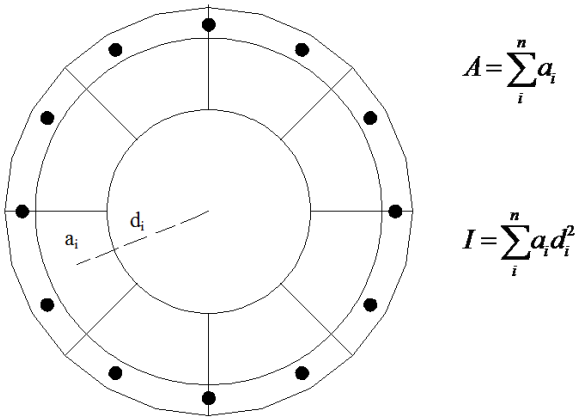

Figure 8.6. Fiber model of a reinforced concrete section

In fiber element modeling, the section is divided into finite number of concrete and steel fiber elements, each represented by the area of the divided element. The summation of each element area is equal to the total area of the section and the summation of area times square of its distance to center of gravity of the section is equal to total moment of

inertia of the section. Then a nonlinear stress strain curve is assigned to each element. The total length of fiber elements are taken equal to the plastic hinge length of the section.

The steel sections are either modeled with fiber sections or lumped P-M-M plastic hinges. The nonlinear soil spring properties are evaluated as defined in Chapter 5 for both cohesive and cohesionless soil.

2-Dimensional structural is modeled with a lumped mass at cap-beam level and therefore it is basically a single degree freedom system. The plastic deformation demands are calculated with nonlinear static procedure by taking advantage of equal displacement approximation. Once the nonlinear pushover analysis is performed, the pushover curve of the structures is drawn in terms of base shear vs. deck displacement. The same pushover curve is then transformed into Modal Capacity diagram. The inelastic deformation demand of pier can be calculated with:

$$S_{di} = S_{de} C_{R1} \tag{8.1}$$

$$C_{R1} = \frac{1 + (R_{y1} - 1) T_s / T_1^{(1)}}{R_{y1}} \geq 1 \tag{8.2}$$

$$R_{y1} = \frac{S_{ae1}}{a_{y1}} \tag{8.3}$$

where S_{di} is the predicted inelastic spectral displacement of the deck, S_{de} is the elastic spectral displacement of the relevant period and spectral displacement ratio, $C_{R1,}$ is equal to unity when the period of the structure is longer than the characteristic period of the design spectrum. R_{y1} is the strength reduction factor of the first mode, S_{ae1} is the elastic spectral pseudo-acceleration demand of the first mode, and a_{y1} is the yield strength of the equivalent SDOF system.

A typical modal capacity curve and predicted inelastic spectral displacement demand of a pier is shown in Figure 8.7.

Once the analysis is complete the inelastic deformations at pile-to-pile-cap connections can be obtained directly as strains since they are modeled with fiber elements. For other elements modeled with lumped plastic P-M-M hinges the out put is in terms of plastic rotations. Once the plastic rotation and corresponding axial force on the section is determined, the plastic rotations are transformed into plastic curvature values with the following relationship.

$$\phi_p = \frac{\theta_p}{L_p} \tag{8.4}$$

$$\phi_t = \phi_p + \phi_y \tag{8.5}$$

where ϕ_t and ϕ_p is the total curvature and total plastic curvature respectively. ϕ_y is the yield curvature of the bi-linearized moment-curvature relation, θ_p is the total plastic rotation and L_p is the plastic hinge length of the section.

After the plastic curvature is determined a moment curvature curve with the associated axial force of the section is drawn. The strain values are then read from the program for corresponding total curvature value. An example of such a calculation for a steel pipe section with 1.00 meter diameter and 0.016 m wall thickness is shown in Figure 8.8.

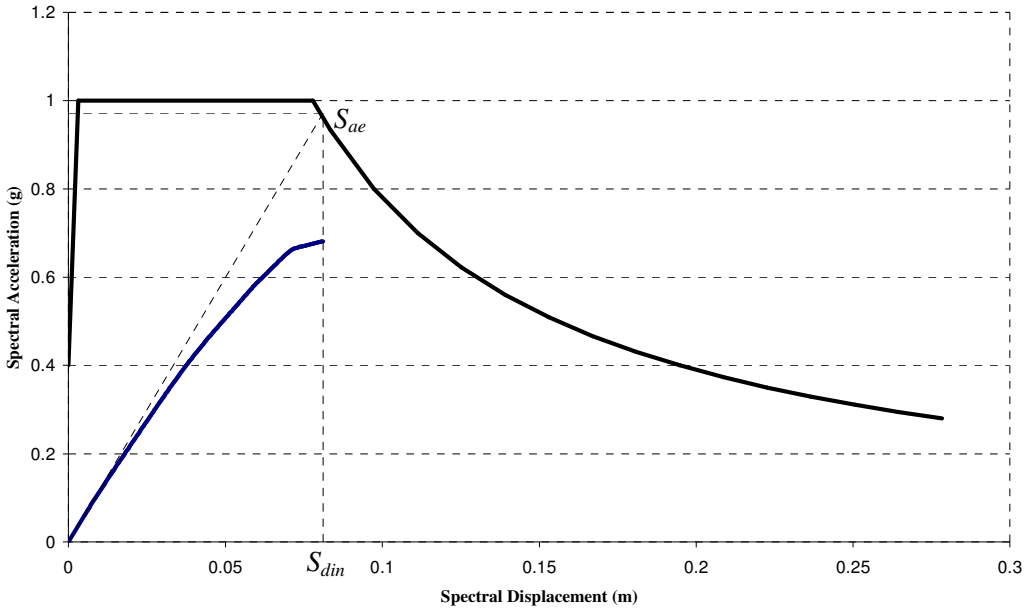

Figure 8.7. Typical modal capacity curve of a pier and estimation of inelastic pier displacement

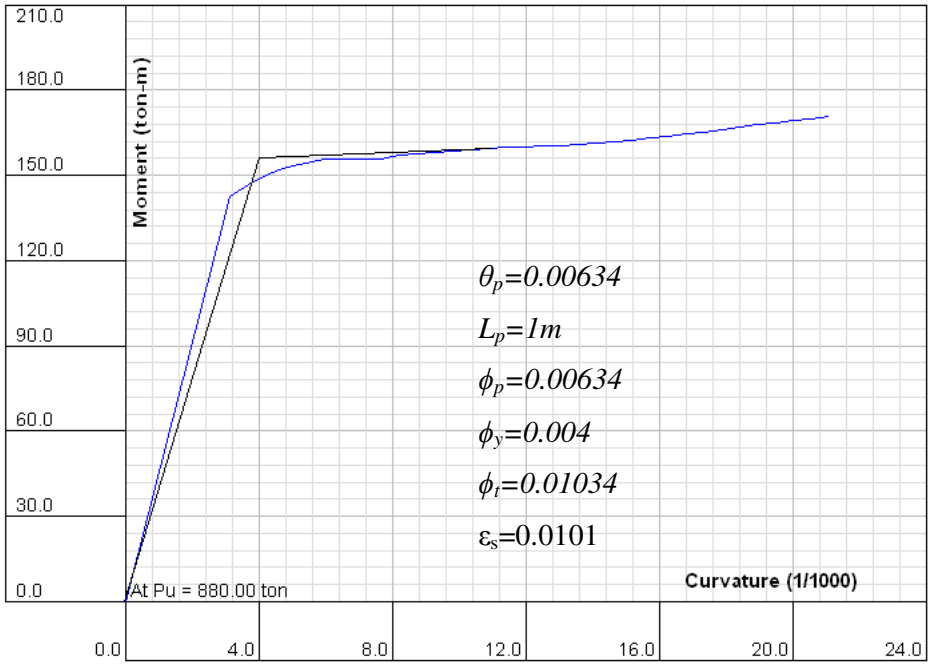

Figure 8.8. Typical moment curvature curve of a steel section and evaluation of steel strains

The structural models are consisted of piers with 24 m short edge length supported by 4 batter piles in the middle and 2 vertical piles on the edges (Figure 8.1). Each frame of the pier is placed 8 meters a part and each model has a lumped mass of 775 kNs^2/m. Also batter piles have two main configurations based on their connection type. The first one is consisted of a concentric pile-to-cap-beam connection and the second one is consisted of an eccentric pile-to-cap-beam connection. A typical section of each configuration is illustrated in Figure 8.9. and 8.10. Each structural configuration is consisted of batter piles with an inclination ranging from α=1/6 to 1/4.

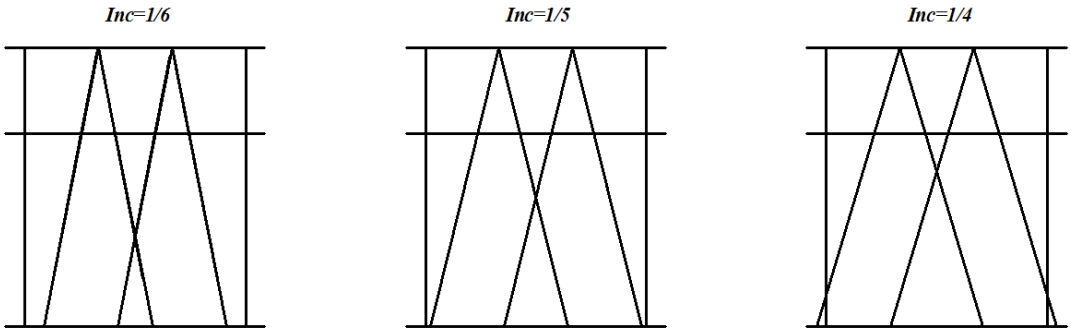

Figure 8.9. A typical section of concentric pile-to-cap-beam connection

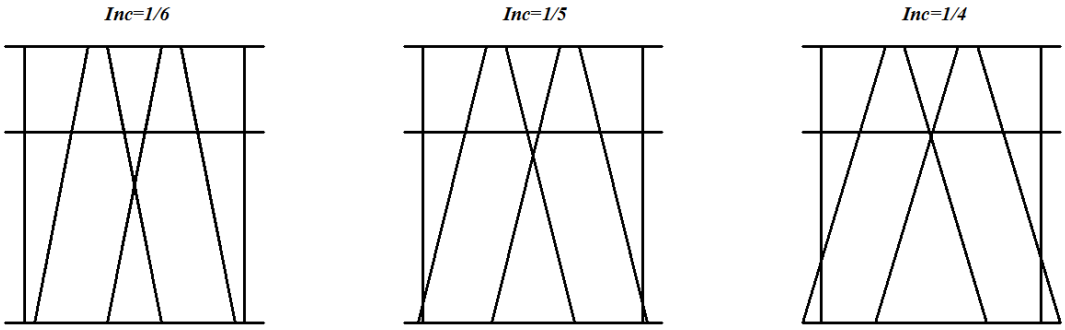

Figure 8.10. A typical section of eccentric pile-to-cap-beam connection

8.1. Significance of Soil Flexibility and Soil Nonlinearity on Response of Batter Piles

A number of codes like MOTEMS and Technical Standards for Ports, Harbor Facilities, Railroads, and Airports in Turkey (2007) encourage the use of soil flexibility and soil nonlinearity as a tool to control or limit the forces transmitted to batter piles or the damage associated to the piles or pile-to-cap-beam connections. This is usually accomplished by limiting the tension capacity of the pile and let it pull-out of the soil at a certain strength level, assuming that the soil has an infinite ductility. Even though limiting the tension capacity of the pile is expected to reduce the plastic deformations related to both pile and pile-to-pile-cap connections, it is expected to increase section design forces of structural elements such as cap-beams or decks that are expected to remain elastic during an earthquake event due to previously explained pole vaulting effect. The pull-out mechanism of pile from the soil and the resulting pole vaulting effect is explained in Figure 8.11.

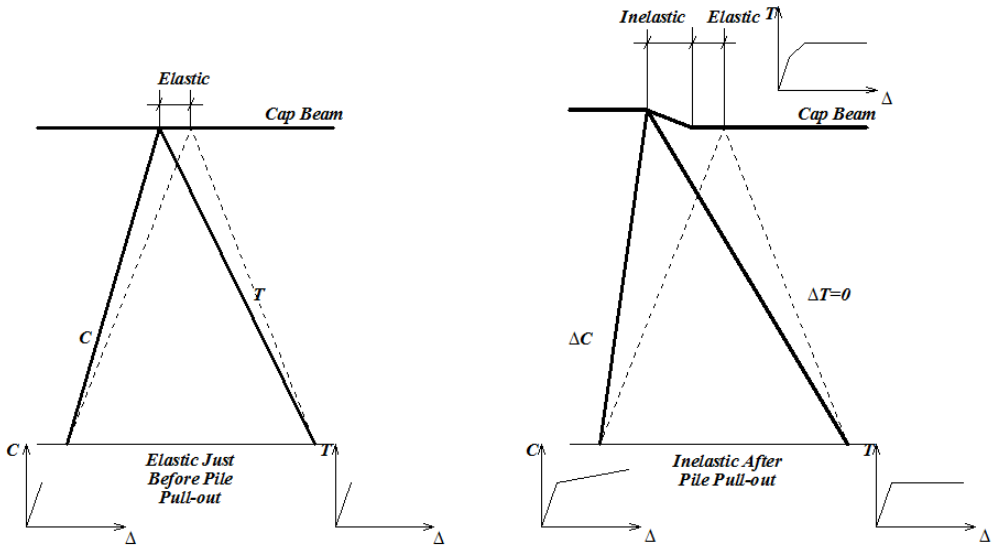

Figure 8.11. Pull-out of pile from the soil and the resulting pole vaulting effect

As it is clearly seen in Figure 8.11 once the pile pulls out of soil it can no longer transmit any more tension forces and the cap-beam and the deck start to rise over the compression pile, in which case will result in an increase at the compression forces of the compression pile and an increase in bending and shear forces at the pile cap or the deck.

To investigate this phenomenon generic pier models have been designed and analyzed with strength reduction factors of R=1.5 and R=3 for the %10/50 earthquake and R=1 for the %50/50 earthquake. The pile lengths are selected based on the fact that the soil will not be able to carry any more tension forces then the ones evaluated with the abovementioned design levels. The full tension capacity of the pile-to-cap-beam connections are selected to be higher than the pile pull-out capacity of the piles. In these structural models, the cap-beam is modeled with a reinforced concrete section of 1.7m x1.7 m dimension (Figure 8.2). The steel pile section properties and the pile lengths inside soil are provided in Table 8.1. The pile-to-pile-cap connection properties and the provided reinforcement are explained in Table 8.2. A section view of the analyzed structures with the soil profile and the corresponding soil properties are given in Figure 8.12.

In these tables and in the following figures, each strength level is associated to a design type. The design with and R=1.5 for %10/50 earthquake is named model 1, R=1 for %50/50 earthquake is named model 2 and R=3 for %10/50 earthquake is named model 3

Table 8.1. Steel pile section and material properties with pile lengths

		Pile Diameter	Wall Thickness	D/t	Material	Pile Length in Soil
Inclination		**m**	**m**			**m**
1/4	**Model 1**	1.00	0.016	62.5	Fe37	20
	Model 2	1.00	0.016	62.5	Fe37	15
	Model 3	1.00	0.016	62.5	Fe37	10
1/5	**Model 1**	1.00	0.016	62.5	Fe37	18
	Model 2	1.00	0.016	62.5	Fe37	14
	Model 3	1.00	0.016	62.5	Fe37	10
1/6	**Model 1**	1.00	0.016	62.5	Fe37	17
	Model 2	1.00	0.016	62.5	Fe37	14
	Model 3	1.00	0.016	62.5	Fe37	10

Table 8.2. Pile-to-cap-beam connection section and material properties with the provided steel reinforcement

Inclination		Con Dia m	Conc Material	Provided ConnectionReinforcement Inclined	Vertical
1/4	Model 1	0.968	BS30	24Φ30	16Φ26
	Model 2	0.968	BS30	20Φ30	16Φ26
	Model 3	0.968	BS30	12Φ28	12Φ22
1/5	Model 1	0.968	BS30	24Φ32	16Φ30
	Model 2	0.968	BS30	20Φ30	16Φ30
	Model 3	0.968	BS30	12Φ28	12Φ26
1/6	Model 1	0.968	BS30	24Φ32	16Φ30
	Model 2	0.968	BS30	20Φ30	16Φ30
	Model 3	0.968	BS30	12Φ28	12Φ26

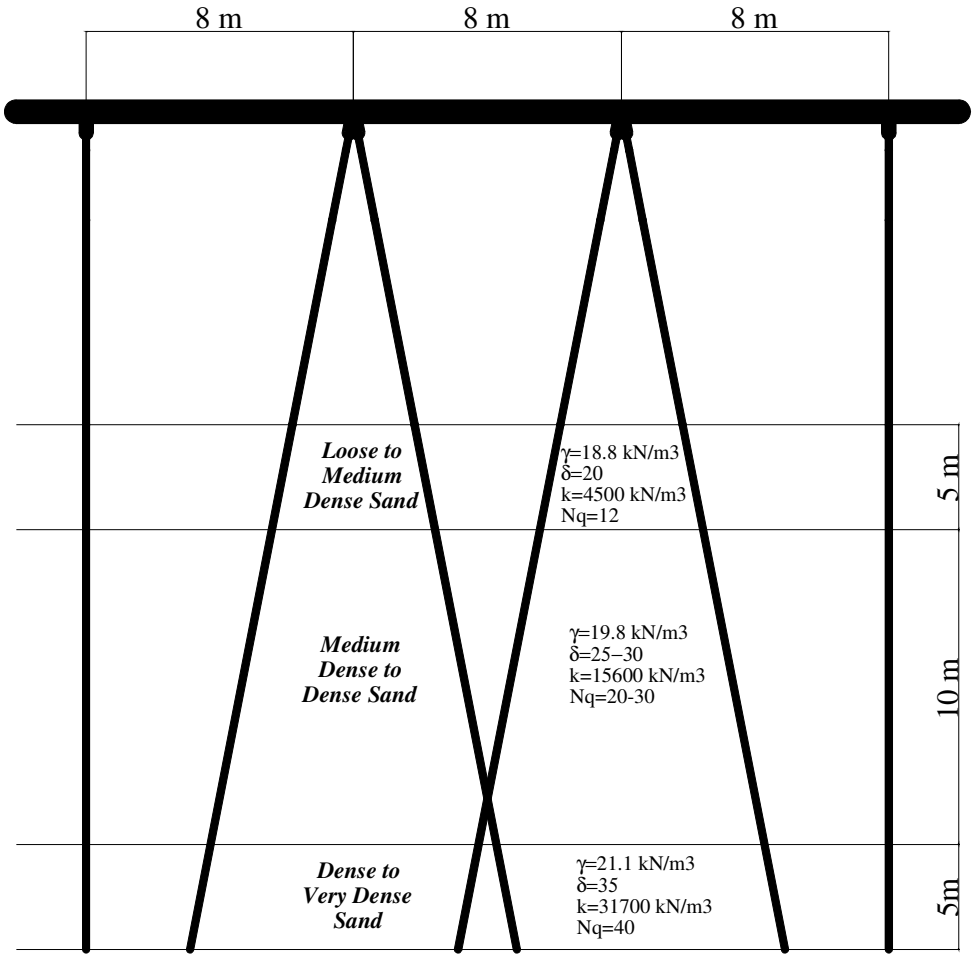

Figure 8.12. Section view of structure and the soil profile

The inelastic deformation demands are evaluated by the use of equal displacement approximation as explained before. The evaluation of inelastic deformation demand and modal capacity curves of a pier having batter piles with an inclination of 1/4 and different strength levels are shown in Figure 8.13. The structural periods and estimated spectral displacements are given in Table 8.3.

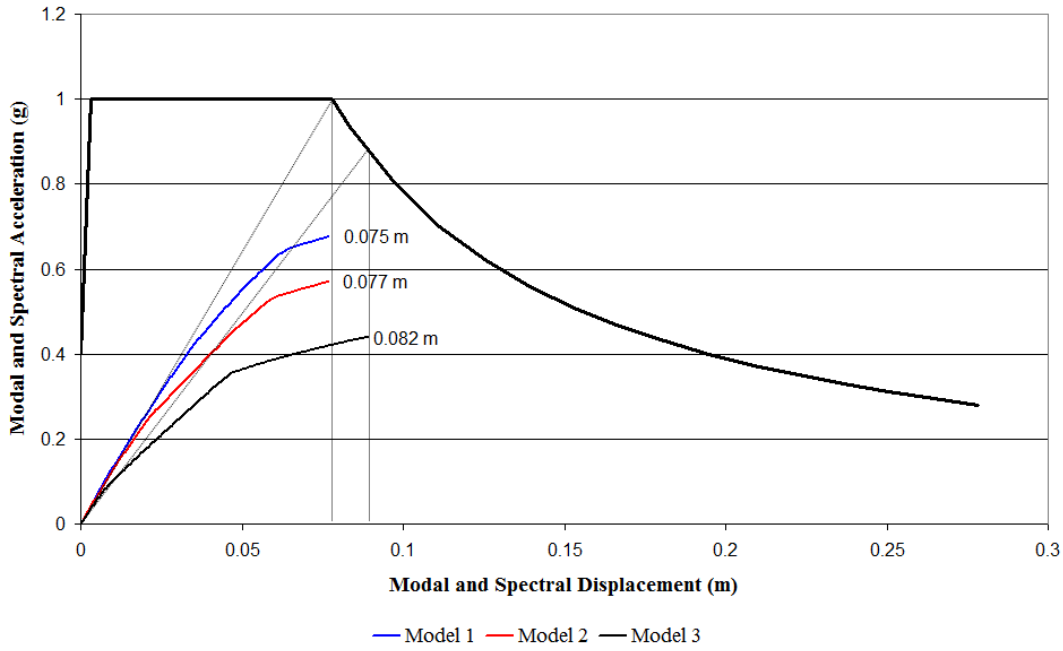

Figure 8.13. Modal capacity curves and estimated inelastic spectral deformation demands of piers with batter piles with an inclination of 1/4 and different strength levels

Table 8.3. Structural periods and corresponding inelastic spectral displacements

		T	S_{di} (m)	
Inclination		**sec**	**%10/50**	**%2/50**
1/4	**Model 1**	0.54	0.075	0.105
	Model 2	0.55	0.077	0.107
	Model 3	0.59	0.082	0.114
1/5	**Model 1**	0.62	0.086	0.120
	Model 2	0.64	0.089	0.124
	Model 3	0.67	0.093	0.130
1/6	**Model 1**	0.7	0.097	0.136
	Model 2	0.71	0.099	0.138
	Model 3	0.74	0.103	0.143

The resulting total steel strains at pile-to-pile-cap connections, composite sections and the steel piles are given in Table 8.4.

Table 8.4. Estimated maximum steel strains

		Pile to Cap Beam Connection Inclination			Composite Section Inclination			Steel Pile Inclination		
	EQ Level	1/4	1/5	1/6	1/4	1/5	1/6	1/4	1/5	1/6
Model 1	%10/50	0.0050	0.0055	0.0066	-	-	-	-	-	-
	%2/50	0.0090	0.0097	0.0113	-	-	-	-	-	-
Model 2	%10/50	0.0055	0.0055	0.0067	-	-	-	-	-	-
	%2/50	0.0089	0.0105	0.0118	-	-	-	-	-	-
Model 3	%10/50	0.0021	0.0113	0.0128	-	-	-	-	-	-
	%2/50	0.0028	0.0176	0.0205	-	-	-	-	-	-

An important indication of pole vaulting effect is the variation of vertical deformation of the pile cap over the compression pile. The pole vaulting starts where the structure starts to rise over the compression pile. The variation of vertical deformation of pile-cap over the compression pile with respect to lateral deformation and the location in which the pole vaulting starts for an %10/50 earthquake event is given in Figure 8.14.

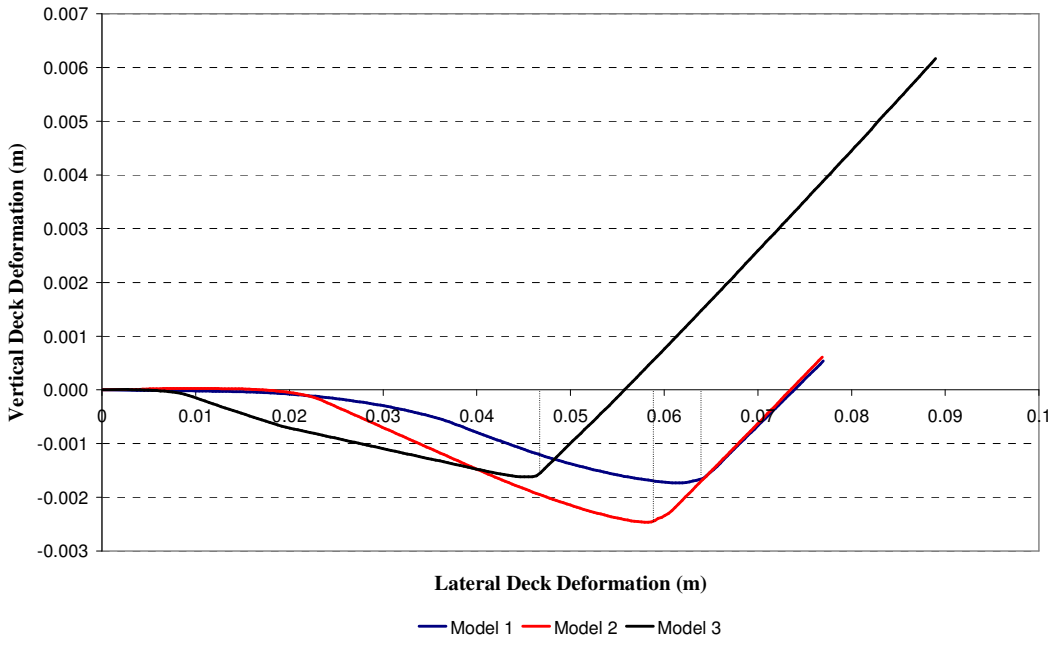

Figure 8.14. Variation of vertical deformation of the pile-cap over compression pile for %10 /50 earthquake event, at a pier having batter piles with an inclination of 1/4 with respect to lateral deformation and strength levels

The most important end product of pole vaulting effect is the amplification of section forces of cap-beam or the deck. The amplification in section design forces of the cap-beam with respect to section design forces evaluated with response modification factors presented in Figure 8.15 and 8.16 for %10/50 and %2/50 earthquakes. In these figures α stands for ratio of bending moments evaluated with nonlinear analysis to bending moments evaluated with response modification factors.

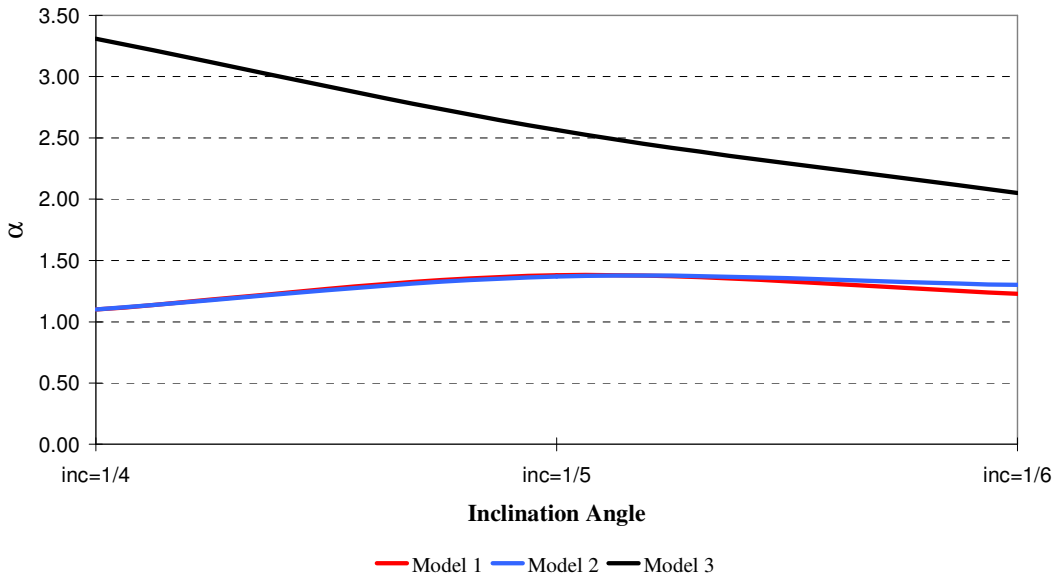

Figure 8.15. Amplification of bending moment at cap-beam due to pole vaulting effect with respect to inclination angle and soil strength at %10/50 earthquake event

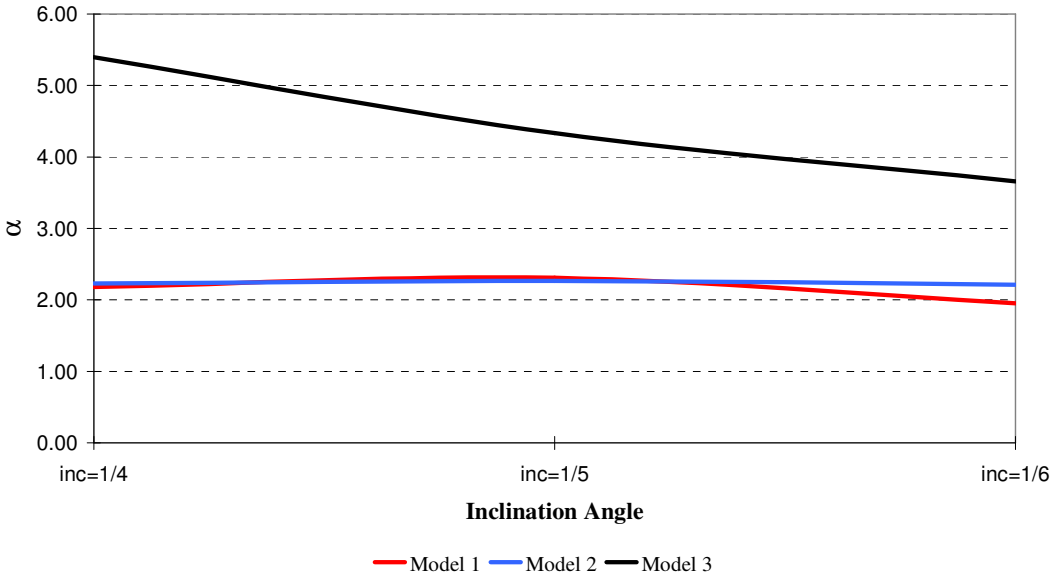

Figure 8.16. Amplification of bending moment at cap-beam due to pole vaulting effect with respect to inclination angle and soil strength at %2/50 earthquake event

After the pile-pulls out of the soil even though the increase in the tension force of the pile is zero the compression force of the batter pile still increases due to shear forces transferred from the elastic pile-cap. The variation of compression forces on the compression pile with respect to lateral deformation and strength levels for a pier, having batter piles with an inclination of 1/4 is shown in Figure 8.17. The dotted lines indicate the lateral deformation where the pole vaulting starts.

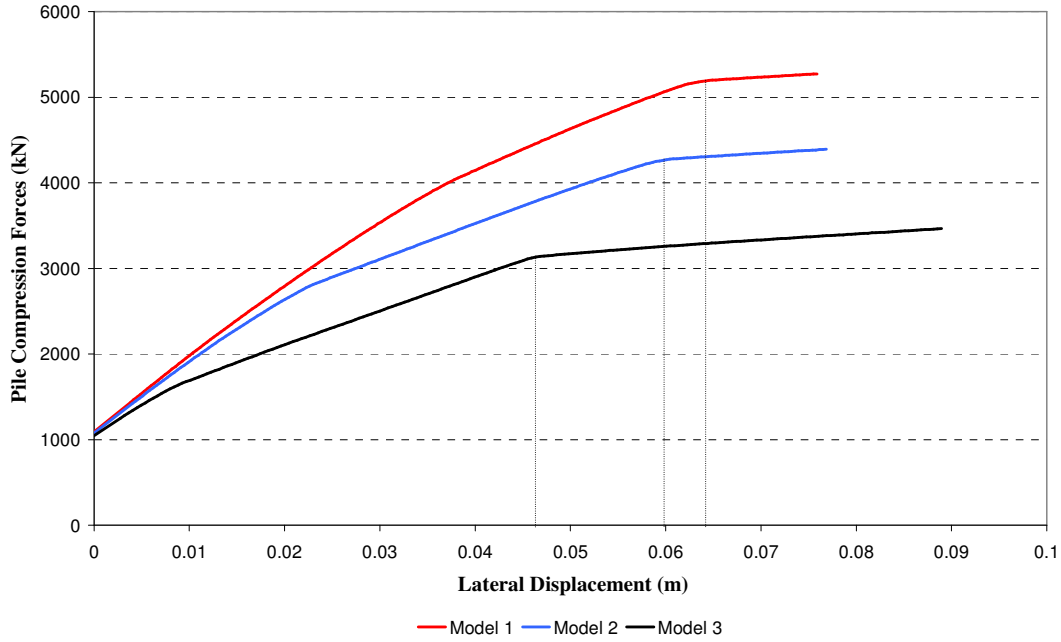

Figure 8.17. Variation of compression forces of the pile for %10 /50 earthquake event at a pier having batter piles with an inclination of 1/4, with respect to lateral deformation and strength levels

Based on the information gathered from nonlinear pushover analysis results the following points have been observed:

- There has been a significant increase in section design forces of the cap-beam due to the pole vaulting effect. This effect is more significant for lower strength levels.
- The amplification is not effected by the inclination for high strength levels but as the strength level decreases the pole vaulting effect is more pronounced by the increasing inclination.
- The high amplification factors observed for low strength level models (R=3) indicates that a force-based analysis will highly underestimate section design forces of a cap-beam and as a consequence may result in plastic deformations and damage to cap beam in multiple locations.
- Event though there has been an increase in axial compression forces of the pile with the pole vaulting effect, the increase is not very significant and since steel piles with compact cross sections have high moment capacity which are likely to yield with the existence of high axial forces, the pull-out of pile by limiting the axial loads

transferred to the pile is more likely to either delay the yielding of steel pile or reduce the plastic deformation.

- In all these models yielding is only observed at the pile-to-cap-beam connections, where the evaluated total steel strain values are well below code limitations.

8.2. Significance of Pile to Cap Beam Connection Yielding with Respect to Inclination Angle and Connection Type in Batter Piles

Engineers in today's design practice usually prefer to use Allowable Stress Design Methods where pile length is evaluated with conservative safety factors instead of ultimate strength of the soil which produce longer pile lengths than needed. In such cases the full tension capacity of the pile-to-cap-beam connection is expected to be much weaker than the soil. In this case the plastic deformations are concentrated at pile-to-cap-beam connection. Unlike the pile pull-out from the soil, the pole vaulting is not significant with the yielding of the pile-to-cap-beam connection. The reinforced concrete section at the connection first yield in combination of bending and tension, as the tension forces increase the bending capacity of the connection decreases until it reaches to the full tension capacity of the provided reinforcement. At that point the bending capacity of the section diminishes and from that point and on, the plastic deformations are only related to the axial deformations. Pole vaulting is more significant from that point. The aforementioned yielding mechanism of pile-to-cap-beam connection is shown on a moment-curvature and yield surface of a reinforced concrete section in Figure 8.18. The resulting pole vaulting effect with the variation of axial forces on the piles and the pile-to-cap-beam connection with respect to lateral deformation is explained in Figure 8.19.

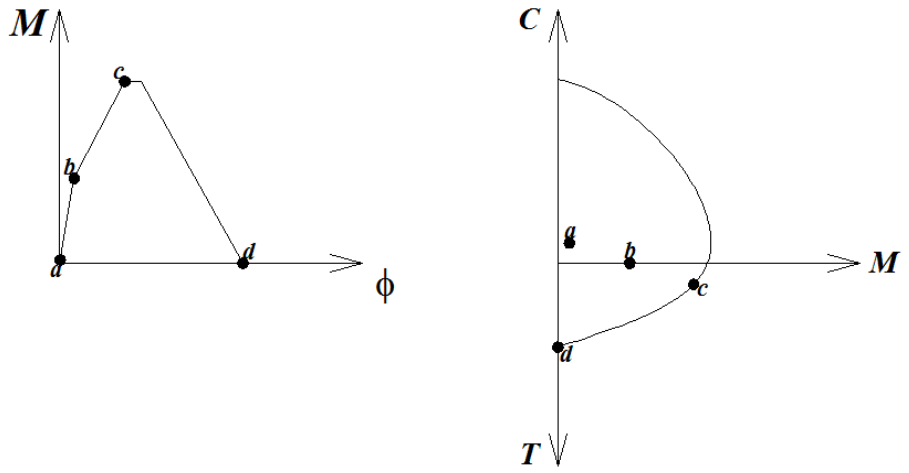

Figure 8.18. Yielding mechanism of pile-to-cap-beam connection in tension

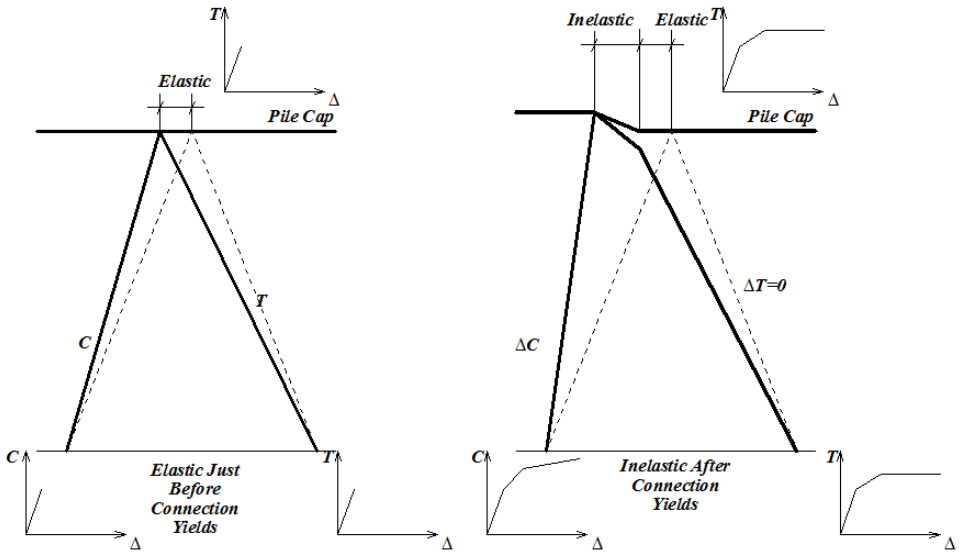

Figure 8.19. Yielding of pile-to-cap-beam connection and the resulting pole vaulting effect

In Figure 8.18, ‘a’ represents the bending moment and axial compression due to gravity loads at the pile-to-cap-beam connection, at point ‘b’, the reinforced concrete section softens due to cracking of concrete with the pure tension force on the section, at point ‘c’, the connection yields with the presence of tension and bending, once the connection yields with the increasing tension of the batter pile the bending strength of the connection travels along the yield surface until it reaches point ‘d’ , where the bending strength totally diminishes and the connection reaches its full tension capacity. From that

point and on, the plastic deformations are pure axial. Once this is accomplished the structure starts to rise significantly over the compression pile. As a result like the pile-pull-out, the cap-beam bending and shear forces significantly increases.

To investigate this phenomenon generic pier models have been designed and analyzed with strength reduction factors of R=1.5 and R=3 for the %10/50 earthquake and R=1 for the %50/50 earthquake and a lateral force equal to 0.15 times the total weight of the structure (Seismic coefficient C=0.15) representing very weak connections. Also to observe the effect of connection type to the structural behavior the piers are modeled with two main configurations based on the configuration of pile-to-cap-beam connection with respect to cap-beam. The first one is a concentric pile-to-cap-beam connection and the second one is an eccentric pile-to-cap-beam connection. The piles are modeled with end bearing supports assuming that the axial deformations in the soil layers will be very small since the soil is not going to yield. In these structural models the cap-beam is modeled with a reinforced concrete section of 1.7m x1.7 m dimensions (Figure 8.2). The steel pile section properties are provided in Table 8.5. The pile-to-cap-beam connection (Figure 8.3) properties and the provided reinforcement are explained in Table 8.6 and 8.7. A section view of the analyzed structures with the soil profile and the corresponding soil properties are given in Figure 8.20 and 8.21.

In these tables and in the following figures each strength level is associated to a design type. The design with and R=1.5 for %10/50 earthquake is named model 1, R=1 for %50/50 earthquake is named model 2 , R=3 for %10/50 earthquake is named model 3 and the design with a lateral force equal to 0.15 times the total weight is named model 4 .

Table 8.5. Steel pile section and material properties for both concentric and eccentric configurations

Inclination		Pile Diameter m	Wall Thickness m	D/t	Material
1/4	Model 1	1.00	0.016	62.5	Fe37
	Model 2	1.00	0.016	62.5	Fe37
	Model 3	1.00	0.016	62.5	Fe37
	Model 4	1.00	0.016	62.5	Fe37
1/5	Model 1	1.00	0.016	62.5	Fe37
	Model 2	1.00	0.016	62.5	Fe37
	Model 3	1.00	0.016	62.5	Fe37
	Model 4	1.00	0.016	62.5	Fe37
1/6	Model 1	1.00	0.016	62.5	Fe37
	Model 2	1.00	0.016	62.5	Fe37
	Model 3	1.00	0.016	62.5	Fe37
	Model 4	1.00	0.016	62.5	Fe37

Table 8.6. Concentric pile-to-pile-cap connection section material properties with the provided steel reinforcement

Inclination		Con Dia m	Conc Material	Provided Connection Reinforcement	
				Inclined	Vertical
1/4	Model 1	0.968	BS30	24Φ30	16Φ26
	Model 2	0.968	BS30	20Φ30	16Φ26
	Model 3	0.968	BS30	12Φ28	12Φ22
	Model 4	0.968	BS30	12Φ20	16Φ16
1/5	Model 1	0.968	BS30	24Φ32	16Φ30
	Model 2	0.968	BS30	24Φ30	16Φ30
	Model 3	0.968	BS30	12Φ28	12Φ25
	Model 4	0.968	BS30	12Φ20	16Φ16
1/6	Model 1	0.968	BS30	24Φ32	16Φ30
	Model 2	0.968	BS30	24Φ30	16Φ30
	Model 3	0.968	BS30	12Φ28	12Φ25
	Model 4	0.968	BS30	12Φ20	16Φ16

Table 8.7. Eccentric pile-to-pile-cap connection section material properties with the provided steel reinforcement

		Con Dia	Conc Material	Provided Connection Reinforcement	
Inclination		**m**		**Inclined**	**Vertical**
1/4	**Model 1**	0.968	BS30	24Φ30	16Φ26
	Model 2	0.968	BS30	20Φ30	16Φ26
	Model 3	0.968	BS30	12Φ28	12Φ22
	Model 4	0.968	BS30	12Φ20	16Φ16
1/5	**Model 1**	0.968	BS30	24Φ32	16Φ30
	Model 2	0.968	BS30	24Φ30	16Φ30
	Model 3	0.968	BS30	12Φ28	12Φ25
	Model 4	0.968	BS30	12Φ20	16Φ16
1/6	**Model 1**	0.968	BS30	24Φ32	16Φ30
	Model 2	0.968	BS30	24Φ30	16Φ30
	Model 3	0.968	BS30	12Φ28	12Φ25
	Model 4	0.968	BS30	12Φ20	16Φ16

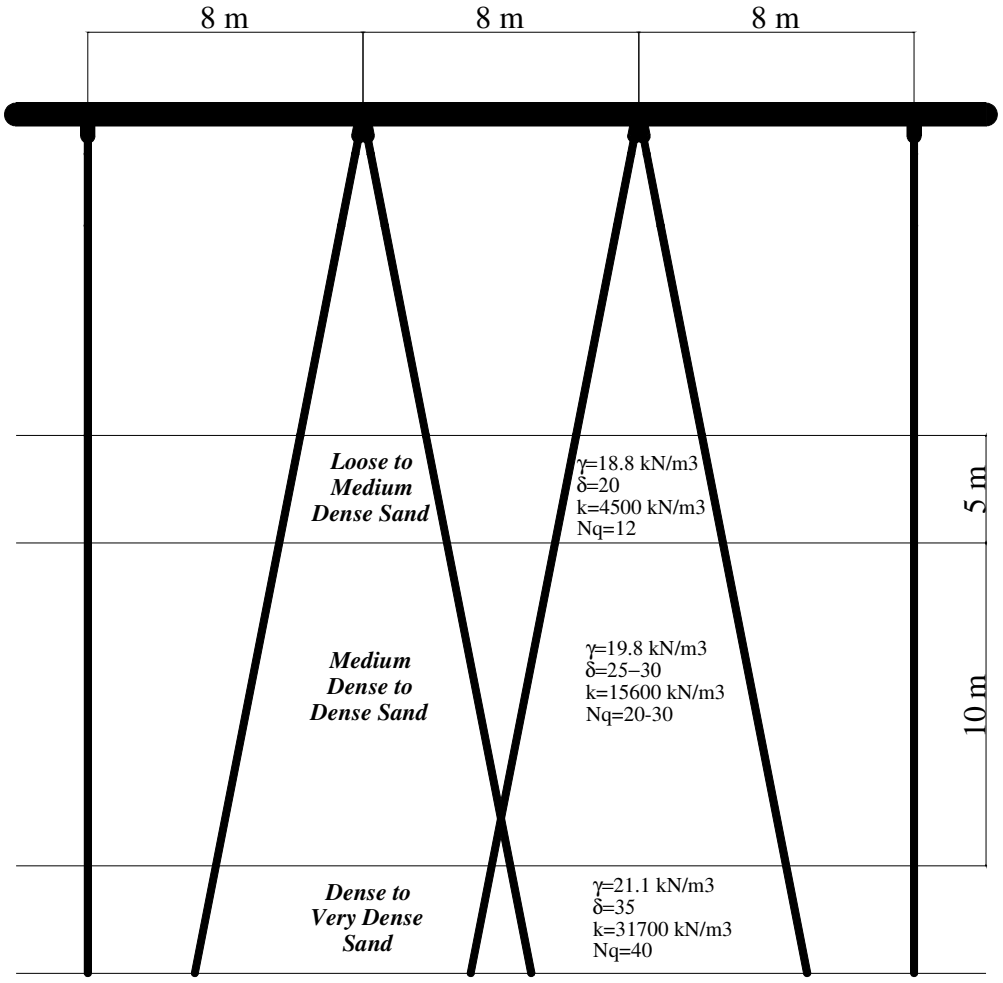

Figure 8.20. Section view of structure with concentric connection and the soil profile

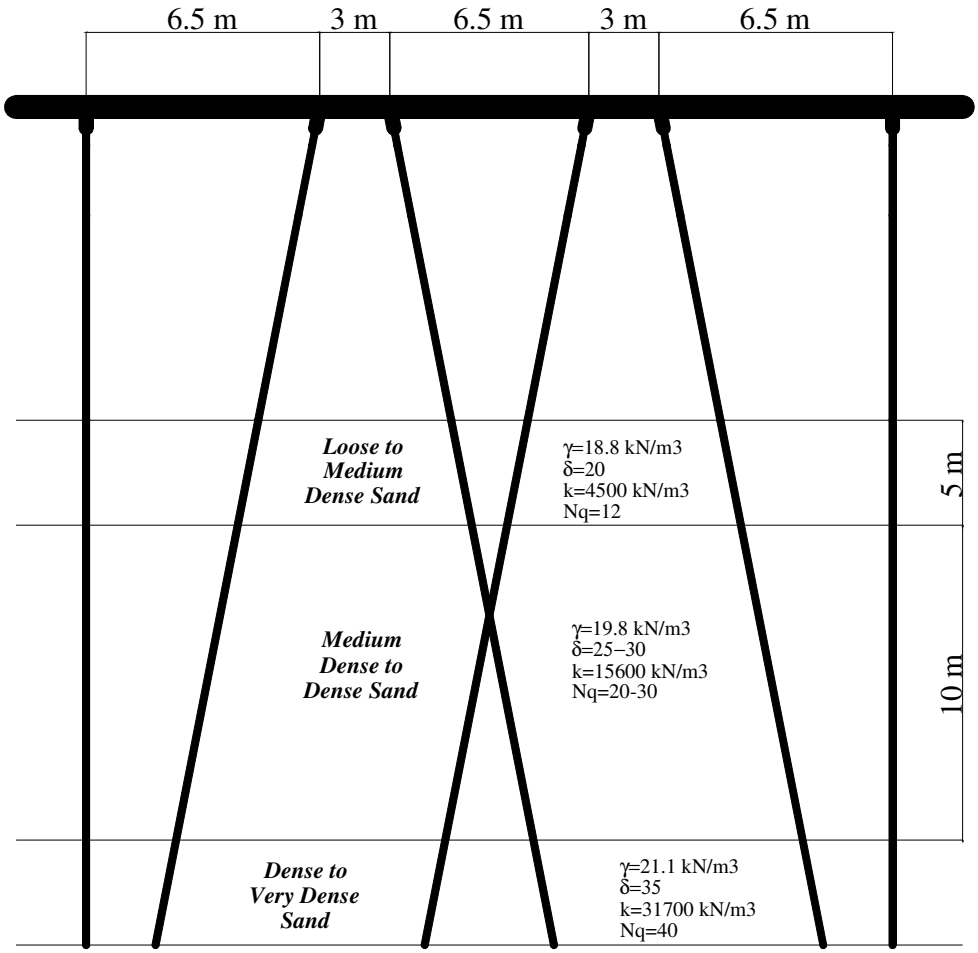

Figure 8.21. Section view of structure with eccentric connection and the soil profile

For model 1 to model 3 the inelastic deformation demands are evaluated by the use of equal displacement approximation as explained before for model 4 the inelastic deformation demands are evaluated by a series of inelastic response history analysis with the strong ground motion data defined in Chapter 7 due to severe deterioration of strength with the fracture of mild steel in tension at pile-to-cap-beam connection. The evaluation of inelastic deformation demand and modal capacity curves of a pier having batter piles with an inclination of 1/4 and different strength levels are shown in Figure 8.22. A displacement history of the same pier for model 4 is given in Figure 8.23. The structural periods and estimated spectral displacements except model 4 are given in Table 8.8. The average pier deformations from inelastic response history analysis of model 4 are given in Table 8.9.

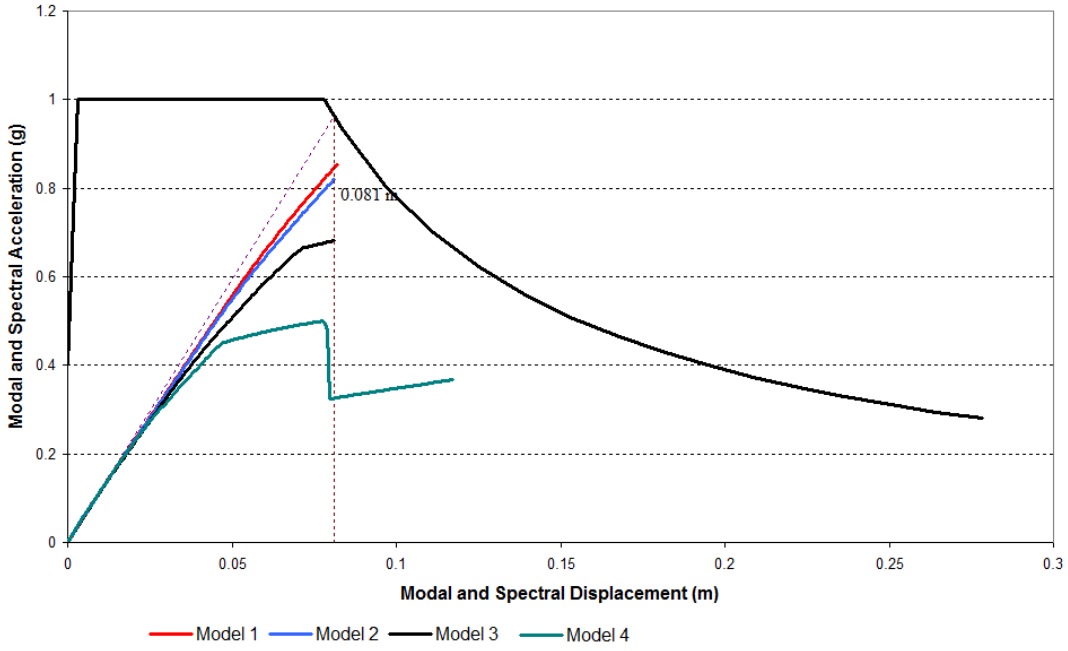

Figure 8.22. Modal capacity curves and estimated inelastic spectral deformations of piers having batter piles with an inclination of 1/4 and different strength levels for %10/50 earthquake event

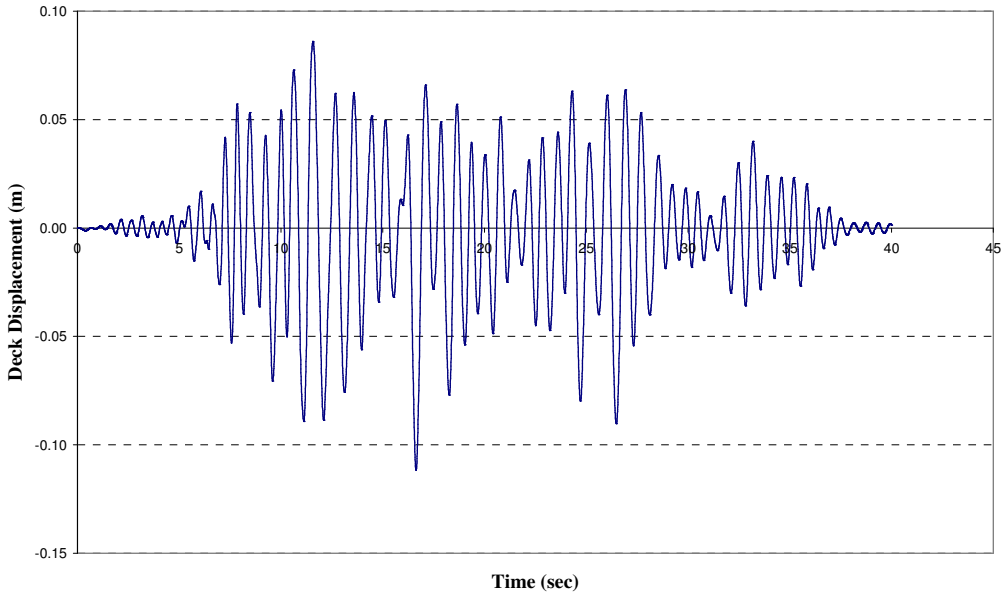

Figure 8.23. Inelastic response history of a pier having batter piles with an inclination of 1/4 for earthquake P0012

Table 8.8. Structural periods and corresponding inelastic spectral displacements

			T	S_{di} (m)	
Configuration	**Inclination**		**sec**	**%10/50**	**%2/50**
Concentric	**1/4**	**Model 1-3**	0.582	0.081	0.113
	1/5	**Model 1-3**	0.666	0.093	0.129
	1/6	**Model 1-3**	0.733	0.102	0.142
Eccentric	**1/4**	**Model 1-3**	0.584	0.081	0.113
	1/5	**Model 1-3**	0.673	0.094	0.130
	1/6	**Model 1-3**	0.738	0.103	0.143

Table 8.9. Structural periods and corresponding inelastic spectral displacements

			T	S_{di} (m)	
Configuration	**Inclination**		**sec**	**%10/50**	**%2/50**
Concentric	**1/4**	**Model 4**	0.582	11.660	-
	1/5	**Model 4**	0.666	13.000	-
	1/6	**Model 4**	0.733	14.670	-
Eccentric	**1/4**	**Model 4**	0.584	11.510	-
	1/5	**Model 4**	0.673	12.470	-
	1/6	**Model 4**	0.738	15.490	-

The resulting steel strains at pile to cap beam connections, composite sections and the steel piles are given in Table 8.10 and 8.11

Table 8.10. Estimated maximum steel strains for concentric connection configuration

		Concentric Pile-to-Cap-Beam Connection			**Composite Section**			**Steel Pile**		
		Inclination			**Inclination**			**Inclination**		
	EQ Level	**1/4**	**1/5**	**1/6**	**1/4**	**1/5**	**1/6**	**1/4**	**1/5**	**1/6**
Model 1	**%10/50**	**0.0076**	**0.0079**	**0.0083**	-	-	-	0.0000	0.0000	0.0000
	%2/50	**0.0148**	**0.0139**	**0.0147**	**-**	**-**	**-**	**0.0094**	**0.0090**	**0.0065**
Model 2	**%10/50**	**0.0095**	**0.0088**	**0.0091**	-	-	-	0.0000	0.0000	0.0000
	%2/50	**0.0210**	**0.0160**	**0.0171**	**-**	**-**	**-**	**0.0090**	**0.0088**	**0.0063**
Model 3	**%10/50**	**0.0320**	**0.0240**	**0.0200**	-	-	-	0.0000	0.0000	0.0000
	%2/50	**0.0550**	**0.0520**	**0.0480**	-	-	-	0.0000	0.0000	0.0000
Model 4	**%10/50**	**>0.12**	**>0.12**	**>0.12**	-	-	-	0.0000	0.0000	0.0000
	%2/50	**>0.12**	**>0.12**	**>0.12**	-	-	-	0.0000	0.0000	0.0000

Table 8.11. Estimated maximum steel strains for eccentric connection configuration

		Eccentric Pile-to-Cap-Beam Connection			Composite Section			Steel Pile		
		Inclination			Inclination			Inclination		
	EQ Level	1/4	1/5	1/6	1/4	1/5	1/6	1/4	1/5	1/6
Model 1	%10/50	0.0074	0.0075	0.0076	-	-	-	0.0000	0.0000	0.0000
	%2/50	0.0142	0.0137	0.0143	-	-	-	0.0111	0.0081	0.0060
Model 2	%10/50	0.0093	0.0078	0.0089	-	-	-	0.0000	0.0000	0.0000
	%2/50	0.0170	0.0154	0.0165	-	-	-	0.0110	0.0100	0.0068
Model 3	%10/50	0.0207	0.0170	0.0171	-	-	-	0.0000	0.0000	0.0000
	%2/50	0.0480	0.0438	0.0402	-	-	-	0.0000	0.0000	0.0000
Model 4	%10/50	>0.12	>0.12	>0.12	-	-	-	0.0000	0.0000	0.0000
	%2/50	>0.12	>0.12	>0.12	-	-	-	0.0000	0.0000	0.0000

The variation of vertical deformation of cap beam over the compression pile with respect to lateral deformation and the location in which the pole vaulting stars from model 1 to model 3 for %10/50 earthquake event is given in Figure 8.24.

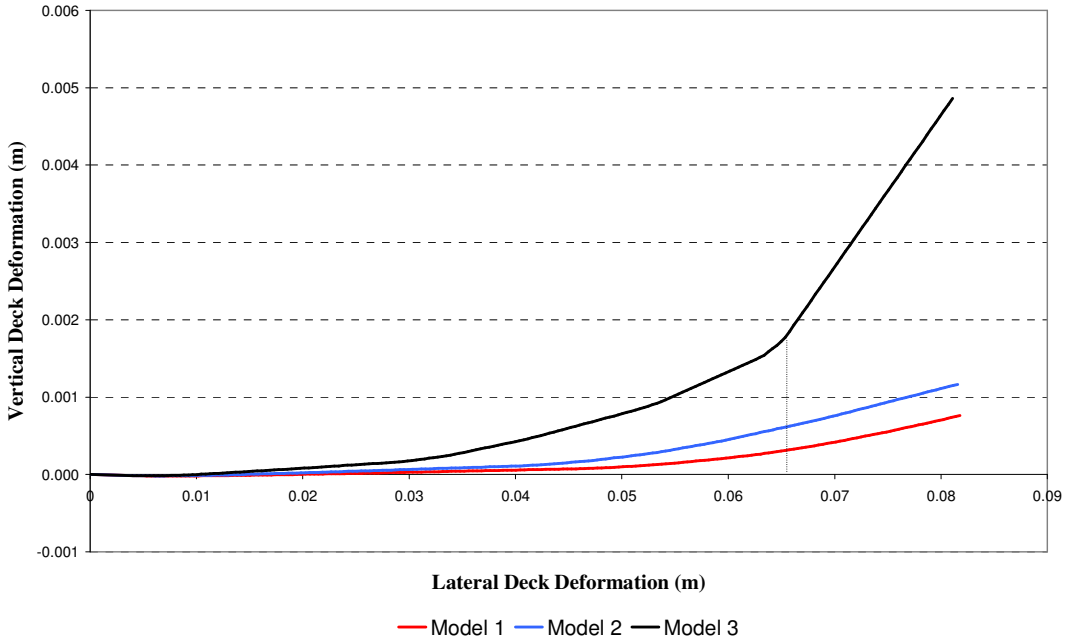

Figure 8.24. Variation of vertical deformation of the cap-beam over compression pile for %10 /50 earthquake event at a pier having batter piles with an inclination of 1/4 with respect to lateral deformation and strength levels

The variation of vertical deformation of cap beam over the compression pile with respect to lateral deformation for model 4 is given in Figure 8.25.

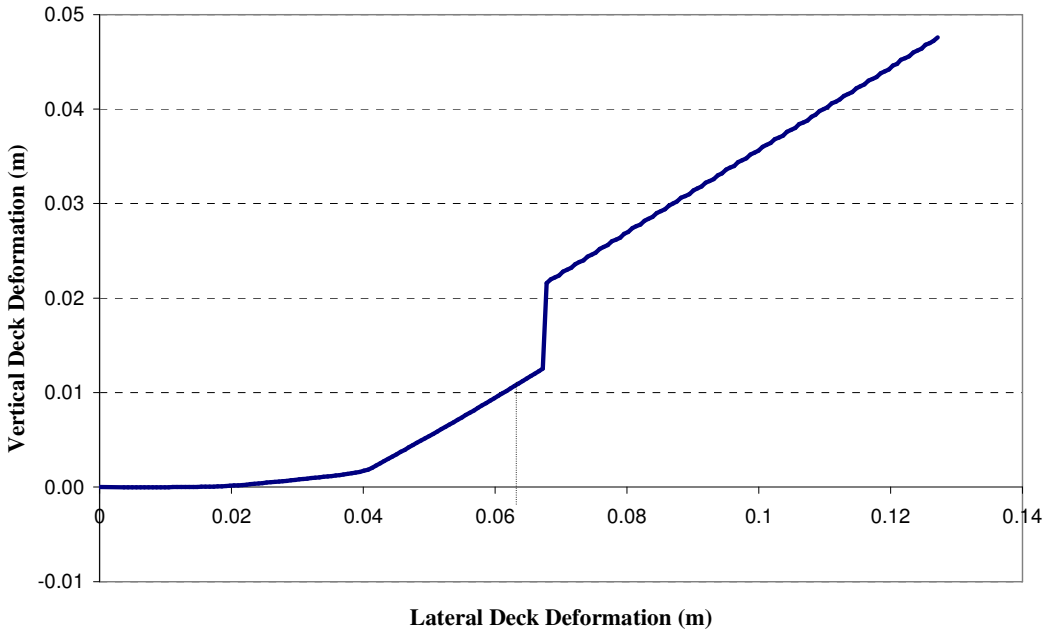

Figure 8.25. Variation of vertical deformation of the cap-beam over compression pile for %10 /50 earthquake event at a pier having batter piles with an inclination of 1/4 with respect to lateral deformation for model 4

The amplification in section design forces of the cap beam with respect to section design forces evaluated with response modification factors presented for each configuration of pile to cap beam connection in Figures 8.26 to 8.29 for %10/50 and %2/50 earthquakes. In these figures α stands for ratio of bending moments evaluated with nonlinear analysis to bending moments evaluated with response modification factors.

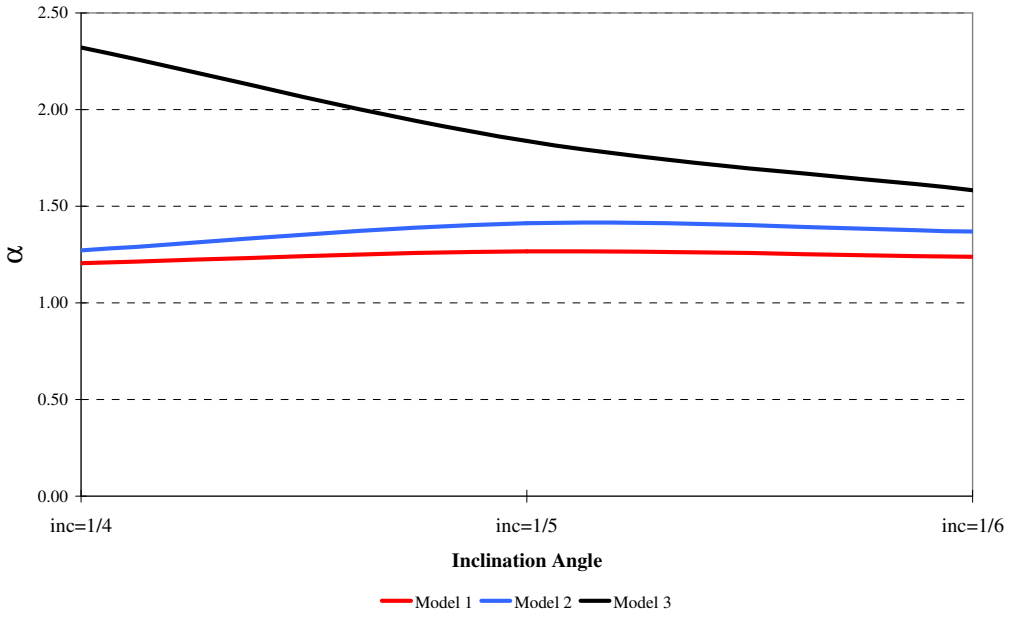

Figure 8.26. Amplification of bending moment at cap-beam with respect to inclination and connection strength with concentric pile-to-pile-cap connection for %10/50 earthquake event

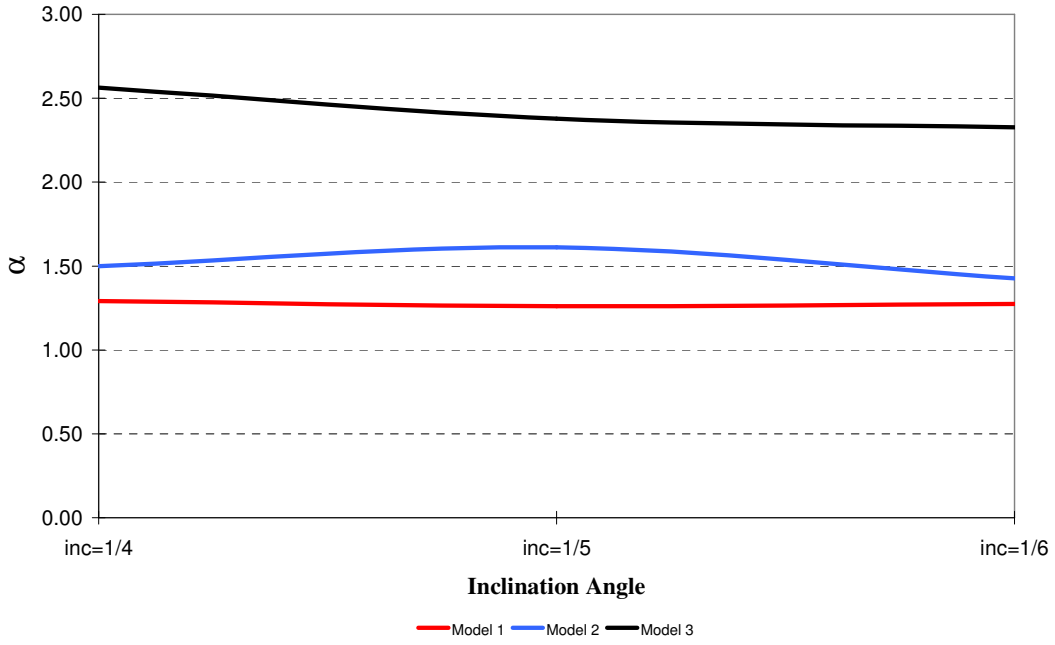

Figure 8.27. Amplification of bending moment at cap-beam with respect to inclination and connection strength with eccentric pile-to-pile-cap connection for %10/50 earthquake event

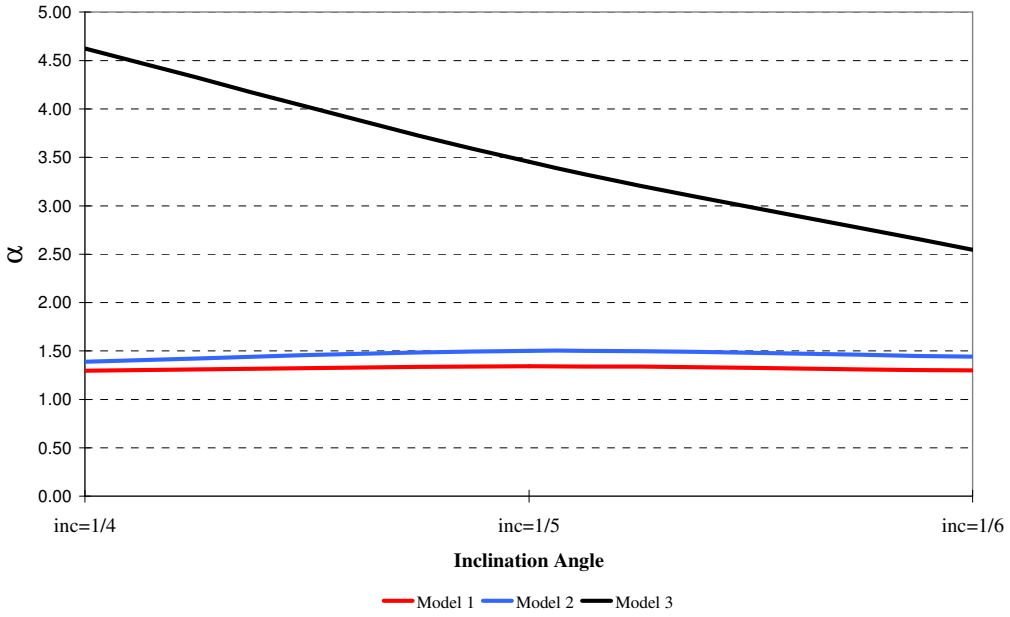

Figure 8.28. Amplification of bending moment at cap-beam with respect to inclination and connection strength with concentric pile-to-pile-cap connection for %2/50 earthquake event

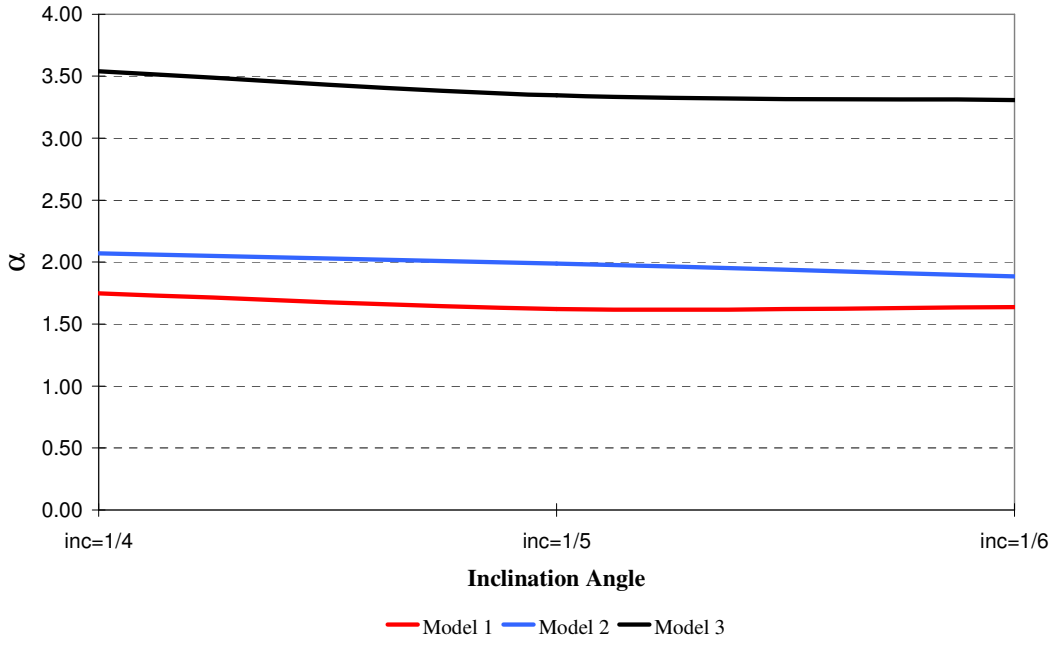

Figure 8.29. Amplification of bending moment at cap-beam with respect to inclination and connection strength with eccentric pile-to-pile-cap connection for %2/50 earthquake event

The amplification in section design forces of the cap beam with respect to section design forces evaluated with seismic coefficient of C=0.15 for %10/50 earthquake is given in Figure 8.30 to 8.31.

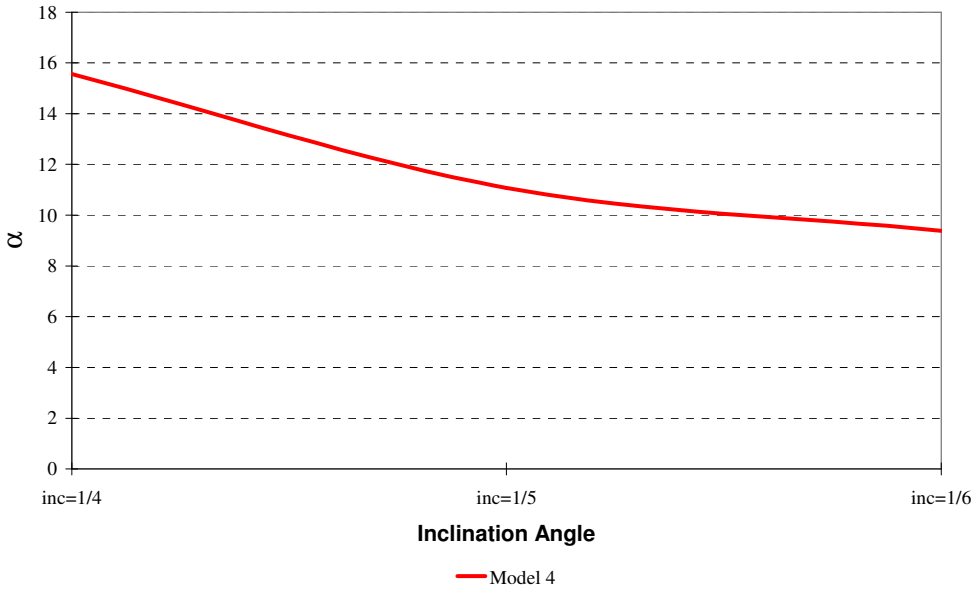

Figure 8.30. Amplification of bending moment at cap-beam with respect to inclination with concentric pile-to-pile-cap connection in %10/50 earthquake

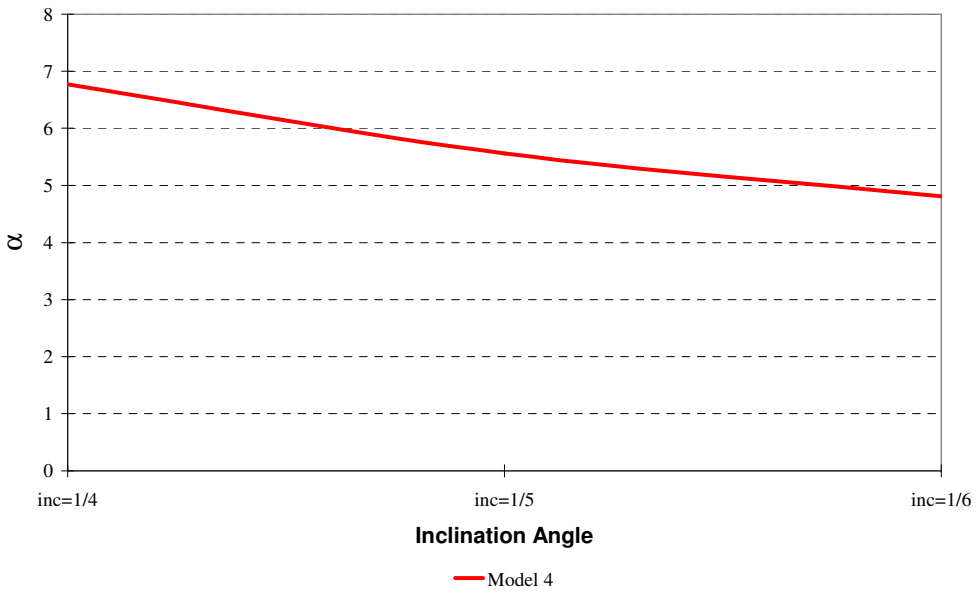

Figure 8.31. Amplification of bending moment at cap-beam with respect to inclination with eccentric pile-to-pile-cap connection in %10/50 earthquake

Based on the information gathered from nonlinear pushover analysis results the following points have been observed;

- There has been a significant increase in section design forces of the cap beam due to the pole vaulting effect for lower strength levels.
- The amplification in concentric pile to pile cap connections is more effected by the inclination angle compared to eccentric connections.
- The high amplification factors observed for low strength level models (R=3 and C=0.15) indicates that a force-based analysis will highly underestimate section design forces of a cap beam and as a consequence may result in plastic deformations and damage to cap beam in multiple locations.
- As expected the plastic deformations at the pile to pile cap connections increase with increased batter and decreased strength.
- The total steel strains are smaller with eccentric pile to pile cap connections.
- For Model 1 to Model 3 total steel strains observed in pile to cap beam connections or the steel pile are with in code limitations
- For model 4 the total steel strains observed in pile to cap beam connections exceed the fracture strain of mild steel causing severe strength deterioration and amplification of structural deformation.

8.3. Significance of Cross Section Compactness on Batter Pile Behavior

Even though steel is an extremely ductile material, the plastic deformation capability of steel sections is more dependent on the section depth-to-thickness ratio namely compactness ratio of the cross section. As explained in detail in Chapter 4, steel sections are classified in to three classes based on their ductility, which is fully compact, semi compact and non-compact section. The fully compact section is expected to behave fully ductile and have full yielding capacity of steel, the semi compact section are expected to have limited ductility with full yielding strength of steel and the non-compact sections are expected to yield before full yielding strength of steel with no plastic deformation capability.

The modeling of inelastic local buckling phenomena is rather a difficult task with out available test data. In literature there are many tests performed with cyclic axial or cyclic bending with constant axial compression. Unfortunately there are no tests performed with both cyclic axial and bending which is close to the behavior of batter piles. When the yielding mechanism of batter piles with steel pipe sections are closely observed, it can be seen that yielding occurs with the existence of high axial compression forces. For this reason the modeling of the steel pile elements in this chapter is based on previously performed compression tests and the derived empiric relationships from these tests.

The critical buckling stress of a steel section can be found with the given ampric formula based on diameter-to-wall thickness ratio of a tube section (Kishida et-al 1984)

$$\sigma_{cr} = (1.16 - 0.0034\frac{D}{t})\sigma_y \tag{8.6}$$

or with the API recommendation (1994) approach

$$\sigma_{cr} = \sigma_y \left[1.64 - 0.23(D/t)^{0.25}\right] \tag{8.7}$$

where σ_{cr} is the critical local buckling stress, σ_y is the tension yield stress, t is the wall thickness and D is the diameter of the steel tube section. The decrease in strength after local buckling can be evaluated by the given formula (Kishida et-al, 1984)

$$\sigma_{sy} = \sigma_y \left[0.69 + 4.4\frac{t}{D}\right] \tag{8.8}$$

where σ_{sy} is the decrease in stress

The skeleton stress-strain curve of the plastic hinge region of a compact and non-compact steel section can be seen in Figure 8.32.

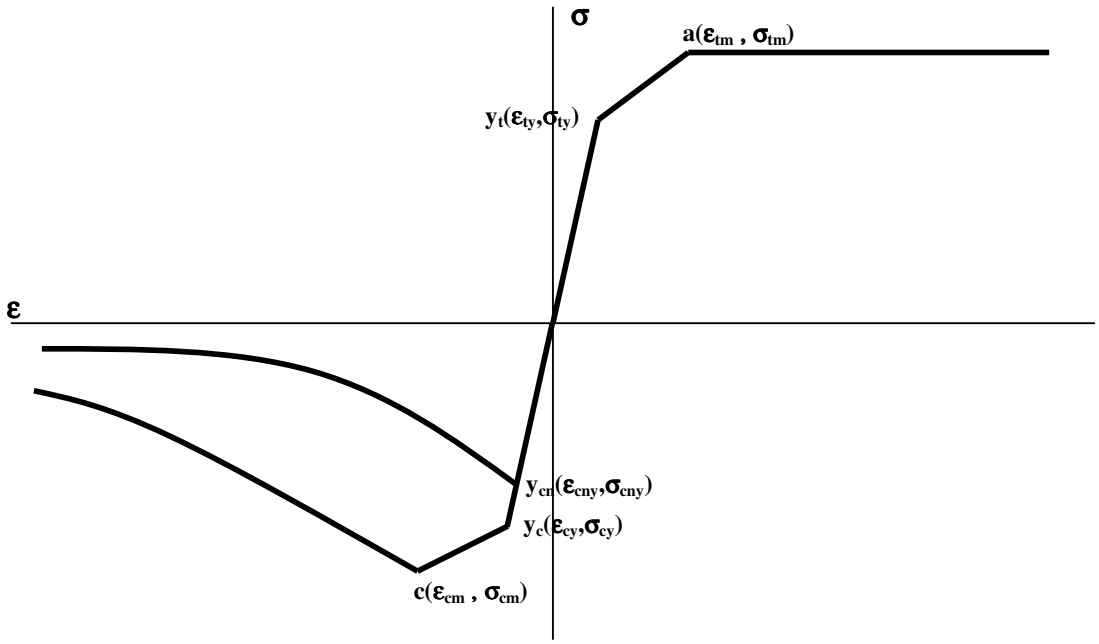

Figure 8.32. Nonlinear skeleton stress strain curve of a compact and non-compact steel section (Modified from Kishida *et-al*, 1984 and Ishizawa *et al*, 2005)

The tensile side of the skeleton curve, as shown in Figure 8.32 is based on the tri-linear curves. Point $y_t(\varepsilon_{ty},\sigma_{ty})$ denotes the yield point steel material. Point $a(\varepsilon_{tm},\sigma_{tm})$ represents the maximum tension stress of the material.

In compression side of the skeleton curve point $y_{cn}(\varepsilon_{cny},\sigma_{cny})$ corresponds to yielding and critical buckling stress of the material for a non-compact section. Point $y_c(\varepsilon_{cy},\sigma_{cy})$ represents the yield point of the material for a compact section. Point $c(\varepsilon_{cm},\sigma_{cm})$ denotes the critical buckling stress point of material for a compact section.

The steel piles are modeled with fiber elements to reflect the severe strength deterioration after inelastic local buckling. The critical buckling stress of non-compact sections is evaluated with Equation 8.7. For over all analysis as shown in Figure 8.33 a steel pile is consists of an elastic beam and a plastic hinge region with a length of L_p, where inelastic local buckling occurs. At first a skeleton curve is determined for the plastic hinge region. The resulting skeleton curve shows strength deterioration on compression side.

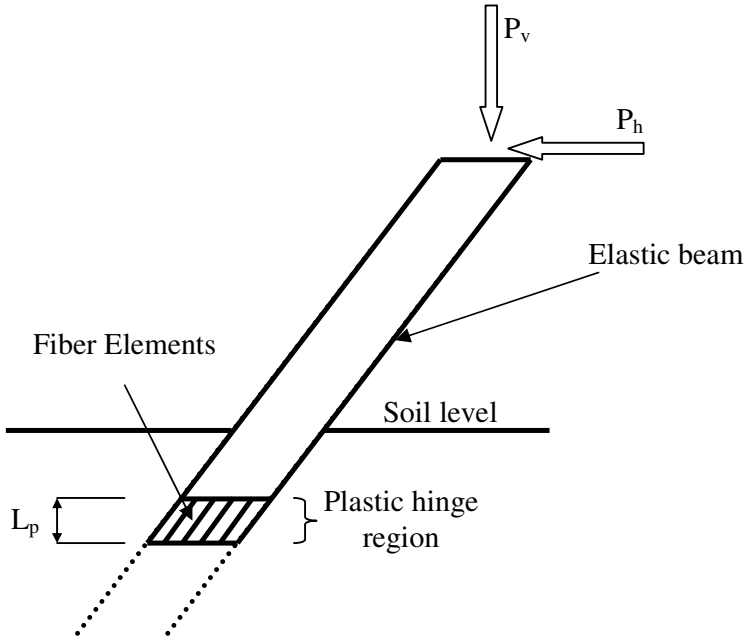

Figure 8.33. Steel pile element model

The plastic hinge length of the steel pile element can be evaluated with the following relationship based on diameter-to-wall thickness ratio and compression force of the section (Ishizawa et al, 2005).

$$L_p = 0.275\left\{\frac{D}{t}\frac{D}{L}\left(\frac{\sigma_y}{E}\right)^{0.5}\left(1-\frac{P_y}{A\sigma_y}\right)^{-0.5}\right\}^{-0.596}\sqrt{I/A} \tag{8.9}$$

where L_p is the plastic hinge length, L is the total length, P_y is the compression force at yield, A is the total area and I is the moment of inertia of the section.

In order to simulate the difference between the compact and non compact section behavior of batter pile systems, a series of nonlinear pushover analysis and inelastic response history analysis is carried out to generic piers. The structural elements of the generic piers are designed with a response modification factor of R=3 for a %10/50 earthquake event. The structural model of the generic piers for compact and non-compact steel pile sections is shown in Figure 8.34.

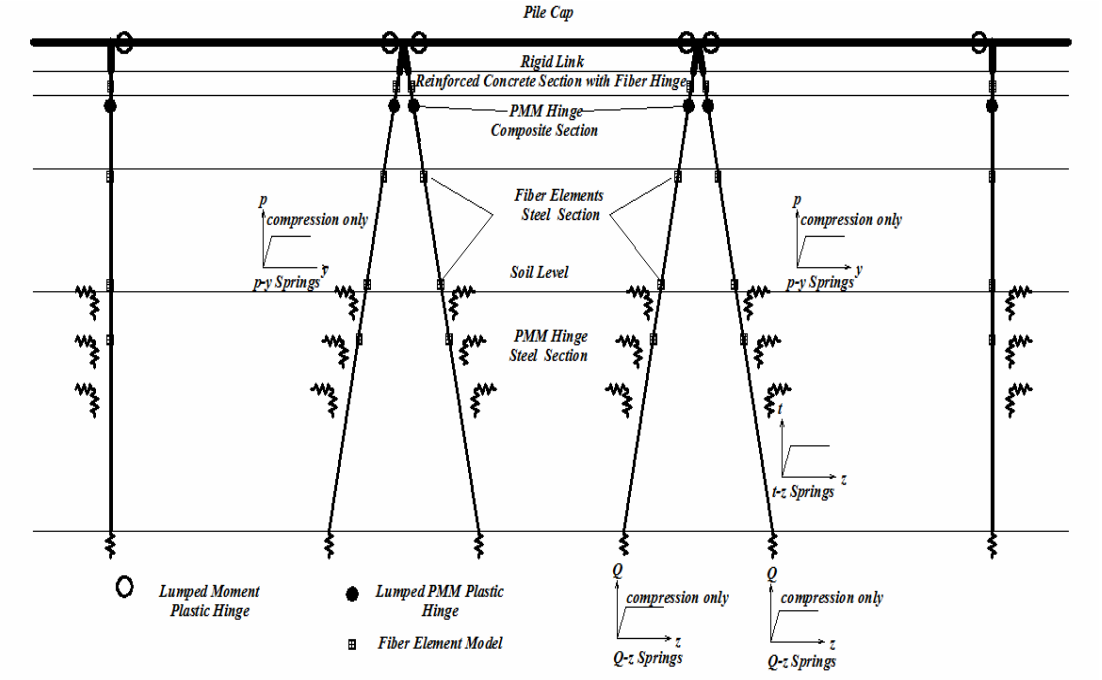

Figure 8.34. 2-Dimensional analysis model of generic pier

In these structural models the cap-beam is modeled with a reinforced concrete section of 1.7m x1.7 m dimensions (Figure 8.2).The pile-cap section properties and the provided steel reinforcement is given in Table 8.12. The steel pile section properties are provided in Table 8.13. The pile-to-pile-cap connection properties and the provided reinforcement are explained in Table 8.14.

Table 8.12. Pile-cap section properties with the provided steel reinforcement

		Pile-Cap Dimension	Cap Beam Reinforcement	
Inclination		**m**	**Top**	**Bottom**
1/4	**Non Compact**	1.7x1.7	16Φ26	16Φ26
	Compact	1.7x1.7	16Φ26	16Φ26
1/5	**Non Compact**	1.7x1.7	16Φ26	16Φ26
	Compact	1.7x1.7	16Φ26	16Φ26
1/6	**Non Compact**	1.7x1.7	16Φ26	16Φ26
	Compact	1.7x1.7	16Φ26	16Φ26

Table 8.13. Steel pile section and material properties for compact and non- compact steel section

Inclination		Pile Diameter m	Wall Thickness m	D/t	Material
1/4	Non Compact	1	0.01	100.0	Fe37
	Compact	0.8	0.014	57.1	Fe37
1/5	Non Compact	1	0.01	100.0	Fe37
	Compact	0.8	0.014	57.1	Fe37
1/6	Non Compact	1	0.01	100.0	Fe37
	Compact	0.8	0.014	57.1	Fe37

Table 8.14. Pile-to-pile-cap connection section and material properties with the provided steel reinforcement

Inclination		Con Diameter m	Conc Material	Provided Connection Reinforcement	
				Inclined	Vertical
1/4	Non Compact	0.98	BS30	12Φ28	12Φ25
	Compact	0.772	BS30	12Φ28	12Φ25
1/5	Non Compact	0.98	BS30	12Φ28	12Φ25
	Compact	0.772	BS30	12Φ28	12Φ25
1/6	Non Compact	0.98	BS30	12Φ28	12Φ25
	Compact	0.772	BS30	12Φ28	12Φ25

Contrary to previous models the pile-caps are modeled with elastic beam elements and lumped plastic moment hinges adjacent to pile-to-pile-cap connections, to simulate the formation of plastic hinging at the pile-cap, due to unbalanced forces after the inelastic local buckling of compression piles.

The inelastic deformation demands of generic piers with compact steel sections are evaluated by the use of equal displacement approximation as explained before. The evaluation of inelastic deformation demands and modal capacity curves of piers with compact sections is shown in Figure 8.35.

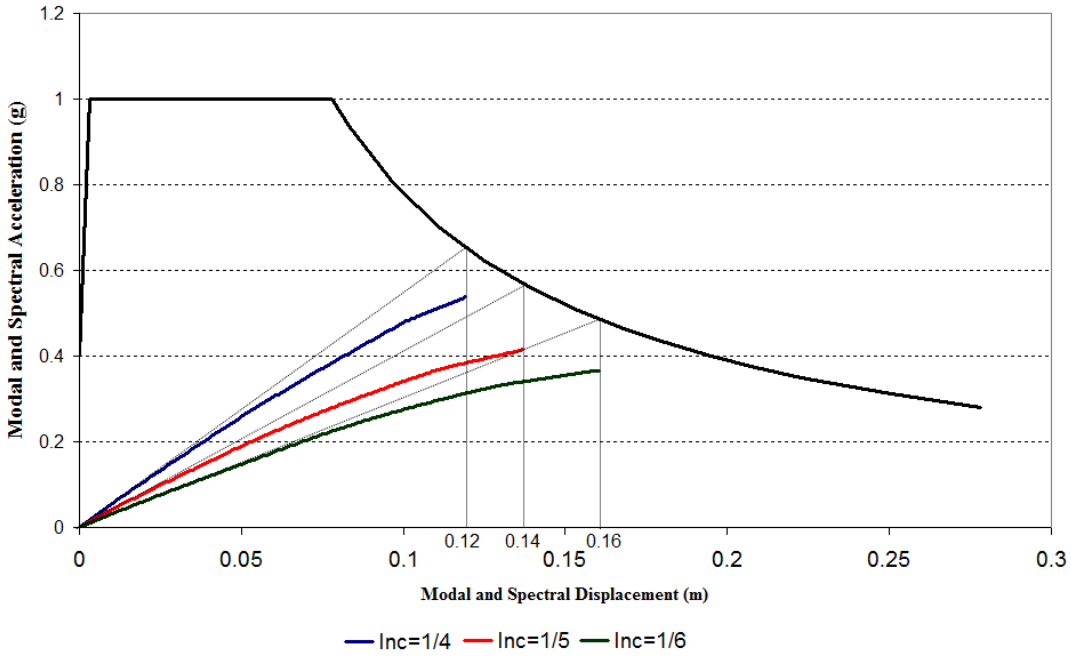

Figure 8.35. Modal capacity curves and estimated inelastic spectral deformation demands of generic piers with compact steel section piles

The inelastic deformation demands for generic piers with non-compact steel pile sections are evaluated through a series of inelastic response history analysis. These inelastic response history analyses have resulted in either substantial residual deformations or total collapse of the generic pier systems. A displacement history of a pier with 1/6 inclination is shown in Figure 8.36. The structural periods and predicted structural displacements are given in Table 8.15.

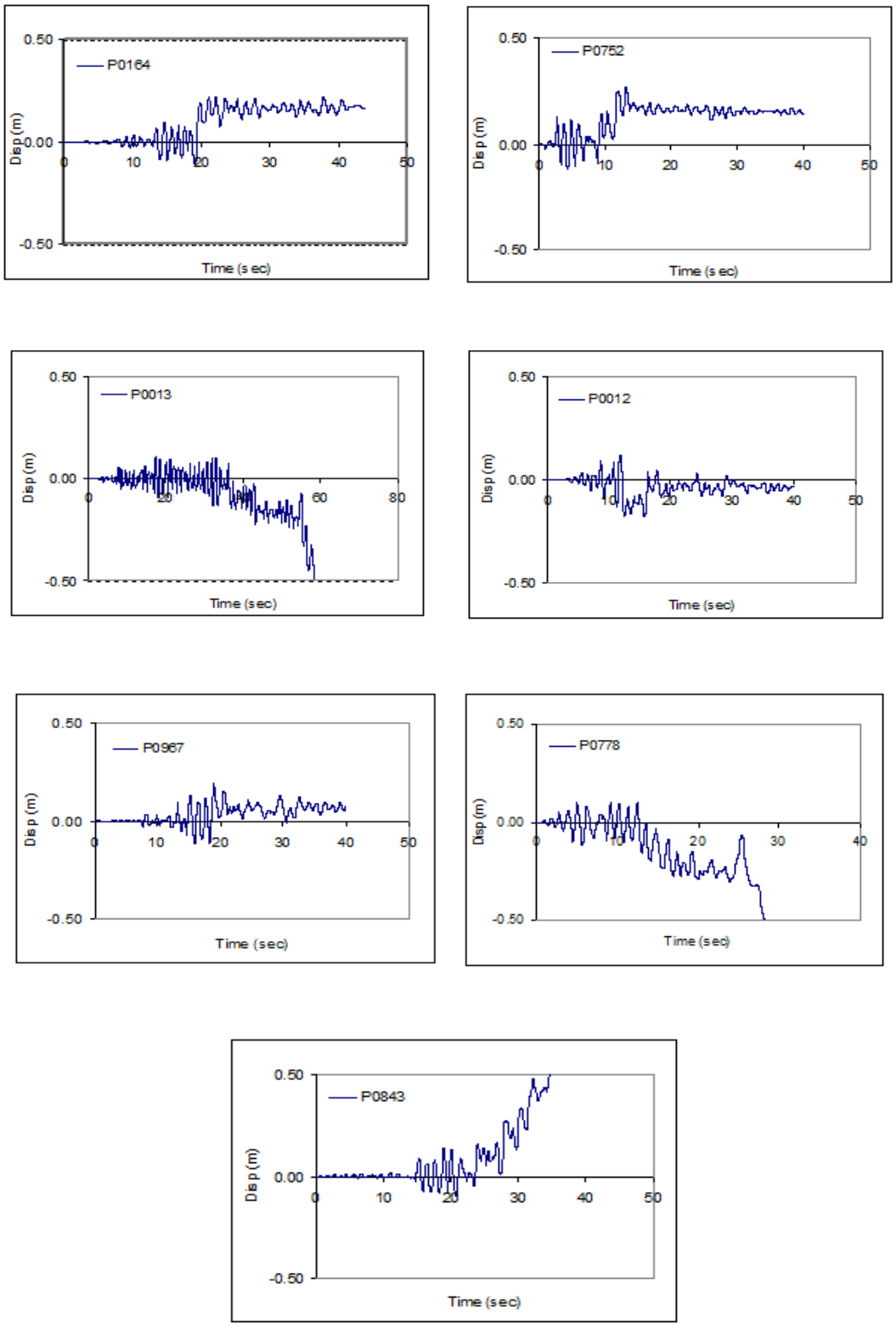

Figure 8.36. Inelastic displacement history of generic pier with non-compact section and inclination of 1/6

Table 8.15. Structural periods and corresponding inelastic spectral displacements

		T	S_{di} (m)	
Steel Pile Section	**Inclination**	**sec**	**%10/50**	**%2/50**
Compact	**1/4**	0.85	0.118	0.165
	1/5	0.98	0.136	0.190
	1/6	1.12	0.156	0.217
Non Compact	**1/4**	0.82	NA	NA
	1/5	0.93	NA	NA
	1/6	1.06	NA	NA

NA* = Not available

A typical pushover curve of a generic pier with 1/6 inclination for both compact and non compact steel sections properties is given in Figure 8.37. The progressive collapse mechanism of the same pier is shown in Figure 8.38.

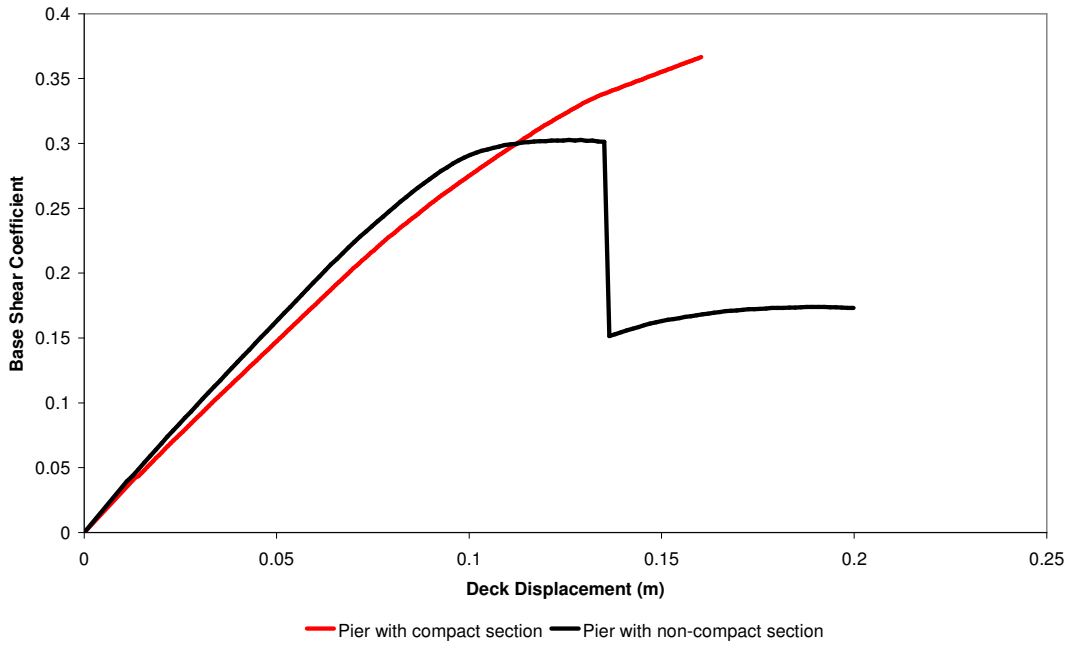

Figure 8.37. Pushover curve of a pier with compact and non-compact sections

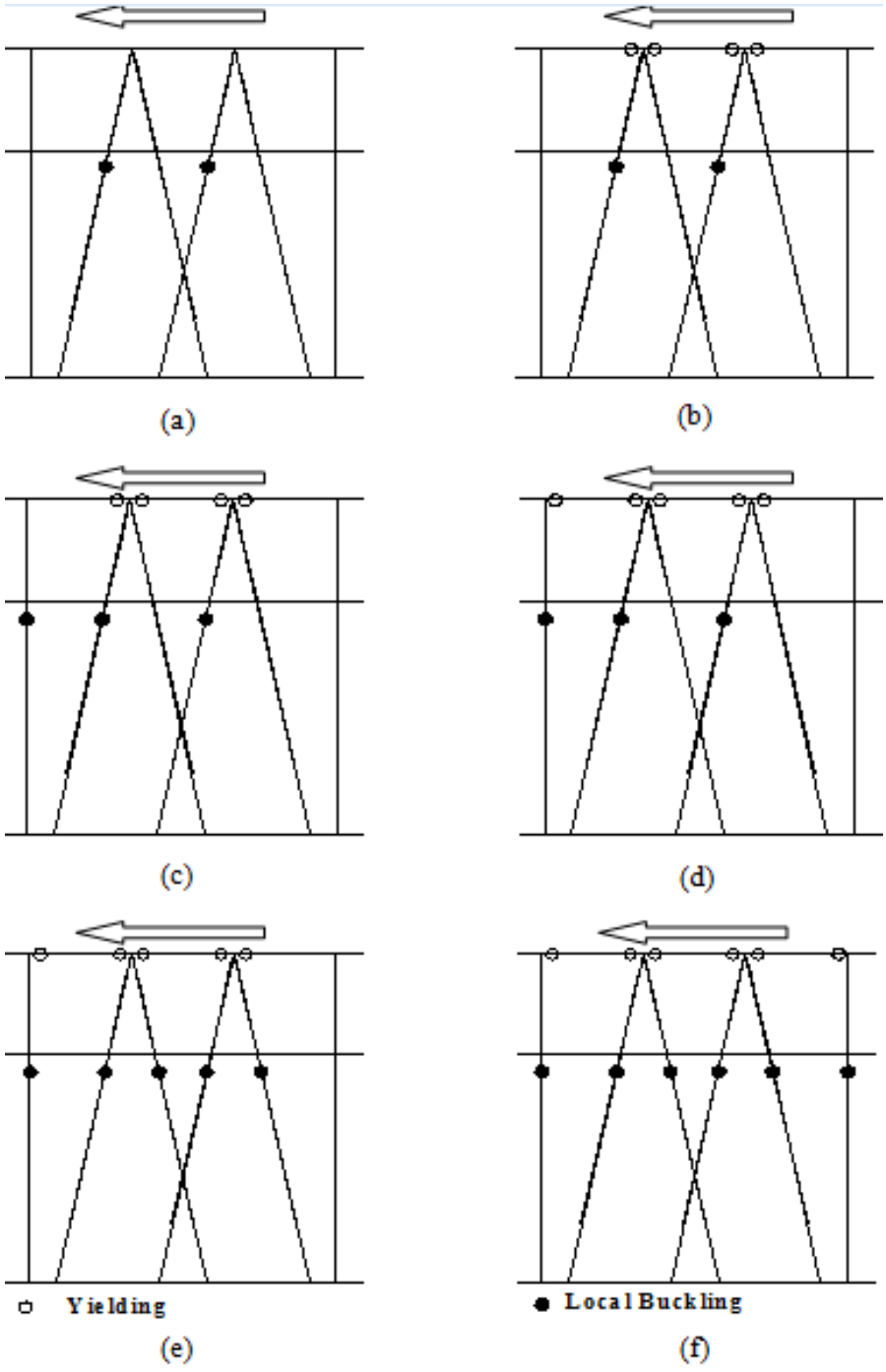

Figure 8.38. Progressive collapse mechanism of a pier with non-compact steel section

The progressive collapse starts with the inelastic local buckling of the compression batter pile as shown in Figure 8.38(a). Once the inelastic local buckling occurs, the cap-beams yield adjacent to batter piles as a result of the un-balanced forces due to severe strength deterioration of the compression pile (Figure 8.38(b)). At this point the structure leans towards to the buckled piles. As the structure continuous to deform inelastic local buckling is observed at the vertical pile in the direction of loading (Figure 8.38(c)). After the formation of inelastic local buckling in the vertical pile, yielding is observed at the pile-cap adjacent to the buckled pile (Figure 8.38(d)). Following this event inelastic local buckling is observed in the rest of the batter and vertical piles and the structure have collapsed (Figure 8.38 (e) and (f)).

Based on the information gathered from nonlinear pushover and inelastic response history analysis the following points have been observed;

- Substantial residual deformations or total collapse have been observed in generic piers with non-compact steel sections.
- Piers designed with compact steel section have shown a stable behavior.

8.4. The use of Structural fuses in Batter Piles and Their Advantages.

Even though the use of structural fuse to limit forces transmitted to structural elements and dissipate energy have been a major design tool in engineering structures over the last two decades, its application for marine structures is very limited due to related erection problems. A new proposed fuse system (Harn, 2004), which is based on limiting the tension forces of a batter pile by controlling the amount of provided mild steel has promising potential. The fuse was simply consisted of mild steel bars debonded by sleeves penetrating in side the pile to lengthen the plastic hinge length of the connection in order to reduce or control steel strains at the reinforcing bar. The debonding length evaluation and a simple drawing of the fuse are provided in Figure 8.39.

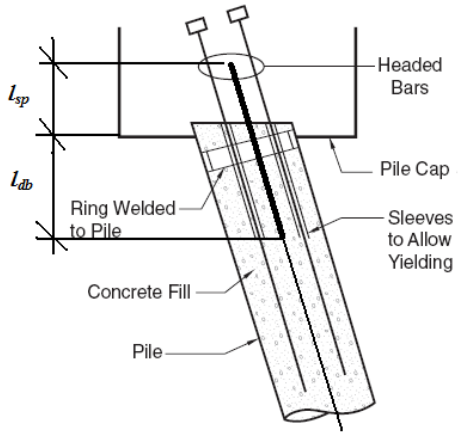

Figure 8.39. Tension fuse

The total debonding length of the fuse l_{db} can be simply evaluated by subtracting the strain penetration length of mild steel l_{sp} from the desired plastic hinge length L_{pfuse}.

To investigate the applicability of such a fuse system, piers having batter piles with an inclination of 1/4 to 1/6 have been designed and analyzed with a strength reduction factor R=4. Later the same models are analyzed with tension fuses. In these structural models the pile cap is modeled with a reinforced concrete section with a 1.7m x1.7 m dimension (Figure 8.2). The steel pile section properties are provided in Table 8.16 (Figure 8.3). The pile to pile cap connection (Figure 8.3) properties and the provided reinforcement and the corresponding plastic hinge length to length of the fuse elements are explained in Table 8.17.

Table 8.16. Steel pile section and material properties

	Pile Diameter	**Wall Thickness**	**D/t**	**Material**
Inclination	**m**	**m**		
1/4	1.00	0.016	62.5	Fe37
1/5	1.00	0.016	62.5	Fe37
1/6	1.00	0.016	62.5	Fe37

Table 8.17. Pile-to-pile-cap connection section and material properties with the provided steel reinforcement and provided fuse and plastic hinge lengths

	Con Dia	Conc Material	Provided ConnectionReinforcement		L_p	L_{pfuse}
Inclination	**m**		**Inclined**	**Vertical**	**m**	**m**
1/4	0.968	BS30	12Φ22	12Φ22	0.4	1
1/5	0.968	BS30	12Φ22	12Φ22	0.4	1
1/6	0.968	BS30	12Φ22	12Φ22	0.4	1

The evaluation of inelastic deformation demands and modal capacity curves of piers with compact sections is shown in Figure 8.40. The structural periods and estimated spectral displacements are given in Table 8.18.

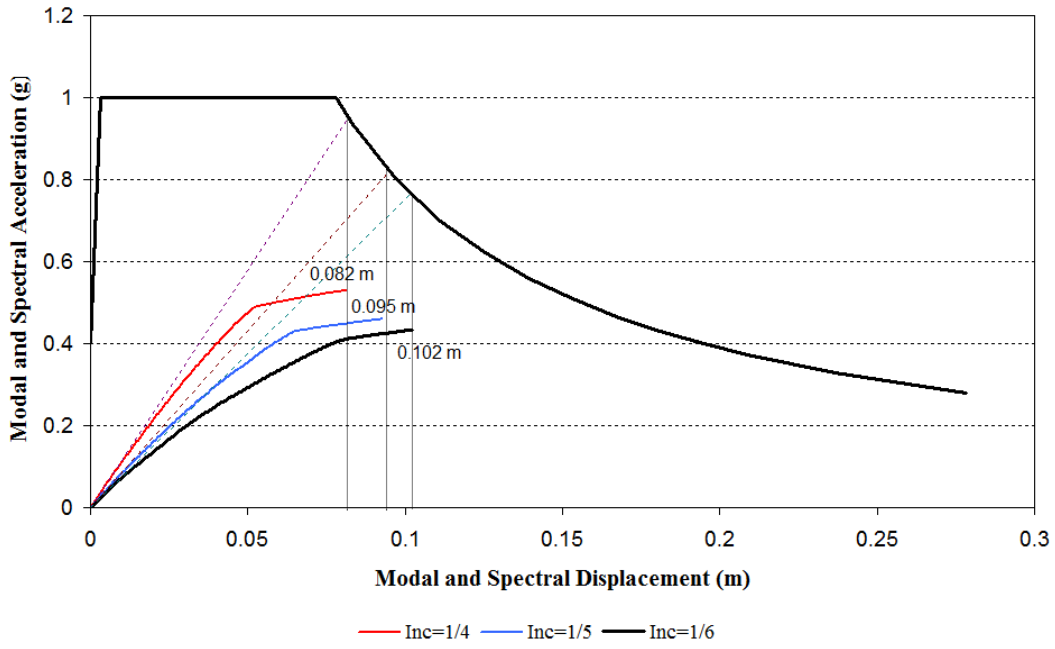

Figure 8.40. Modal capacity curves and estimated inelastic spectral deformation demands of generic piers

Table 8.18. Structural periods and corresponding inelastic spectral displacements

	T	S_{di} (m)	
Inclination	**sec**	**%10/50**	**%2/50**
1/4	0.59	0.082	0.114
1/5	0.68	0.095	0.132
1/6	0.73	0.102	0.141

This fuse system is designed to control steel strains of a pile to pile cap connection by lengthening the plastic deformation length of the plastic hinge. This allows the designer to control the transmitted axial forces to the piles and helps them to create more economical designs by assigning a proper strength level to the pile-to-pile-cap connection. The design process is therefore controlled by the pole vaulting phenomena rather than the plastic deformations. Reduction of total steel strains at the pile to pile cap connection can be seen in Figure 8.41 and 8.42 for %10/50 and %2/50 earthquake events with the relevant strength levels.

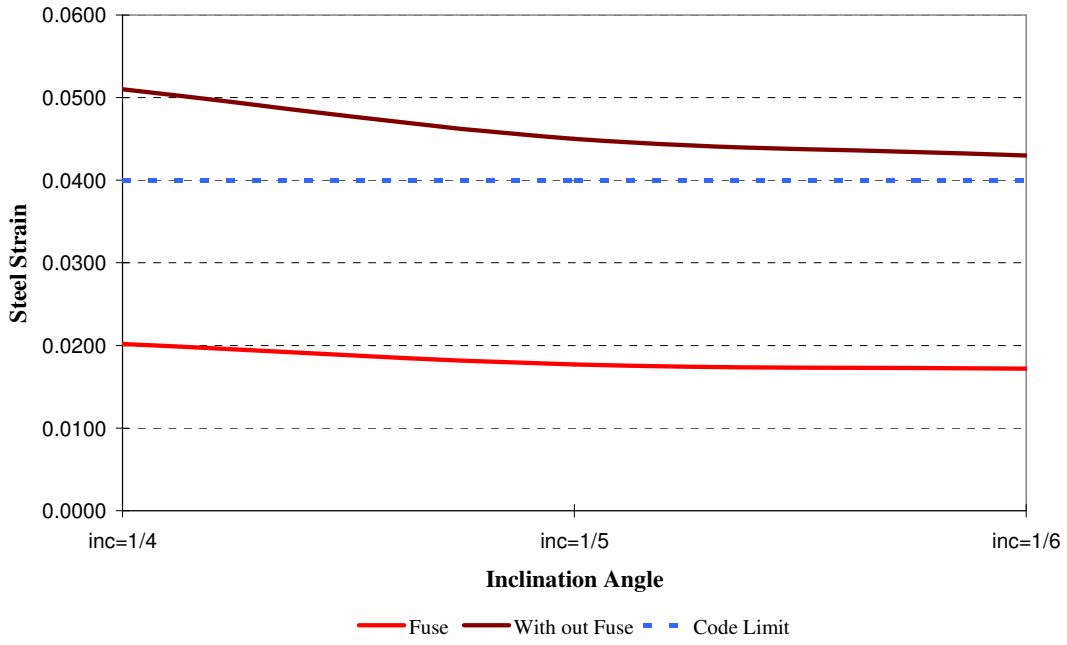

Figure 8.41 Variation of steel strain with and with out fuse at pile to pile cap connection with respect to inclination angle at %10/50 earthquake event

Figure 8.42. Variation of steel strain with and with out fuse at pile to pile cap connection with respect to inclination angle at %2/50 earthquake event

The amplification in section design forces of the pile-cap with and without fuse is presented in Figure 8.43 for %10/50 earthquake event. In this figure α stands for ratio of bending moments evaluated with nonlinear analysis to bending moments evaluated with response modification factors.

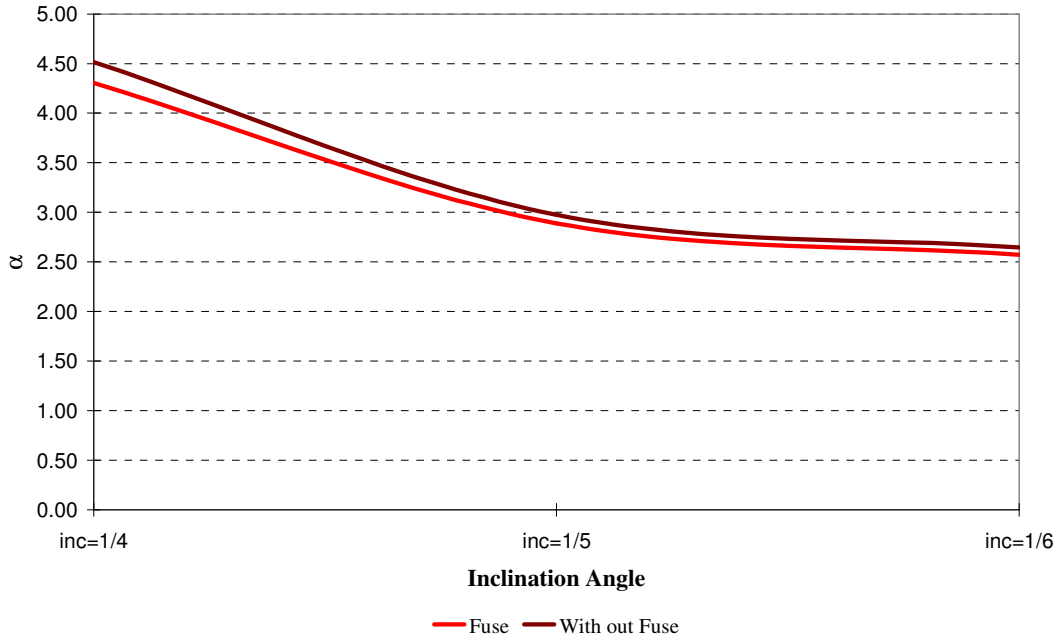

Figure 8.43. Amplification of bending moment at pile-cap with respect to inclination at %10/50 earthquake event with and with out fuse

Based on the information gathered from nonlinear pushover analysis results the following points have been observed;

- As expected the plastic deformations at the pile to pile cap connections have reduced significantly.
- The amplification of section design forces of the pile-cap due to pole vaulting effect remained almost the same, since fuse has the same uplift deformation of a traditional pile-to-pile-cap connection. The high amplification factors observed for fused models indicates that force-based design methods will highly underestimate section design forces of a cap beam and as a consequence may result in plastic deformations and damage to cap beam in multiple locations.

9. ACCURACY OF NONLINEAR STATIC PROCEDURES.

The behavior of irregular structures like wharfs or L or T shape piers needs special attention, which is very difficult to be simulated by simple pushover analysis tools with single mode approach. Even though inelastic response history analysis is the best tool to predict inelastic deformations, the complexity of performing such an analysis, often times forces engineer to look for other solutions. The improved nonlinear static procedures, which includes more than one vibration mode are promised to be an intermediate solution to over come the problems associated to a single mode push over analysis and introduce a simpler solution to the engineer. In this chapter the accuracy of such a method proposed by Chopra et al (2003) will be investigated by comparing the average response of inelastic response history analysis results to MPA and single mode pushover results.

A typical wharf structure is selected to test MPA, where the fundamental mode in the direction of loading is coupled with torsion (parallel to the seaward edge). A three dimensional time history analysis is performed parallel to the seaward edge with a series of strong ground motions described in Chapter 7, in which the average response spectrum of strong ground motion data match the design spectrum with a reasonable margin. Then a three dimensional push over analysis is performed with MPA and single mode pushover procedure parallel to the sea ward edge. In the tables and figures from this page, MPA stands for Multi-Mode Push-over Analysis and SMPA stands for Single Mode Pushover Analysis.

The cap-beams in this wharf structure are modeled with non-yielding frame elements, consisted with the design philosophy. In a typical modern wharf construction the steel pipe piles are usually cut below the bottom reinforcement bar of the cap-beam. The full-moment connection of the steel pile to the-cap beam is provided by mild steel bars extending from the concrete fill of the steel pipe-pile to cap-beam. The pile in this zone has the strength and stiffness properties of a reinforced concrete section with a length equal to twice the strain penetration length of the reinforcing bar, which is also equal to the plastic hinge length of the section. The pile-to-cap-beam elements are modeled with elastic beam elements and lumped plastic P-M-M hinges, located under the pile-cap.

From the pile-to-cap-beam connection to the end of the concrete fill, the pile has the stiffness and strength properties of a full composite section. In this zone, the pile is modeled with elastic beam elements and lumped plastic P-M-M hinges, located under the pile-to-cap-beam element.

From the concrete fill to the tip, the pile has the stiffness and strength of the bare steel section properties. The pile is modeled with elastic beam and lumped plastic P-M-M hinges under the concrete fill. For short piles a plastic hinge is lumped to each pile element with a length equal to the depth of the pile section. For long piles there is another plastic hinge located just over the pile-soil interface. The plastic hinge length of steel pipe section is assumed to be one half of the section depth above the pile-soil interface and one section depth below the soil level.

The stiffness and strength of the soil surrounding the piles are modeled with nonlinear axial spring elements connected to each pile element.

The steel pile section properties are provided in Table 9.1. The pile-to-pile-cap connection properties and the provided reinforcement are explained in Table 9.2. A plan and a section view of the analyzed structure with the soil profile and the corresponding soil properties are given in Figure 9.1 and 9.2.

The total lumped lateral mass of the wharf is 3877 kNs^2/m and the total mass moment of inertia of the structure is 723790 $kNms^2$. A section view of the structural model is illustrated in Figure 9.3.

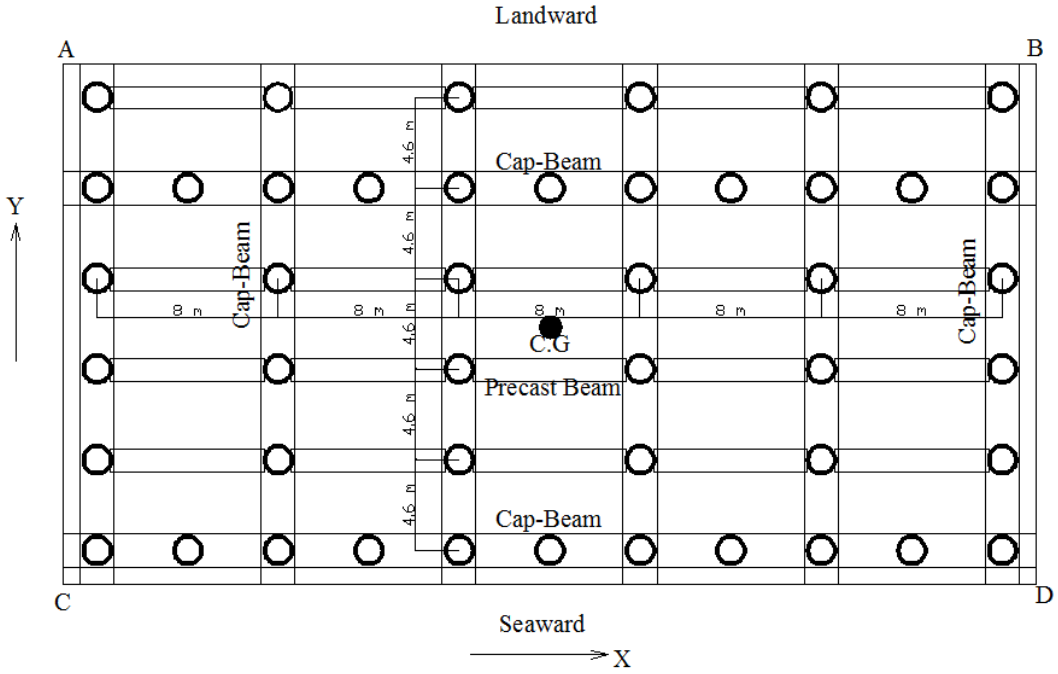

Figure 9.1 Plan view of the wharf

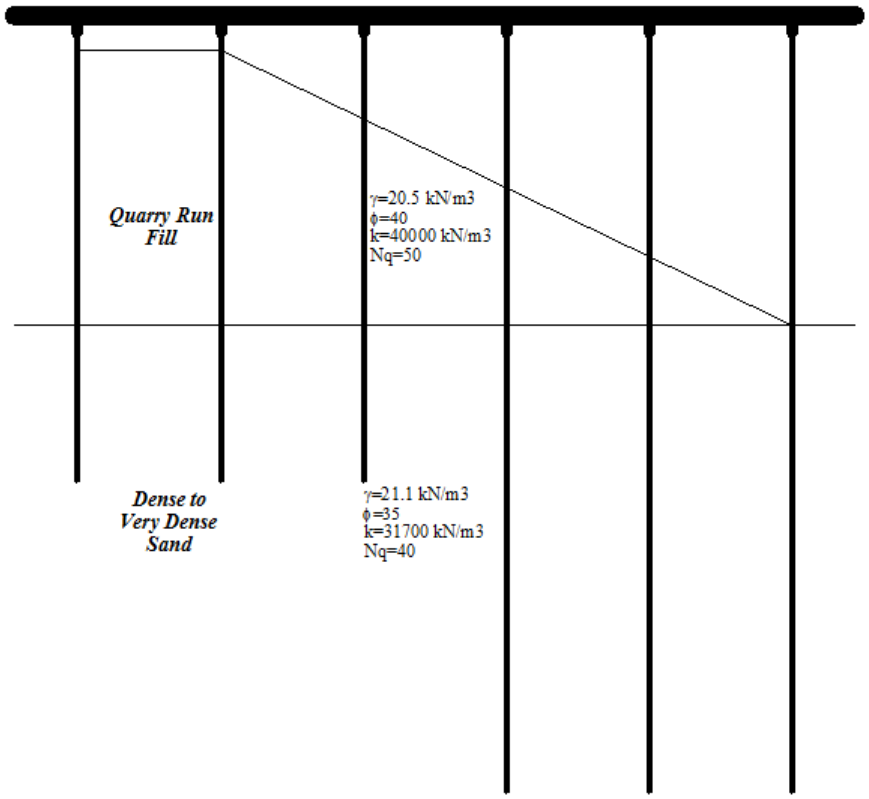

Figure 9.2. Section view of the wharf and the soil profile

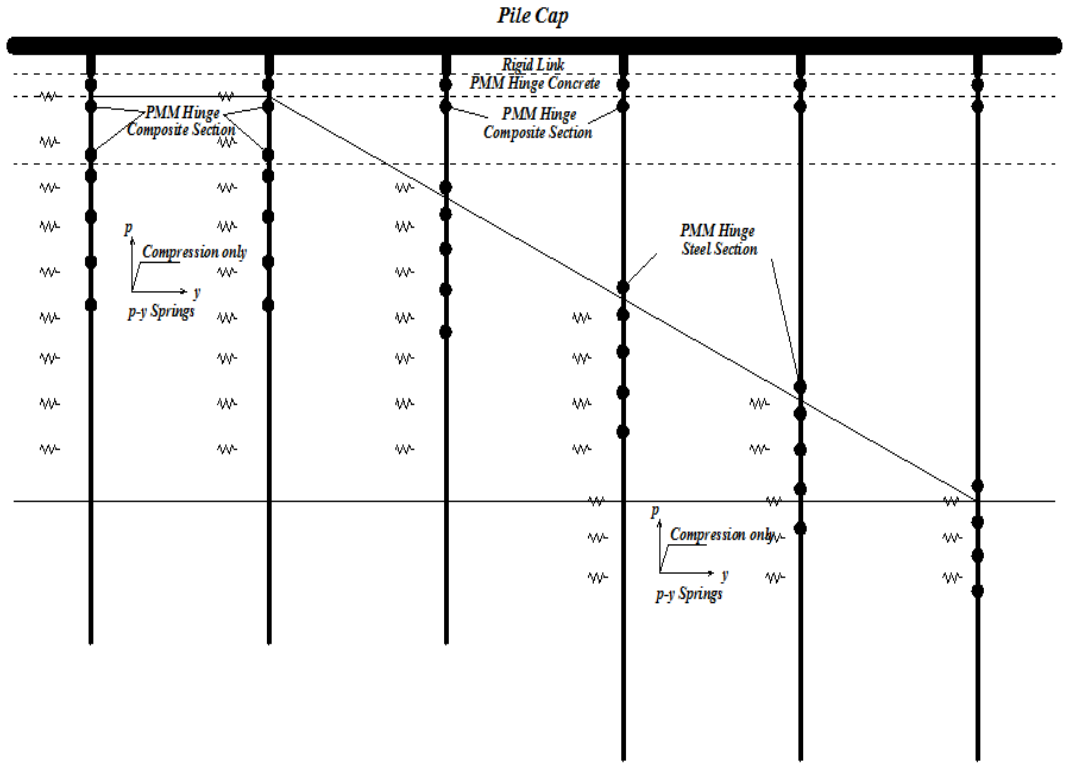

Figure 9.3. Structural model of the wharf

Table 9.1. Steel pile section and material properties

	Pile Diameter	Wall Thickness	D/t	Material
Rows**	**m**	**m**		
1 st Row	0.60	0.016	37.5	Fe52
2 nd Row	0.60	0.016	37.5	Fe52
3 nd Row	0.60	0.016	37.5	Fe52
4 nd Row	0.60	0.016	37.5	Fe52
5 nd Row	0.60	0.016	37.5	Fe52
6 nd Row	0.60	0.016	37.5	Fe52

Table 9.2. Pile-to-pile-cap connection section and material properties with the provided steel reinforcement

	Con Dia	Conc Material	Provided ConnectionReinforcement
Rows**	**m**		
1 st Row	0.468	BS30	12Φ28
2 nd Row	0.468	BS30	12Φ28
3 nd Row	0.468	BS30	12Φ22
4 nd Row	0.468	BS30	12Φ22
5 nd Row	0.468	BS30	12Φ22
6 nd Row	0.468	BS30	12Φ22

**The rows are named from the landward edge to sea ward edge

The modal properties of the structure are given in Table 9.3.

Table 9.3. Modal properties of the wharf

Mode Number	Period	Mass Participation Ratio		
	sec	m_x	m_y	m_{oo}
1	0.6031	0.7048	0	0.29
2	0.473	0	1	0
3	0.3545	0.2952	0	0.71

9.1. Comparison of MPA to IRHA and SMPA in Loading Direction Parallel to Seward Edge

The evaluated deformations will be given in 5 different locations as shown in Figure 9.1. These points are center of gravity of the wharf and the corner points A, B, C and D. The evaluated effective periods and estimated inelastic spectral deformations for each mode at the center of gravity of the wharf are given in Table 9.4.

Table 9.4. Estimated inelastic spectral deformation demands for each mode parallel to seaward edge

	Ti	Te	S_{di} (m)	Δ_{di} (m)
Mode Number	**sec**	**sec**	**%10/50**	**%10/50**
1	0.6031	0.69	0.097	0.068
3	0.3595	0.6031	0.084	0.025

The modal capacity curves and the estimated inelastic spectral deformations parallel to seaward edge are shown in Figure 9.4.

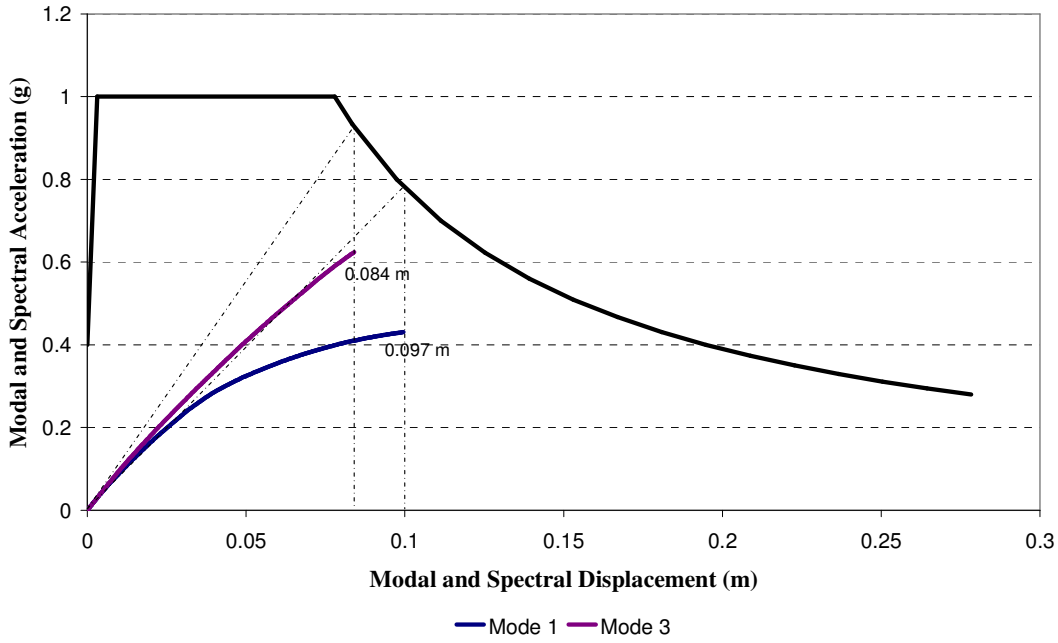

Figure 9.4. Modal capacity curves and estimated spectral deformations of wharf, parallel to seaward edge

The deformations evaluated with the inelastic response history of analysis at the center of gravity of the wharf parallel and perpendicular to seaward edge is given in Figure 9.5 and 9.6. The evaluated maximum deformations at center of gravity and each corner of the wharf are given in Table 9.5.

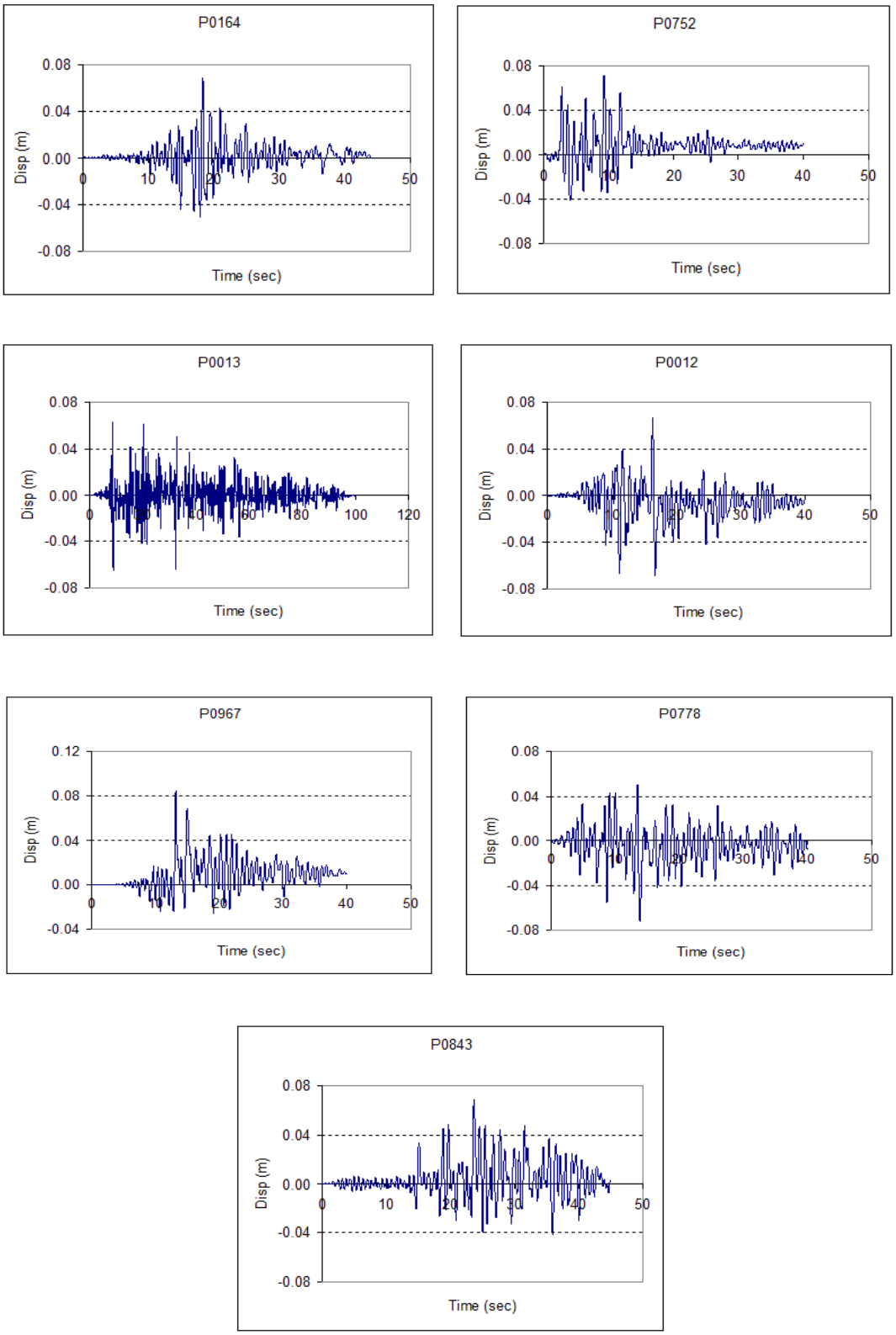

Figure 9.5. Inelastic displacement history at center of gravity of wharf parallel to seaward edge

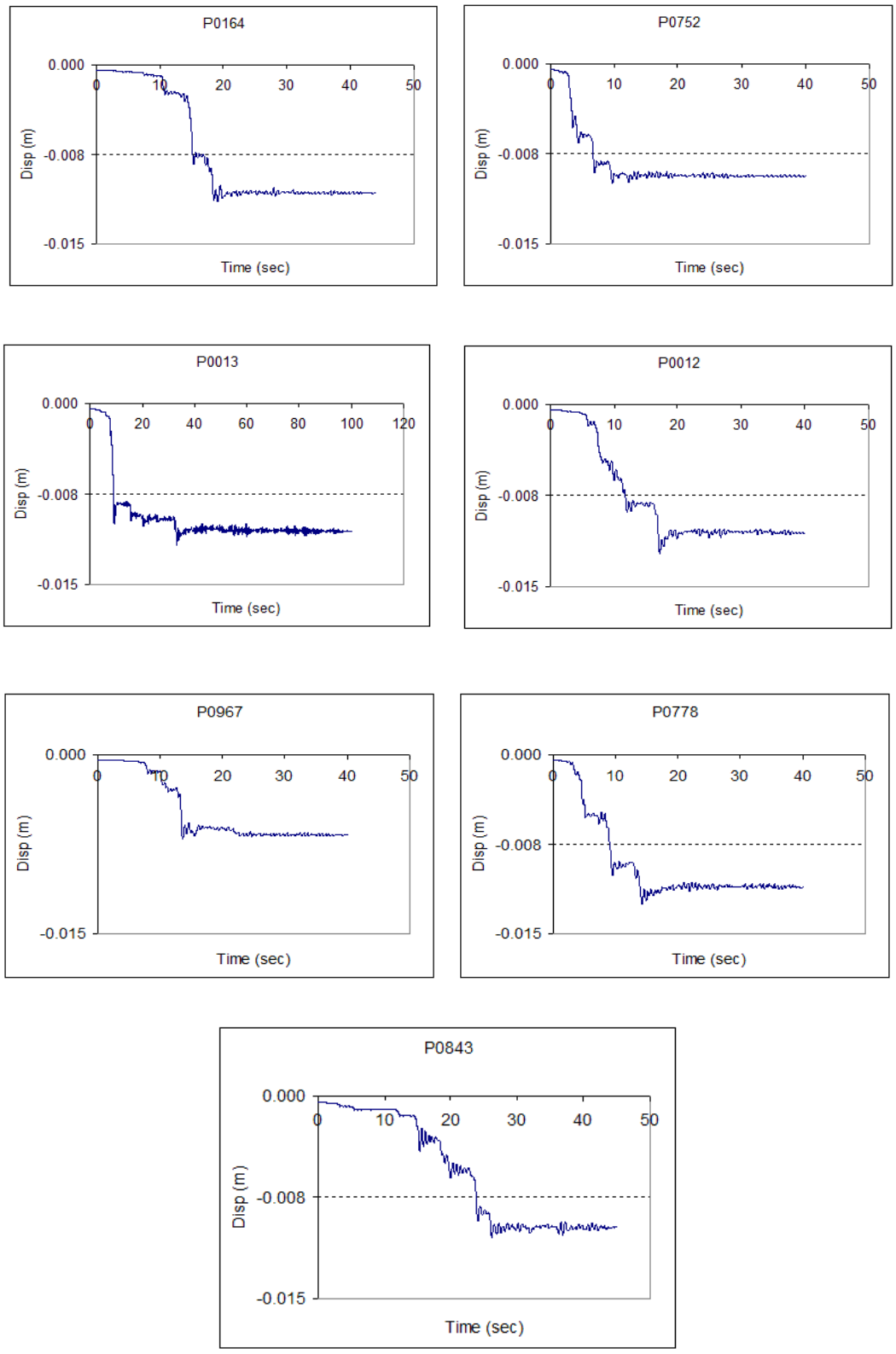

Figure 9.6. Inelastic displacement history at center of gravity of wharf perpendicular to seaward edge

Table 9.5. Evaluated maximum deformations at controlling points

	Corner A (m)		Corner B (m)		Corner C (m)		Corner D (m)		Center of Gravity (m)	
EARTHQUAKE	**X**	**Y**	**X**	**Y**	**X**	**Y**	**X**	**Y**	**X**	**Y**
P0164	0.041	0.078	0.041	0.078	0.105	0.063	0.105	0.063	0.069	0.011
P0752	0.049	0.068	0.049	0.068	0.101	0.060	0.101	0.060	0.071	0.010
P0013	0.047	0.071	0.047	0.071	0.094	0.075	0.094	0.075	0.065	0.012
P0012	0.044	0.066	0.044	0.066	0.105	0.085	0.105	0.085	0.069	0.012
P0967	0.058	0.069	0.058	0.069	0.116	0.060	0.116	0.060	0.085	0.007
P0778	0.052	0.070	0.052	0.070	0.108	0.076	0.108	0.076	0.072	0.013
P0843	0.052	0.076	0.052	0.076	0.108	0.062	0.108	0.062	0.072	0.010
Avg.	0.049	0.071	0.049	0.071	0.105	0.069	0.105	0.069	0.072	0.011

Comparisons of estimated deformations by MPA and SMPA with respect to evaluated deformation with inelastic response history analysis are given in Figure 9.7 to Figure 9.9 for center of gravity, landward and seaward edge of the wharf.

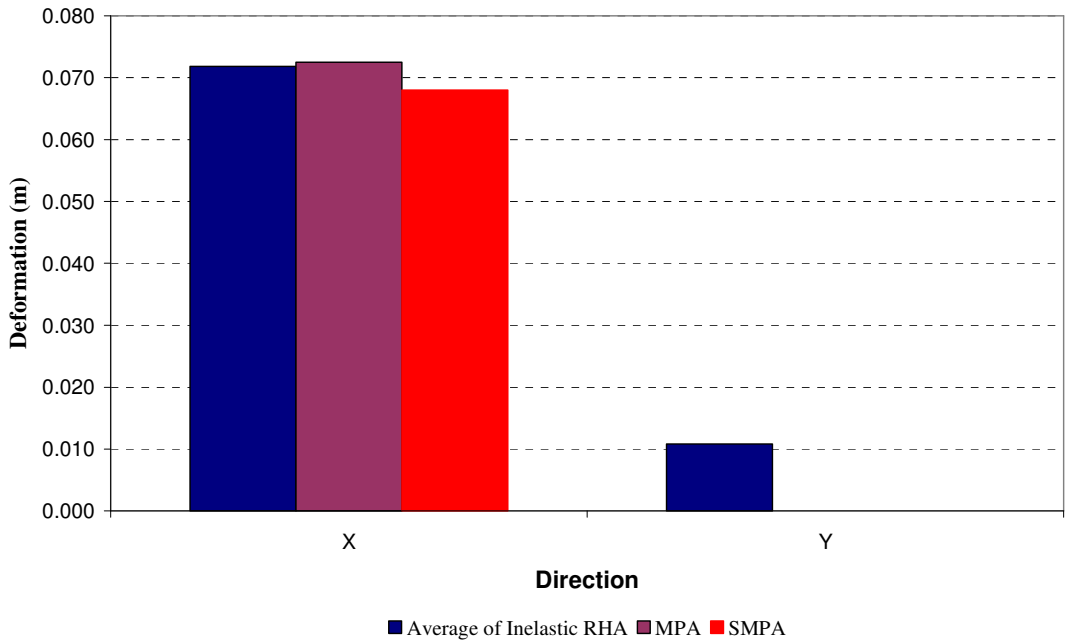

Figure 9.7. Estimated deformation with MPA and SMPA with respect to average of evaluated deformations with IRHA at the center of gravity of the wharf

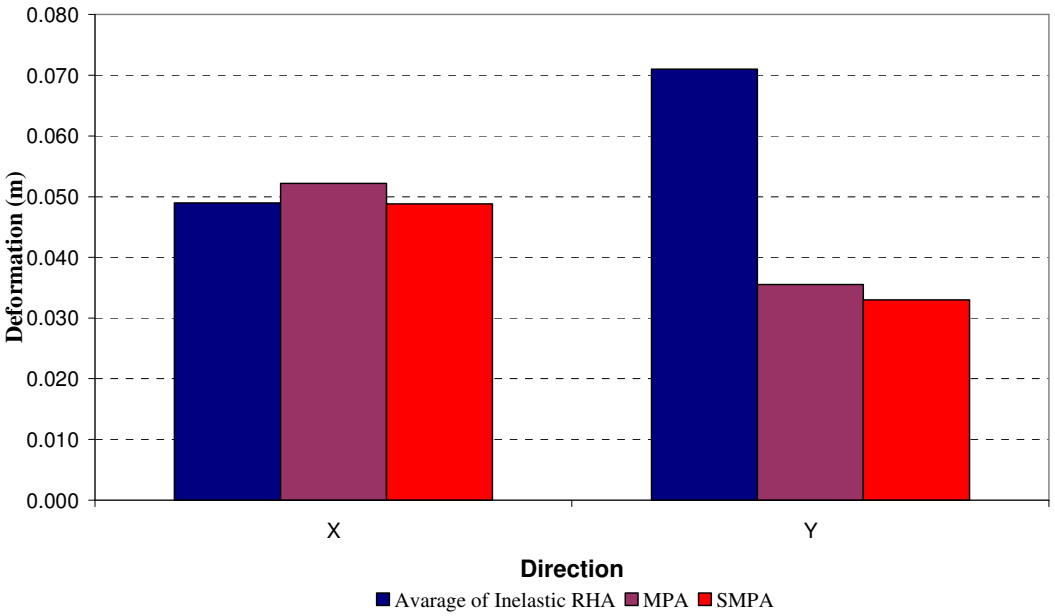

Figure 9.8. Estimated deformation with MPA and SMPA with respect to average of evaluated deformations with IRHA at the landward edge of the wharf

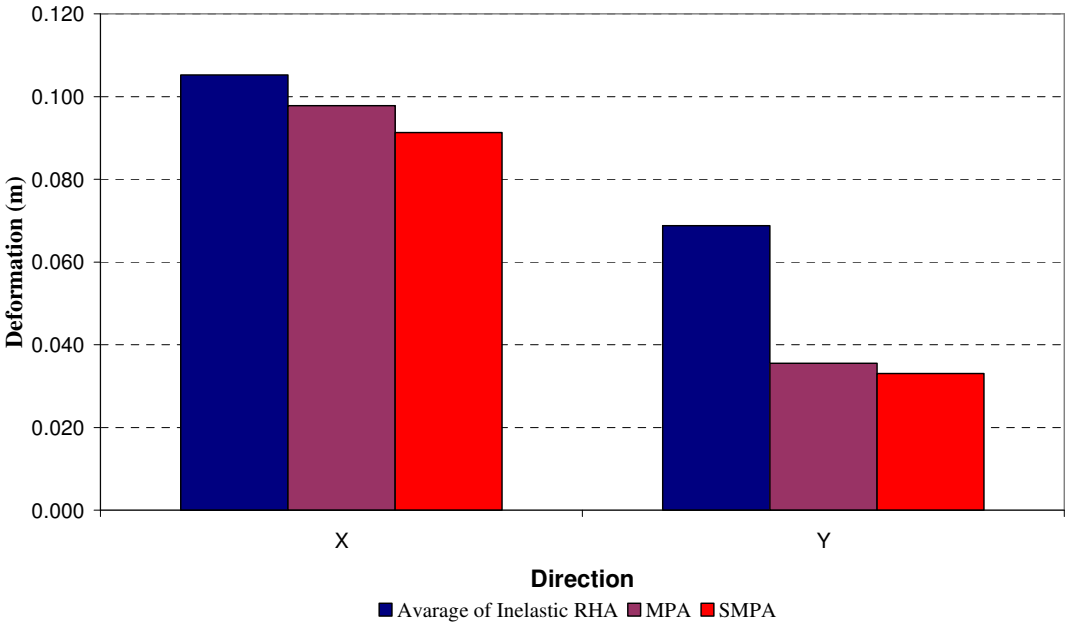

Figure 9.9. Estimated deformation with MPA and SMPA with respect to average of evaluated deformations with IRHA at the seaward edge of the wharf

Comparison of estimated plastic rotations by MPA and SMPA with respect to average of evaluated plastic rotations with inelastic response history analysis is given in Figure 9.10.

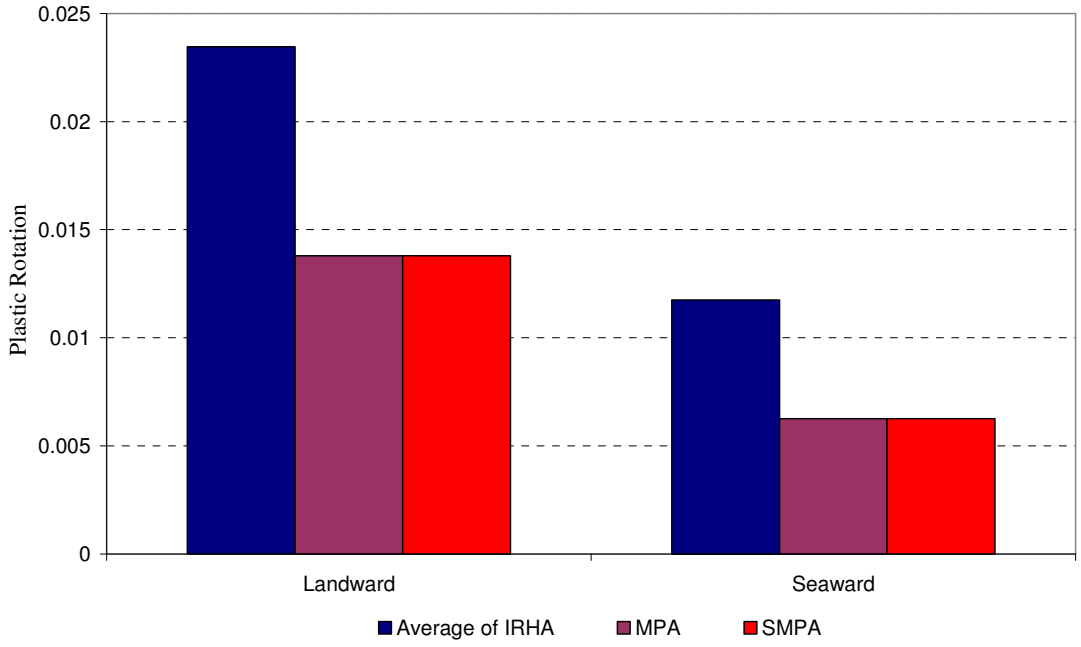

Figure 9.10. Estimated plastic rotations with MPA and SMPA with respect to average of evaluated plastic rotations with IRHA at the seaward edge of the wharf

Based on the information gathered from inelastic response history analysis and nonlinear pushover analysis results the following points have been observed;

- Both MPA and SMPA are successful in estimating deformations at center of gravity, seaward edge and landward edge of the deck at the direction of loading but fails to estimate deformations normal to the direction of loading at the same locations.
- Both MPA and SMPA estimate similar plastic deformations at seaward and landward edge of the structure and both failed to estimate these plastic deformations with a reasonable accuracy with respect to IRHA results.

10. RECOMENDATIONS

Most of modern design codes allow the pile pull-out in the soil to limit the transmitted loads to the piles as well as control the amount of plastic deformations in structural elements through the use of nonlinear soil springs representing the axial resistance of soil. This method though has shown to be effective for design purposes the following is recommended to be considered during design.

- In order for the pile to pull-out of soil the compression capacity of the pile should be higher than the tension capacity of the pile with a reasonable margin.
- For reasons given in the Chapter 8, the design should be based on nonlinear pushover or inelastic response history analysis since any amplification of section design forces for the cap beam can not be reasonable estimated by force-based design methods.
- Since the design will be iterative a response modification factor R=3 is felt to be appropriate for preliminary dimensioning of structural elements and for the selection of pile length.
- In the absence of available test data at the site the analysis should be carried out with reasonable upper bound and lower bound limits defined for soil properties. The plastic deformations in structural elements should be taken from the upper bound analysis and the design section forces for cap beams and decks should be evaluated with the lower bound analysis.
- The full tension strength of the pile to cap beam connection evaluated with expected yield strength of mild steel should be higher than the upper bound tension capacity of the pile to ensure that majority of plastic deformation to be through pile pull-out.

The application of a tension fuse have shown to be very efficient in the previous chapter but in case of using such a structural fuse element the following is recommended to be considered during design.

- For reasons given in Chapter 8, the design should be based on nonlinear pushover or inelastic response history analysis since any amplification of section design forces

for the cap beam in a fuse system is as the same with out a fuse system which can not be reasonable estimated by force-based design methods.

- Since the design will be iterative a response modification factor R=5 is felt to be appropriate for the preliminary dimensioning of the structural elements.
- The nonlinear analysis should be carried out with upper bound strength calculated with to expected strength of mild steel to evaluate maximum compression forces transmitted to the compression piles and with lower bound strength calculated with characteristic strength of mild steel to evaluate the design section forces for cap beams and the maximum total strains at the fuse connection.
- The use of tension fuse system is strongly recommended instead of pile pull-out from the soil since the forces transmitted in such a connection can be accurately predicted while it is rather difficult to rely on soil since there are many parameters that may affect the pull-out capacity of the pile.
- The use of tension fuse system is strongly recommended instead of conventional pile to cap beam connections since the proposed plastic hinge lengths in literature for these types of connections are based on empirical relationships evaluated from different tests. It is again rather difficult to evaluate the true plastic hinge length of a section; therefore the use of such a fuse system provides a plastic hinge length that can be accurately defined by the engineer.

11. CONCLUSION

The poor performance of marine structures with batter piles discouraged owners and engineers, even a number of seismic design codes from their use. The possible cause of this poor behavior however has been studied by a limited number of researchers in the last decade. Traditionally those structures were designed with force-based design methods assuming that the plastic deformations will be concentrated at the piles and the cap beams and the decks which carry heavy gravity loads will remain elastic. Previous studies revealed that this assumption with out considering the post-yielding behavior modes like "pole vaulting" effect of batter pile systems highly underestimates the design section forces of cap beams and decks.

Amplified section forces, particularly adjacent to pile to cap beam connections are probable to cause unexpected yielding of the cap beam both in bending and shear which may lead to premature failure modes under the existence of high gravity loads, if the magnified section forces are not taken into account. Practically this amplification in section forces is not addressed in force-based design methods and therefore is not taken into account.

Subsequently it has been observed that the majority of marine structures supported by steel piles with non-compact sections are prone to premature failure modes in the form of inelastic local buckling. Only a few codes including the Technical Standards for Ports, Harbor Facilities, Railroads, and Airports in Turkey (2007) provided limitation to cross section compactness of steel piles to prevent such premature failure modes.

A new trend in engineering world is to use special pile to cap beam connections in batter pile systems, namely structural fuses, for the purpose of concentrating the inelastic deformation of the marine structures to the inelastic axial deformation of the connection. The use of such fuses allows the engineer to use lower strength level connection and limit the amount of forces transmitted to the piles both in compression and tension.

Most of the modern design codes use displacement-based design approaches, which require the application nonlinear analysis methods such as pushover analysis. The behavior of irregular structures such as wharfs and L or T shape piers are very difficult to be simulated by conventional pushover analysis tools. It is believed that the accuracy of such methods needs further investigation.

Nonlinear pushover analysis and inelastic response history analysis is performed to force-based design generic pier frames, having batter piles with different strength levels and different inclination angles, to investigate the post yielding modes represented both in pile pull-out of the soil and the yielding of pile to cap beam connections. The results of the inelastic response history analysis and the pushover analysis have revealed that there has been a significant increase in section forces of cap-beams with increasing batter and decreasing strength of both pile to cap beam connection or the pile pull-out capacity of the soil. It is has been observed in the case of pile pull-out the amplifications in section forces is more significant than the pile-to-cap-beam connection yielding due the fact that the plastic deformations in pile pull-out is pure axial where in the latter case in is also interacting with the bending deformations resulting in higher vertical uplift deformations.

The results of the nonlinear analysis clearly indicated that the a force-based design method is not suitable for marine structures with batter piles that in the end may lead to hinging and high plastic deformations at the cap-beam which is undesirable in structural elements carrying heavy gravity loads.

The post yield behavior of piers having batter piles with non-compact sections have been evaluated through a series of nonlinear pushover and inelastic response history analysis of piers with varying batter. The nonlinear time history analysis and the nonlinear pushover analysis have clearly shown that the piers designed with non-compact steel sections resulted in either total or partial collapse. The analysis results indicate that the use of non-compact sections in marine structures should be strongly discouraged.

The feasibility of tension fuses have been evaluated through a series of pushover analysis of piers with varying batter. The nonlinear pushover analyses have clearly shown that the use of tension fuse can significantly reduce plastic deformation and force

transmitted to the pile elements and therefore may allow the engineer to provide more economical design solutions. It should also be noted that the fuse can not be designed very weak due to increase in section design forces of the cap beam, as the pole vaulting effect is becoming more significant with decreasing strength of the fuse element.

The accuracy of multi mode pushover analysis method MPA suggested by Chopra(2003) have been investigated through a series of inelastic response history analysis of a wharf structure with a loading direction parallel to seaward edge. The results of the inelastic response history analysis have clearly revealed that the method though is successful in predicting inelastic deformations at the direction of loading, have failed to predict deformations perpendicular to the direction of loading and the maximum plastic deformations with a reasonable accuracy. This is mainly due to elastic contribution of the higher mode and its inability to reflect the effect of changes of modal properties of the structure during the earthquake excitation. It should also be noted that a nonlinear static analysis method with adaptive load distribution may successfully predict such deformations.

APPENDIX A: TIME HISTORY RECORDS USED IN THIS STUDY

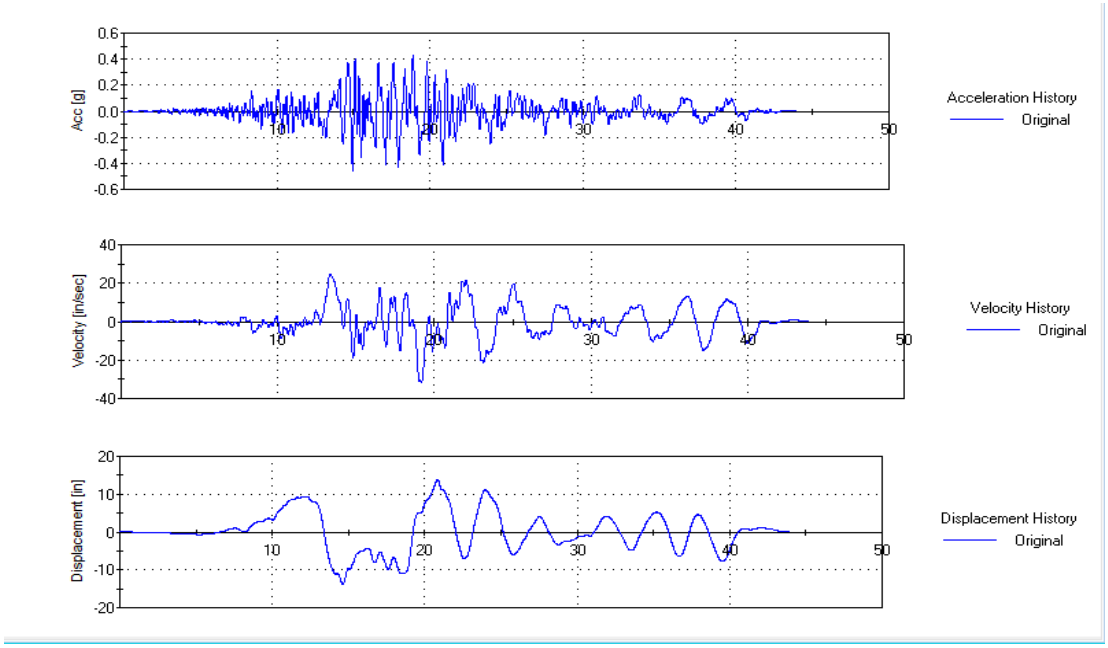

Figure A1 Acceleration-Velocity and Displacement History of Earthquake Record P0164

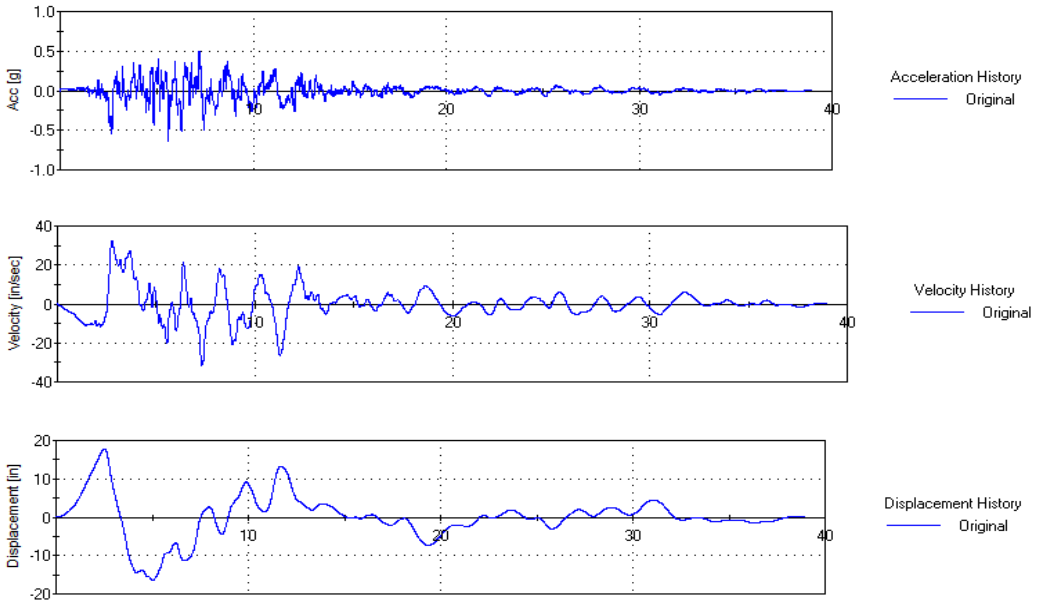

Figure A2 Acceleration-Velocity and Displacement History of Earthquake Record P0752

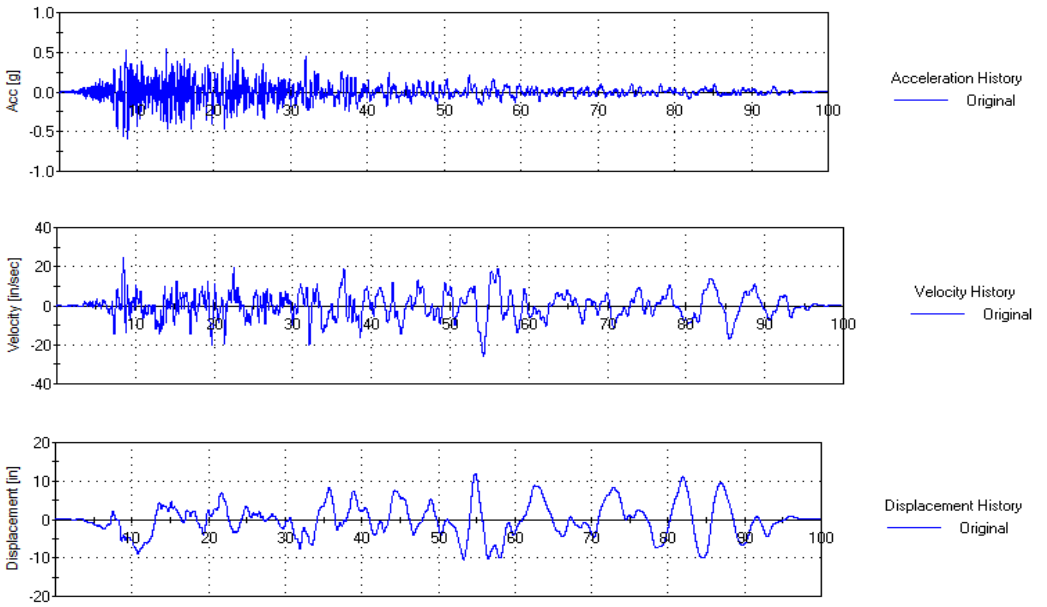

Figure A3 Acceleration-Velocity and Displacement History of Earthquake Record P0013

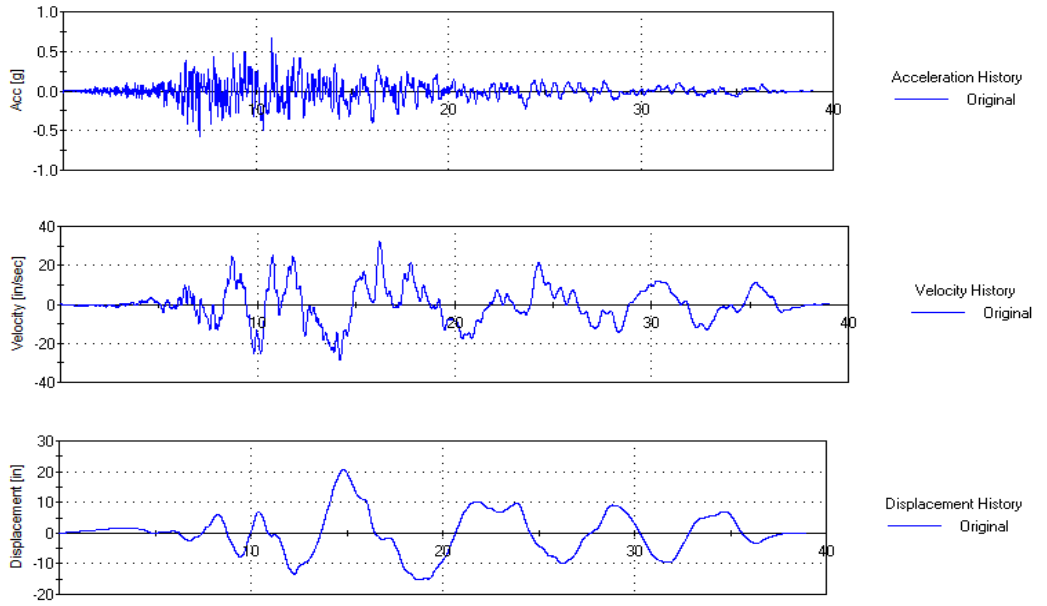

Figure A4 Acceleration-Velocity and Displacement History of Earthquake Record P0012

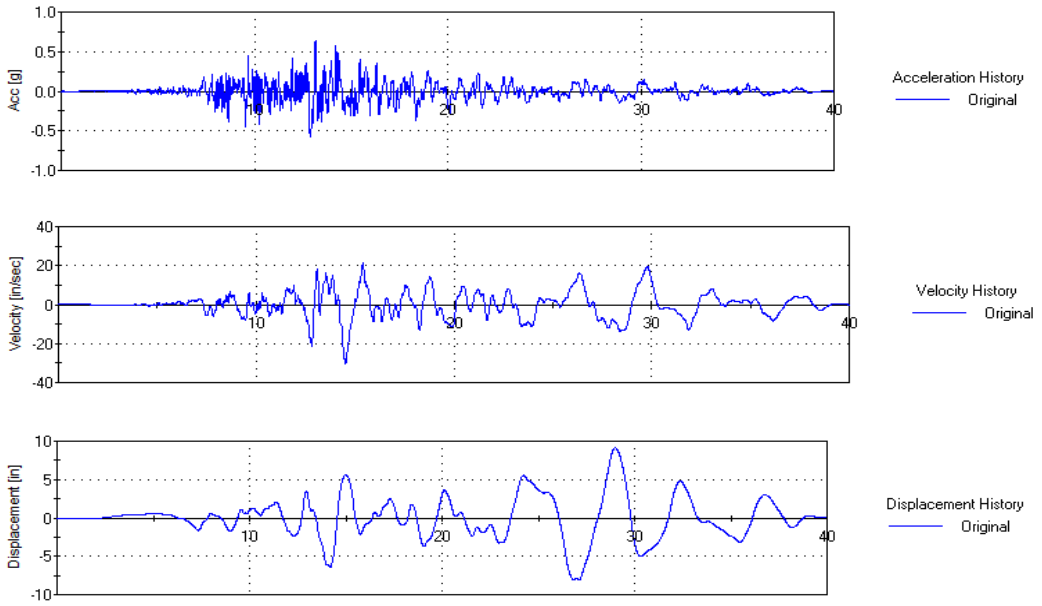

Figure A5 Acceleration-Velocity and Displacement History of Earthquake Record P0967

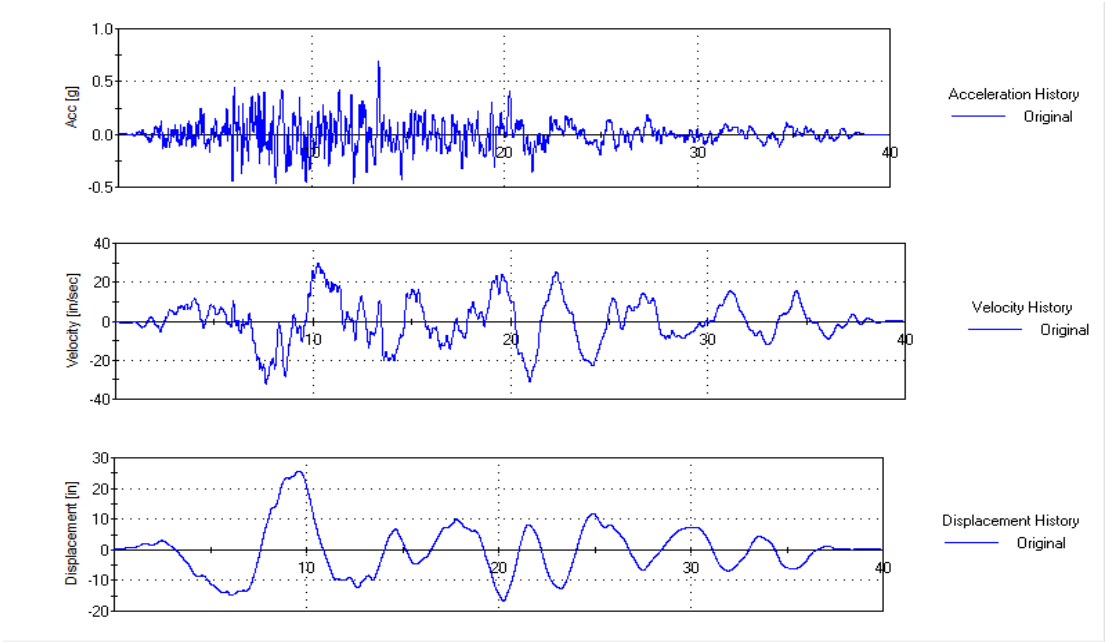

Figure A6 Acceleration-Velocity and Displacement History of Earthquake Record P0778

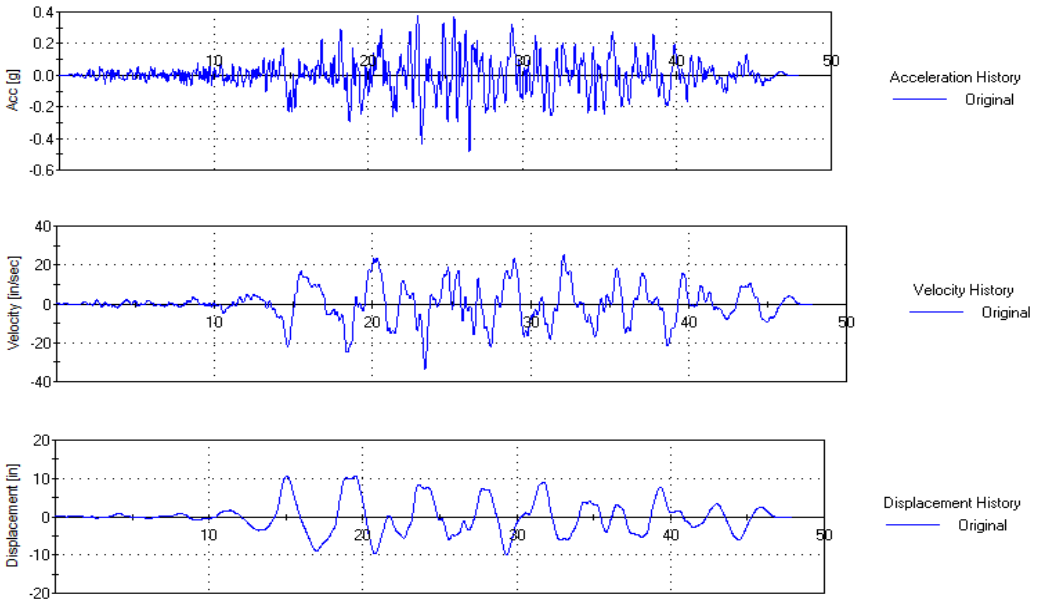

Figure A7 Acceleration-Velocity and Displacement History of Earthquake Record P0843

REFERENCES

API. "Recommended practice for planning, designing and constructing fixed offshoreplatforms—Working stress design." 20th Edition, *American Petroleum Institute*,Washington, DC, 1994.

ATC-40 (1996). "Seismic Evaluation and Retrofit of Concrete Buildings", Applied Technology Council, Redwood City, California.

Boulanger, R. W., S. Iai, A. Ansal, K.Ö. Çetin, I.M. Idriss, B. Sunman, K. Sunman, 2000, "Performance of Waterfront Structures" *Earthquake Spectra Special Issue on 1999 Izmit Earthquake* pp. 295-310.

Bowles, J.E. *Foundation Analysis and Design*, 5th edition, McGraw-Hill, New York, NY, 1997.

Brown, D. A., C. Morrison, and L.C. Reese, 1988, "Lateral Load Behaviour of Pile Group in Sand." *ASCE Journal of Geotechnical Engineering*, 114(11), pp. 1261-1276.

Charles, W. Roeder, Robert Graff, Jenifer L. Soderstrom, Jung Han Yoo, 2001, "Seismic Performance of Pile Wharf Connections", PEER 2002/07.

Chopra, A.K., R.K. Goel, 2003, "A Modal Pushover Analysis Procedure to Estimate Seismic Demands for Un-symetric Plan Buildings", *Earthquake Engineering Research Center University of California,* EERC-2003-8.

Davidson, B.J., D.K. Bell, and S.F. George, 1988, "The Implementation of Seismic Isolation in the Retrofit of a Large Wharf", Asia pacific workshop on seismic design and retrofit of structures, Taipei, Taiwan

EQE International., 1995, "The January 17, 1995 Kobe Earthquake: An EQE Summary Report".

Fajfar, P and M. Fischinger, 1988, "N-2 – A Method for Nonlinear Seismic Analysis of Regular Structures", *Proceedings of 9th World Conference on Earthquake Engineering*, Tokyo.

FEMA (1997). "NEHRP Guidelines for the Seismic Rehabilitation of Buildings (FEMA 273)", *Federal Emergency Management Agency*, Washington D.C.

Ferrito, J.M., 1997, " Design Criteria for Earthquake Hazard Mitigation of Navy Piers and Wharfs" Technical Report TR-2069-SHR, Naval Facilities Engineering Service Center .

Ferrito, J.M ,S.E. Dickenson, M.J.N Pristley, S.D. Werner , & C.E. Taylor , 1999, "Seismic Criteria for Marine oil Terminals" ,Technical Report TR-2103-SHR, Naval Facilities Engineering service Center.

Freeman S.A., J.P. Nicoletti, and J.V. Tyrell, 1975, "Evaluations of Existing Buildings for Seismic risk – A Case Study of Puget Sound Naval Shipyard, Bremerton, Washington", *Proceedings of 1st U.S. National Conference on Earthquake Engineering*, EERI, Berkeley, pp.113-122.

Harn, Robert E. 2004 "Have Batter Piles Gotten a Bad Rap in Seismic Zones?(Or Everything You Wanted to Know About Batter PilesBut Were Afraid to Ask)" *Ports 2004* ,ASCE, doi: 10.1061/40727(2004)13.

International Navigation Association, (PIANC), 2001, "Seismic Design Guidelines for Port Structures:Working Group No. 34 of the Maritime Navigation Commission", A. A. Balkema Publishers, Exton, Penn.

Ishizawa, T. and M. Iura, 2005, " Analysis of Tabular Steel Bridge Piers", *Earthquake Engineering and Structural Dynamics*, doi. 10.1002/eqe.465.

Johnson, R.K., R. Riffenburgh, R. Hodali, Y. Moriwaki, & P. Tan, 1998, "Analysis and Design of Container Terminal Wharf at the Port of Long Beach", *PORT 98*, ASCE, pp.436-444.

Kishida, H. and A. Takano, 1990, "The Buckling of Steel Piles and the Method of Strengthen the End of Steel Piles", *Transactions of the Architectural Institude of Japan* No.213, pp. 29-38.

Klusmeyer, L. and R.E. Harn, 2004, "Displacement-Based Seismic Design of a Large Naval Pier", *Ports 2004* ,ASCE, doi: 10.1061/40727(2004)123.

Kraft, L.M., R.P. Ray, and T. Kagawa., 1981, "Theoretical T-Z curves." *Journal of Geotechnical Engineering,* ASCE, 107(11), , pp. 1543–1561.

Lam, I. P. and G.R. Martin, 1986, "Seismic Design of Highway Bridge Foundations, " Volume I, Executive Summary; Volume II, Design Procedures and Guidelines; Volume III, Example Problems and Sensitivity Studies, Report Nos. FHWA-RD-86-101, 102, and 103, (NTIS/PB87-133062, PB88-157276, and PB88-157284).

Landers, P., 2001, "Kobe Disaster Offers Clues on Rebuilding", *Wall Street Journal*, New York, NY, pp A19.

McClelland, B., and J.A. Focht, 1956, "Soil Modulus for Laterally Loaded Piles." *Journal of the Soil Mechanics and Foundation Division*, Proceedings Paper (101),pp. 1049-1063.

McCullough, N.J., S.E. Dickenson, 2004, " The Behavior of Piles in Sloping Rock Fill at Marginal Wharves",*Ports 2004* ,ASCE, pp. 1-10

Mokwa R. L., J.M. Duncan, 2001, "Lateral Loaded Pile Group Effects and P-y Multipliers", *ASCE Geotechnical Special Publication*, N0 113, pp.728-742

Poulos, H. G., 1971, “Behavior of Laterally Loaded Piles: Part II - group piles.” *ASCE Journal of the Soil Mechanics and Foundations Division*, 97(SM5), pp. 733-751.

Poulos, H. G., 1980, “Comparisons Between Theoretical and Observed Bhavior of Pile Foundations.” *Australia-New Zealand Conference on Geomechanics*, pp. 95-104. Poulos, H. G., and E.H. Davis, (1980) “Pile Foundation Analysis and Design”, John Wiley and Sons, New York.

Powel, G. H., 2006, “PERFORM 3-D, Program for Nonlinear Analysis and Performance Assesment of 3-D Structures”, Computer and Structures, Inc.

Reese, L.C., W.R. Cox, and F.D. Koop, 1974, “Analysis of Laterally Loaded Piles in Sand.”, *Proceedings of the Offshore Technology Conference*, Houston, Texas, Vol II, Paper No. 2080, pp. 473-484.

Silva, P. F., F. Seible, 2001, "Seismic Performance Evaluation of CISS Piles,” *ACI Structural Journal*, Vol. 98, No. 1, pp. 36-49.

Standards, Canada, 1994, “Canadian Standart Association (CSA). Limit states design of steel structures-CAN/CSA-S16.1-M94.” ,Rexdale Ont., Canada

Standards, California, 2003, “Marine Oil Terminal Engineering and Maintenance Standards”, MOTEMS, California State Land Commission.

Standards, California, 2002, “Ports of Los Angeles Code for Seismic Design, Upgrade and Repair of Container Wharfs”, POLA, California State Land Commission.

Standards, Europe, 2005, “EN 1993 1-1, Eurocode 3: Design of steel structures - Part 1-1: General rules and rules for buildings”, Comité Européen de Normalisation, Brussels.

Standards, Japan, 1999, “Technical Standards for Ports and Harbor Facilities in Japan”, Ministry of Transport, Japan.

Standards, Turkey, 2007, “Technical Standards for Ports, Harbor Facilities, Railroads, and Airports in Turkey”, DLHA, Turkey.

Standards, USA, 1994, “American Institude of Steel Construction (AISC). Load and resistance factor design-Manual of steel construction”, 2nd Ed., Chicago.

Tsinker, Gregory P. “Port Engineering: Planning, Construction, Maintenance, and Security”, Wiley , March 2004.

Unified Facilities Criteria, (2005), “Design: Piers and Wharves”, US Army Corps of Engineering.

Wang, S.T. and L.C. Reese, 1993, “COM624P – Laterally Loaded Pile Analysis Program for the Microcomputer, Version 2.0.”, U.S. Dept. of Transportation, Federal Highway Administration (FHWA), Publication No FHWA-SA-91-048.

Werner, Stuart D., ASCE, 1998, “Seismic Guidelines for Ports”, Technical Council on Lifeline Earthquake Engineering (TCLEE) Monograph No. 12, Aston, ISBN: 0-7844-0327-9.

Zmuda, R., M. Weismair, & M. Caspe, 1995, “Base Isolating a Wharf Using Sliding Friction Isolators at the Port of Los Angeles”, *PORTS 1995*, ASCE , pp. 1263-1274

REFERENCES NOT CITED

Aydınoğlu, M.N., 2003, "An Incremental Response Spectrum Analysis Procedure Based on Inelastic Spectral Displacements for Multi-Mode Performance Evaluation", *Bulletin of Earthquake Engineering*, Vol. 1, pp. 3-36.

Aydınoğlu M. N. (2004). "An Improved Pushover Procedure for Engineering Practice: Incremental Response Spectrum Analysis (IRSA)". International Workshop on "Performance-based Seismic Design: Concepts and Implementation", Bled, Slovenia, *PEER Report* 2004/05, pp. 345-356.

Chopra, A.K. (2001). "Dynamics of Structures: Theory and Applications to Earthquake Engineering", 2nd Edition, New Jersey, Prentice Hall.

Chopra, A. K. and R.K. Goel, 2002, "A Modal Pushover Analysis for Estimating Seismic Demands for Buildings", *Earthquake Engineering and Structural Dynamics*; 31(3), pp. 561-582.

Clough , R.W. and J. Penzien, 1993, *Dynamics of Structures*, 2nd International Edition, McGraw Hill Inc., Singapore.

CSI, 2006, "SAP 2000, Static and Dynamic Finite Element of Structures", Computers and Structures Inc., Berkeley, California, USA.

FEMA (2000). "Prestandard and Commentary for the Seismic Rehabilitation of Buildings (FEMA 356)". *Federal Emergency Management Agency*, Washington D.C.

Fahjan Y.M., Z. Ozdemir and M. Al-Qaryouti, 2005, "Selection and Scaling of Real Earthquake Accelerograms to Fit the New Jordanian Design Spectra", Paper No. 27, *The International Earthquake Engineering Conference*, November 21-24, Dead Sea/Jordan

Mander, J.B., M. J. N. Priestley, and R. Park. 1988. "Theoretical Stress-Strain Model for Confined Concrete." *Journal of Structural Engineering* 8, pp. 1804-1826.

Naeim, F., A. Alimoradi and S. Pezeshk, 2004, "Selection and Scaling of Ground Motion Time Histories for Structural Design Using Genetic Algorithms", *Earthquake Spectra*, Vol. 20 No 2, pp 413-426

Naeim, F. and J.M. Kelly, 1999, "Design of Seismic Isolated Structures: From Theory to Practice", John Wiley & Sons, 289 pp.

Priestley, M.J.N., 2003, "Myths and Fallacies in Earthquake Engineering, Revisited", *The Mallet Milne Lecture*, IUSS Press, Pavia, ITALY.